

**STUDIES ON HIGH MOLECULAR WEIGHT FIBROBLAST
GROWTH FACTOR-2 ISOFORMS PRODUCED BY RAT
AND HUMAN CARDIAC MYOFIBROBLASTS**

BY

JON-JON RODRIN SANTIAGO

A Thesis Submitted to the Faculty of Graduate Studies of

The University of Manitoba

in partial fulfillment of the requirements

for the degree of

DOCTOR OF PHILOSOPHY

Department of Physiology and Pathophysiology

Faculty of Health Sciences

College of Medicine

University of Manitoba

Winnipeg, Manitoba

Copyright © 2014

Table of Contents

Table of Contents	i
Dedication	v
Acknowledgments	vi
Abstract	viii
List of Figures	xi
List of Abbreviations	xv
Chapter 1: Review of the Literature	1
1.1 Fibroblast Growth Factor-2 (FGF-2): general history.....	1
1.2 Gene expression and translational regulation.....	4
1.3 FGF-2 in cell/subcellular, tissue, and extracellular matrix.....	6
1.4 Export mechanisms of FGF-2.....	9
1.5 Biological effects of extracellular-acting FGF-2.....	11
1.5.1 FGF-2 isoforms in knock out mouse models.....	13
1.6 FGF-2 signaling transduction pathways.....	14
1.6.1 Angiotensin II signaling transduction pathways.....	17
1.7 FGF-2 isoforms in heart disease.....	19
1.8 Myofibroblasts and FGF-2.....	23
1.8.1 Matricellular proteins and myofibroblasts.....	26
1.9 <i>In vitro</i> model of cardiac myofibroblasts.....	28
1.10 Rationale and hypotheses of the study.....	29
Chapter 2: Materials and Methods	32
2.1 Rat primary cultures.....	32
2.2 Human tissues, primary cultures, and pericardial fluid.....	33
2.3 Adult rat cardiomyocytes isolation.....	34

2.4 Mouse embryonic fibroblasts (MEFS).....	35
2.5 Reagents.....	36
2.6. Antibodies.....	37
2.7 Expression of human FGF-2 isoforms by gene transfer.....	38
2.8 Isolation of anti-human Hi-FGF-2 antibodies by affinity chromatography.....	38
2.9 Immunoprecipitation with anti-human Hi-FGF-2 antibodies.....	38
2.10 Cell treatments.....	39
2.11 High salt elution of extracellular, cell associated FGF-2.....	39
2.12 Heparin-Sepharose fractions.....	40
2.13 Tissue/cell extraction for analysis by Western blotting.....	40
2.14 Western blotting.....	41
2.15 Hypertrophy <i>in vitro</i>	42
2.16 qRT-PCR.....	43
2.17 Immunolocalization.....	44
2.18 Secretome analysis by LC-MS/MS.....	45
2.19 Zymography.....	47
2.20 Statistical analysis.....	47
Chapter 3: Results.....	49
3.1. Production of Hi-FGF-2 by rat cardiac myofibroblasts. Some of the results in this section have been published in M1.....	49
3.1.1 FGF-2 isoforms in cardiac cells.....	49
3.1.2 Hi-FGF-2 export and caspase-1.....	50
3.1.3 Secreted Hi-FGF-2 is pro-hypertrophic.....	51

3.1.4 Autocrine effects of Hi-FGF-2.....	52
3.2 Expression and role of human Hi-FGF-2. Results in this section have been published in M2.....	67
3.2.1 Human FGF-2 isoform expression in human cardiac tissue.....	67
3.2.2 FGF-2 isoform expression in human atria-derived myofibroblasts.....	71
3.2.3 Regulation of human FGF-2 isoform production by Angiotensin II, <i>in vitro</i>	76
3.2.4 Human Hi-FGF-2 export.....	78
3.2.5 Biological activity of human Hi-FGF-2.....	80
Chapter 4: Discussion.....	110
4.1 Rat Hi-FGF-2. This Discussion section corresponds to Results in section 3.1.....	110
4.1.1 The mechanism of rat Hi-FGF-2 export requires caspase-1 activity.....	110
4.1.2 Biological effects of extracellular-acting rat Hi-FGF-2.....	112
4.2 Human Hi-FGF-2. This Discussion section corresponds To results in section 3.2.....	117
4.2.1 Hi-FGF-2 in the human atria.....	118
4.2.2 Expression of human Hi-FGF-2 in hMFs.....	120
4.2.3 The role of Ang II signaling in human Hi-FGF-2 accumulation by hMFs.....	121
4.2.4 Secretion/release of human Hi-FGF-2.....	123
4.2.5 Biological activity of human Hi-FGF-2.....	125
Chapter 5: Conclusions: Clinical Relevance and Future Directions...129	
Chapter 6: References.....133	
Appendix A.....150	

This thesis contains materials (Figures/Results/Discussion) published in two peer-reviewed manuscripts as listed below. Permissions have been obtained from the Journals for reproducing copyrighted materials and are included as an Appendix A.

Manuscript 1 (M1). By Santiago *et al.*, “Preferential accumulation and export of high molecular weight of FGF-2 by rat cardiac non-myocytes”. *Cardiovasc Res* 2011;89**:139-147.**

I contributed 85% of the figures (6 out of 7 figures) and wrote 70% of the first draft of manuscript including revisions.

Manuscript 2 (M2). By Santiago *et al.*, “High molecular fibroblast growth factor-2 in the human heart is a potential target for prevention of cardiac remodeling”. *PLoS One*, 2014 May 14;9(5):e97281.

I contributed 74% of the figures (14 out of 19 figures including supplementary materials) and wrote 70% of the first draft of manuscript including revisions.

For

Dina

Genico

Giada

Daddy Jorge

Mommy Lucy

Luigina

Domenico

Because all of me loves all of you

Acknowledgements

I am very grateful to my supervisor and mentor, **Dr. Elissavet Kardami**. I want to express my deepest gratitude for your profound influence in my career as a scientist. One thing that I will take with me is your constant motivation for me to think critically at all times, especially in my own work. Your passion for science is contagious and the depth of knowledge you carry is phenomenal. Thank you for the encouragements, support, and understanding especially in most difficult times. Your training has enormously impacted me from the very first day I step into your lab. I am proud to be a Kardami student and that I will cherish forever.

I would also like to give a special thank you to my advisory committee (past and present) for getting me where I am now. Thank you **Dr. Peter Zahradka, Dr. Ian Dixon, Dr. Nasrin Mesaeli, Dr. Thomas Netticadan, and Dr. Jeff Wigle**. Your advice and constructive criticism on my research have proven to be essential during my training. Thank you for the never ending questions, open door policy, and countless reference letters. I would also like to extend my appreciation of **Dr. Janice Dodd** for the interest in my project and the emails full of positive comments which helped me realized that I belong in research and can be competitive in the scientific community. Special thank you to **Dr. Peter Cattini** for his unwavering support and encouragement.

My work during my Ph.D. training would not have been possible without the members of the Kardami Lab. I am forever in debt to each lab members past and present: **Robert Fandrich, Barb Nickel, Sarah Jimenez, Maya (Madhu) Jeyaraman, Xin Ma, Wattamon Srisalkuldee, and Navid Koleini**. Thank you

my dear friends for the technical expertise, constant encouragements, and for providing all the laughs that made each day enjoyable. I am also grateful to the support staff at the Institute of Cardiovascular Sciences and the Department of Physiology. Thank you all for the team-oriented setting you have provided.

I would also like to give my appreciation to the funding agencies. I am grateful to the St. Boniface Hospital Research Centre, CIHR, and the University of Manitoba and all its affiliates. As well, I would like to thank MHRC and NSERC for funding my salary throughout my degree. Thank you for the financial assistance to conduct my research.

I can never survive the intense post-graduate training without my love ones. I want to thank my wife, **Dina**. You have been very supportive and understanding throughout my studies. Thank you for listening to me when I would practice my talks even though “it’s a little too much science” for you. I would also like to give my appreciation to my parents, **Daddy Jorge**, whom I missed so much, and **Mommy Lucy**, for believing in me and setting a good example as parents. Thank you to all my immediate and extended family and this includes my in-laws for your unconditional love. Last but not the least is my son **Genico** and my daughter **Giada**, you have both been a bundle of joy in our lives and I thank you for all the happiness you have provided making my research worthwhile. With this, I wish to end by thanking **GOD** for all His blessings.

Abstract

Fibroblast growth factor-2 (FGF-2) is a ubiquitous and multifunctional heparin binding growth factor, that exists as high molecular weight (> 20 kDa, Hi-FGF-2), or a low molecular weight, (18 kDa, Lo-FGF-2) isoforms with distinct biological functions. Most studies to-date have focused on Lo-FGF-2, while the biology of Hi-FGF-2 is less well understood. In addition, very little is known about the production and secretion of Hi-FGF-2 by human cardiac myofibroblasts. We hypothesized that pathology-associated stimuli such as Angiotensin II (Ang II) stimulate the upregulation and release of human Hi-FGF-2 that promote cardiomyocyte hypertrophy (via paracrine action) as well as stimulate pro-fibrotic, pro-inflammatory protein expression (via autocrine action). A series of studies were undertaken to investigate the following : (1) secretion of Hi-FGF-2 is mediated by caspase-1, (2) extracellular-acting Hi-FGF-2 stimulates cardiomyocyte hypertrophy and production of fibrosis-related extracellular matrix proteins by myofibroblasts, and (3) human Hi-FGF-2 is upregulated by the Angiotensin II (Ang II) /Ang II receptor/ERK pathway in cardiac myofibroblasts.

In the first series of studies, we used rat ventricular myofibroblast cultures stimulated with Ang II, in the absence or presence of YVAD, a peptide inhibitor of caspase-1. Our results showed that caspase-1 activity was required for the Ang II-stimulated Hi-FGF-2 secretion, but that caspase-1 did not prevent intracellular FGF-2 accumulation. Secreted rat Hi-FGF-2 was shown to be biologically active and capable of stimulating neonatal as well as adult cardiomyocyte hypertrophy *in vitro*.

In a second series of studies, we compared the effect of extracellular-acting Hi- versus Lo-FGF-2 on the secretome of rat cardiac myofibroblasts by mass spectroscopy (LC-MS/MS). Secretome profiles suggested that Hi-FGF-2 was more potent than Lo-FGF-2 in upregulating several matricellular and fibrosis-associated proteins, most prominently periostin, follistatin-like protein 1, plasminogen activator inhibitor-1, and tenascin. Western blotting of myofibroblast-conditioned media with specific antibodies confirmed these MS/MS findings. Mouse embryonic fibroblasts expressing only Hi-FGF-2 accumulated significantly higher levels of periostin compared to those from mice expressing only Lo-FGF-2. These cells also displayed increased expression of procollagen and EDA-Fibronectin, consistent with a more prominent myofibroblast phenotype.

The third study examined the translational potential of our findings with rat Hi-FGF-2 in the human context. Human heart (atrial) tissue, pericardial fluid, and human tissue-derived myofibroblasts were shown to accumulate predominantly Hi-FGF-2. Human myofibroblasts were shown to export Hi-FGF-2 and Ang II up-regulated Hi-FGF-2 in these cells, via activation of: type 1 or type 2 Ang II receptors (AT-1R, AT-2R); the ERK pathway; and matrix metalloprotease-2. Treatment with neutralizing antibodies specific for Hi-FGF-2 (neu-Ab^{Hi-FGF-2}) reduced expression of proteins indicative of fibroblast to myofibroblast conversion and fibrosis. Blocking the autocrine action of Hi-FGF-2 on human atrial myofibroblasts with neu-Ab^{Hi-FGF-2} resulted in the down-regulation of periostin, as well as α -smooth muscle actin, pro-collagen, embryonic smooth muscle myosin, and extra domain A fibronectin, consistent with a reversal from

activated myofibroblast to fibroblast phenotype. Conditioned media from stimulated human atrial myofibroblasts increased cardiomyocyte size and protein synthesis (hypertrophy) *in vitro*, effects that were abolished by neu-Ab^{Hi-FGF-2}. Furthermore, stimulation of human atrial myofibroblasts with recombinant human Hi-FGF-2 was significantly more potent than recombinant human Lo-FGF-2 in upregulation of pro-interleukin-1 β and plasminogen-activator inhibitor-1, considered to be pro-inflammatory proteins.

Our data, taken together, indicate that exported, extracellular-acting Hi-FGF-2 has pro-fibrotic, pro-inflammatory, and pro-hypertrophic properties by contributing to the 'activated fibroblast' phenotype. Prevention of Hi-FGF-2 export, down-regulation of Hi-FGF-2 accumulation, or conversion of Hi-FGF-2 into a beneficial Lo-FGF-2 isoform, may be considered as potential therapeutic strategies to prevent the undesirable autocrine and paracrine effects of Hi-FGF-2.

List of Figures

We have used a dual listing system for some of the Figures. The first listing (Figures 1, 2, etc.) numbers the Figures as they appear in this thesis. The second listing represents the corresponding Figure number within published manuscripts (Manuscript 1; Santiago *et al.*, 2011 and Manuscript 2; Santiago *et al.*, 2014). For example, Figure 1 in this thesis is described as Figure 1/M1-Fig.1.

Figure 1/M1-Fig.1	Expression of Hi-FGF-2 by neonatal heart -derived non-myocytes (CNMs) and cardiomyocytes (CMs)....56
Figure 2/M1-Fig.2	Expression of FGF-2 by adult heart cells.....57
Figure 3/M1-Fig.6	Caspase-1 inhibition prevents Hi-FGF-2 export.....58
Figure 4/M1-Fig.7	Secreted Hi-FGF-2 is pro-hypertrophic.....59
Figure 5	Hi-FGF-2 stimulates gene expression of BNP in neonatal rat cardiomyocytes.....60
Figure 6	Hi-FGF-2 increases adult rat cardiomyocyte cell size.....61
Figure 7	Secretome profile of rat cardiac myofibroblasts stimulated with Hi- or Lo-FGF-2 and analyzed by LC-MS/MS.....62
Figure 8	Western blot of conditioned medium of rat cardiac myofibroblasts analyzed for specific antibodies detecting matricellular fibrosis-promoting proteins....63

Figure 9	Western blot of total cell lysates of rat cardiac myofibroblasts analyzed for specific antibodies detecting matricellular fibrosis-promoting proteins...64
Figure 10	Western blot of total cell lysates of MEFs analyzed for specific antibodies detecting matricellular fibrosis-promoting proteins.....65
Figure 11	Western blot of total cell lysates of MEFs analyzed for specific antibodies detecting myofibroblastic-promoting proteins.....66
Figure 12/M2-Fig.1	Detection of Hi-FGF-2 in human atrial tissue.....85
Figure 13/M2-Fig.S1	Comparison of Western blot signal for recombinant FGF-2 (12.5-200 pg/lane) with anti-FGF-2 signal representative human atrial lysate samples.....87
Figure 14/M2-Fig.S2	Localization of Hi-FGF-2 in cardiomyocytes and non-myocytes in human atrial tissue.....88
Figure 15/M2-Fig.S3	Anti-human Hi-FGF-2 antibodies detect overexpressed human Hi-FGF-2 but not human Lo-FGF-2, <i>in situ</i>89
Figure 16/M2-Fig.S4	Specificity of anti-human Hi-FGF-2 antibodies for denatured and native Hi-FGF-2.....90
Figure 17/M2-Fig.S5	Identification of human patient atria-derived cells as myofibroblasts (hMFs).....92
Figure 18/M2-Fig.2	Detection of Hi-FGF-2 in human atrial myofibroblasts.....93

Figure 19/M2-Fig.S6	Production of Hi- and Lo- FGF-2 isoforms by cardiac myofibroblasts from different sources, and endothelial cells.....	95
Figure 20/M2-Fig.3	Angiotensin II promotes upregulation of cell-associated human Hi-FGF-2 via AT-1R and AT-2R.....	96
Figure 21/M2-Fig.4	ERK and MMP-2 activities are required for the Ang II-induced Hi-FGF-2 upregulation in hMFs.....	98
Figure 22/M2-Fig.5	Both AT-1R and AT-2R mediate the Ang II-induced ERK activation in hMFs.....	99
Figure 23/M2-Fig.S7	MMP activity is not affected by Ang II receptor activation nor extracellular-acting FGF-2.....	100
Figure 24/M2-Fig.6	Detection of Hi-FGF-2 in the extracellular environment <i>in vitro</i> and <i>in vivo</i>	101
Figure 25/M2-Fig.S8	Human adult ventricular myofibroblasts export Hi-FGF-2.....	102
Figure 26	Exported human Hi-FGF-2 levels depend on Caspase-1 activity.....	103
Figure 27/M2-Fig.7	Selective neutralization of extracellular human Hi-FGF-2 attenuates expression of pro-fibrotic proteins.....	105
Figure 28	Neu-Ab ^{Hi-FGF-2} antibodies decrease periostin accumulation.....	106

Figure 29/M2-Fig.8	Effect of extracellular-acting FGF-2 isoforms on the accumulation of pro-IL-1 β and PAI-1 by hMFs.....	107
Figure 30/M2-Fig.9	Human Hi-FGF-2 exerts pro-hypertrophic effect.....	108

List of Abbreviations

Ang II	angiotensin II
AT-1R	angiotensin type 1 receptor
AT-2R	angiotensin type 2 receptor
α -SMA	alpha-smooth muscle actin
ANOVA	analysis of variance
ANP	atrial natriuretic peptide
BCA	bicinchoninic acid
BHK-21	baby hamster kidney cells
BNP	B-type natriuretic peptide
BSA	bovine serum albumin
CMF	calcium magnesium free
CMs	cardiomyocytes
CNMs	cardiac non-myocytes
DMSO	dimethylsulfoxide
DTT	dithiotreitol
ECL	enhanced chemiluminescence
ECM	extracellular matrix
EDA-FN	extra-domain fibronectin
ELISA	enzyme-linked immunosorbent assay
Erg1	early growth response-1
ERK	extracellular signal-regulated kinase
ET-1	endothelin 1
FBS	fetal bovine serum
FGF	fibroblast growth factor

FGF-2	fibroblast growth factor-2
FGFR	fibroblast growth factor receptor
FSTL-1	follistatin-like protein 1
GAPDH	glyceraldehyde-3-phosphate dehydrogenase
GPCR	G-protein coupled receptor
HEK293	human embryonic kidney cells
HEPES	4-(2-hydroxyethyl)-1-piperazineethanesulfonic acid
Hi-FGF-2	high molecular weight fibroblast growth factor-2
HSPG	heparan sulfate proteoglycans
hMFs	human cardiac myofibroblasts
IGF-1	insulin-like growth factor 1
IgG	immunoglobulin
IL-1 β	interleukin 1, beta
IL-6	interleukin 6
IRES	internal ribosome entry site
LDH	lactic dehydrogenase
Lo-FGF-2	low molecular weight fibroblast growth factor-2
LC-MS/MS	liquid chromatography, tandem mass spectrometry
MAPK	mitogen activated protein kinase
MCF-7	mammary carcinoma cells
MEFs	mouse embryonic fibroblasts
MF20	striated muscle myosin
MHC	myosin heavy chain
MMP2	matrix metalloproteinase-2
mRNA	messenger ribonucleic acid

neu-AB ^{Hi-FGF-2}	neutralizing antibodies to Hi-FGF-2
neu-AB ^{FGF-2}	neutralizing antibodies to total FGF-2
NHCF-A	human adult atrial fibroblasts
NHCF-V	human adult ventricular fibroblasts
NIH	National Institute of Health
NLS	nuclear localization sequence
N.S.	not significant
ORF	open reading frames
PAGE	polyacrylamide gel electrophoresis
PAI-1	plasminogen activator inhibitor-1
PBS	phosphate buffered saline
pI	isoelectric point
PIC	protein inhibitor cocktail
PKA	protein kinase A
PKC	protein kinase C
PMSF	phenylmethylsulfonylfluoride
PPIC II	phosphate inhibitor cocktail II
PPIC IV	phosphate inhibitor cocktail IV
PRMT5	arginine methyltransferase 5
qRT-PCR	quantitative real-time polymerase chain reaction
RIPA	Radioimmunoprecipitation assay
rpm	rotations per minute
SD	standard deviation
SDS	sodium dodecyl sulfate
SEM	standard error of the mean

SH2	Src homology domain 2
SHP-1	SH2-containing phosphatase 1
Sp1	stimulating protein 1
SMemb	non-muscle heavy chain myosin
SPE	solid phase extraction
TBS-T	tris-buffered saline with Tween
TCA	trichloroacetic acid
TGF β	transforming growth factor beta
TnT	troponin
U	units
UTR	untranslated region

1.1 Fibroblast Growth Factor-2 (FGF-2): general history

Early studies showed that extracts from bovine pituitary glands were capable of stimulating proliferation of fibroblasts (Abraham *et al.*, 1986). Within these brain extracts, fibroblast growth factor (FGF) was discovered as was first published by Amerlin in 1973 (Amerlin, 1973), followed by Gospodarowicz in 1974 (Gospodarowicz *et al.*, 1974). FGF was purified by heparin-Sepharose chromatography based on its high affinity to sulphated oligosaccharide heparin. However, further fractionation based on isoelectric points indicated the presence of dual peaks, the first peak having an acidic isoelectric point or pI of 5 was designated as acidic FGF or FGF-1; and the second peak with a basic pI between 8 - 10 was designated as basic FGF or FGF-2. Although, both polypeptides share a high degree of amino acid sequence identity, they were determined to be biologically distinct mitogens.

We now know that FGF-2 is a prototypic member of a large family of heparin-binding proteins comprised of 23 members to date (Yamashita *et al.*, 2000). Family of fibroblast growth factors (FGFs) are composed of structurally related proteins that are required for development, homeostasis, response to injury, and metabolism (Itoh *et al.*, 2011). In vertebrates, FGFs can be classified based on functions as having paracrine (FGF-1 to FGF-10, FGF-16, -17, -18, -20, -22), intracrine (FGF-11 to FGF-14), and endocrine (FGF-15, -19, -21, -23) activities. Intracrine signaling act independently of FGF receptors (FGFR) while both paracrine and endocrine activities act via cell surface receptors (Itoh *et al.*,

2011). Most of the FGF family have amino terminal signal peptides that allow them to be secreted from cells. However FGF-1, -2, -9, -16, -20 lack the signal peptide sequences but can also be secreted by cells to the cell surface and extracellular space via unconventional protein secretion (Ornitz *et al.*, 2001). Targeted mutagenesis of FGF genes in mice has elucidated various cellular processes in development and metabolism. FGF-21 has been shown to act on many tissues to coordinate carbohydrate and lipid metabolism by enhancing insulin sensitivity, decreasing triglycerides, causing weight loss, and ameliorating obesity-associated hyperglycemia and hyperlipidemia (Li *et al.*, 2013). The prototypic members of the FGF family are FGF-1, FGF-2, and FGF-3. Both FGF-2 and FGF-3 have high molecular weight isoforms that are translated at the upstream non-conical start codons. FGF-2 has been shown to play a major role in cardiac healing.

FGF-2 exists in several isoforms differing in their N-terminal extensions. In humans, five isoforms have been identified, all of which are considered to be products of regulation at the translational level, arising from a single gene within chromosome 4 of q26 to q27 region of the human genome (Yu *et al.*, 2007). Translation initiation from the AUG start codon generates the smallest variant at 18 kDa and is designated as low molecular weight FGF-2 (Lo-FGF-2), whereas translation from four CUG start codon in-frame of the AUG codon generates the high molecular version of FGF-2 (Hi-FGF-2) at 22, 22.5, 24, and 34 kDa, as reviewed in (Kardami *et al.*, 2004). In rat, three isoforms have been identified, 18, 20, 21.5 kDa, while in mice, 18, 20.5, 21 kDa variants were isolated. Both Hi-

FGF-2 and Lo-FGF-2 bind and activate plasma membrane tyrosine kinase receptors, FGFR, (Klint *et al.*, 1999), and have been shown to have diverse biological activities. Overexpression and ablation studies of FGF-2 demonstrated biological roles of FGF-2 in controlling vascular tone (Zhou *et al.*, 1998), brain development, blood pressure control (Dono *et al.*, 1998), and wound healing (Ortega *et al.*, 1998). In addition, in FGF-2 knockout mice studies, FGF-2 is involved in the induction of pathological hypertrophy (Pellieux *et al.*, 2001). Our lab has shown that FGF-2 promotes acute and sustained cardioprotection (associated with enhanced angiogenesis) after myocardial infarction (Kardami *et al.*, 2007). There is evidence that the diverse biological activities of FGF-2 may reflect isoform specific properties.

Hi-FGF-2 is reported to be present mainly within the nucleus whereas Lo-FGF-2 can be present in both the cytoplasm and nucleus. Studies have reported or implied that Lo-FGF-2 is the only FGF-2 that is capable of being secreted into the extracellular matrix thus it is the only FGF-2 that can have paracrine or autocrine activities (Delrieu, 2000; Chlebova *et al.*, 2009). However, there is increasing evidence from several laboratories, including our own that Hi-FGF-2 can also be released into the extra-cellular environment where it can exert potentially detrimental paracrine activities. Cardiac rat fibroblasts have been shown to preferentially release Hi-FGF-2, which would be predicted to stimulate cardiomyocyte hypertrophy, and/or secretion of remodeling-associated cytokines by fibroblasts (Jiang *et al.*, 2007). The biological activities of secreted Hi-FGF-2

by cardiac fibroblasts is the main focus of this thesis in both rat and human models.

1.2 Gene expression and translational regulation of FGF-2

Hi-FGF-2 production is regulated at both the transcriptional and translational level. The *FGF-2* gene has been shown to be transcribed into multiple polyadenylated sense and also antisense mRNAs (Delrieu, 2000). Variations in gene locus exist in different species. In humans, *FGF-2* gene is located in chromosome 4q26-27 region. The human *FGF-2* gene consists of two introns of 1.6 kbp in size integrated in between three exons. Assessment of *FGF-2* promoter revealed a lack of canonical TATA or CCAAT consensus sequences (Shibata *et al.*, 1991), instead the promoter region contains five GC-rich regions that binds Sp1 and Egr-1 transcription factors (Jimenez *et al.*, 2004). Studies have identified two known negative regulatory elements within the 5'-promoter area that is not transcribed and within the 3' of the promoter region that is transcribed but not translated (Shibata *et al.*, 1991; Baird *et al.*, 1991). A variety of stimuli can induce *FGF-2* gene expression including stress stimuli such as ischemia, cytokines, and growth factors; FGF-2 has been shown to activate the *FGF-2* gene promoter and activate its own expression in cardiomyocytes (Jimenez *et al.*, 2004).

Studies to date have reported and documented five mRNA transcripts, all of which containing 5' untranslated region (UTR) as well as AUG-initiated open reading frames (ORF) along with various length of polyadenylation at the 3'-UTR

(Chlebova *et al.*, 2009). The difference between various FGF-2 mRNA species can then be attributed to the different 3'UTR polyadenylation lengths. Translational regulation of FGF-2 has been investigated mainly by Prats and colleagues. They have shown that the length of 3'UTR poly A tail could play a role in selectively initiating the translation of specific FGF-2 isoforms (Touriol *et al.*, 2000).

Translation of FGF-2 occurs by both conventional cap-dependent as well as internal ribosome entry site (IRES) cap-independent pathways (Bonnal *et al.*, 2003). Both Lo-FGF-2 and the 22-24 kDa Hi-FGF-2 can be translated via the IRES pathway, although the 34 kDa human Hi-FGF-2 is translated by a cap-dependent and IRES-independent mechanism (Delrieu, 2000).

Translation regulation of FGF-2 is not well understood especially how cells selectively use AUG versus CUG start codons. Studies have shown that stress inhibits the cap-dependent mechanism of translation while promoting the IRES-dependent FGF-2 translation (Prats *et al.*, 2002), which resulted in the production and accumulation of both Hi- and Lo-FGF-2 isoforms (excluding the 34 kDa isoform). It is of interest that the tumor suppressor p53 inhibits FGF-2 translation by promoting a conformational change in the FGF-2 mRNA structure (Galy *et al.*, 2001).

FGF-2 is subject to several post-translational modifications including methylation, phosphorylation, and limited degradation/cleavage. Studies done by Bruns *et al.*, (2009) indicated that several arginines at the N-terminal region of Hi-

FGF-2 can be methylated by an enzyme known as arginine methyltransferase 5 or PRMT5. This modification is an essential requirement for nuclear localization of Hi-FGF-2. Treatment of cells with PRMT5 inhibitors resulted in an increase accumulation and localization of Hi-FGF-2 within the cytoplasm and significantly decreased amount of nuclear Hi-FGF-2. Other studies have shown that Protein Kinase A and Protein Kinase C are able to phosphorylate FGF-2 itself, which stimulated an increase in activities by binding to FGF-2 receptor (Baird *et al.*, 1989). This event occurs at the cell surface of cytoplasmic membrane acting upon extracellular-bound FGF-2. In regards to the cleavage of Hi-FGF-2, serine protease thrombin, a key coagulation factor and inflammatory mediator with selective proteolytic activities can cleave Hi-FGF-2 into a Lo-FGF-2-like mitogen that stimulated endothelial cells to proliferate and migrate (Yu *et al.*, 2008).

1.3 FGF-2 in cells, tissues, and extracellular matrix

Early studies indicated that FGF-2 isoforms may accumulate in tissues in relative fixed molar ratios that varies with cell type and developmental stage (Riese *et al.*, 1995). Extracts of atrial and ventricular heart from chicken, rat, sheep, and cow have been shown to contain FGF-2 (Kardami *et al.*, 1989). Hi-FGF-2 was reported to be predominantly expressed only in transformed cell lines whereas primary cells were thought to express the Lo-FGF-2 isoform (Vagner *et al.*, 1996). These early studies are likely to have underestimated the relative Hi-FGF-2 content of cells/tissues. FGF-2 levels are often assessed by enzyme-linked immunoabsorbent assays (ELISA) that do not discriminate between the

isoforms as they are raised against the core Lo-FGF-2 sequence. In addition, the N-terminal extension of Hi-FGF-2 is vulnerable to limited degradation during tissue extraction, producing the 18 kDa isoform (Doble *et al.*, 1990; Kardami *et al.*, 2004). Furthermore, studies associating Hi-FGF-2 with cellular transformation fail to account for predominant expression of Hi-FGF-2 isoforms in fully differentiated adult tissues such as the brain (Liu *et al.*, 1993).

Exposing cells to stress stimuli including heat shock, oxidative stress, and γ -irradiation resulted in an increase expression and translation of Hi-FGF-2 (Vagner *et al.*, 1996). Hypothyroidism was associated with increased Hi-FGF-2 accumulation in rat hearts (Liu *et al.*, 1993), a transient increase in Hi-FGF-2 accumulation was also observed after isoproterenol-induced cardiac injury (Padua *et al.*, 1993).

FGF-2 isoforms are believed to have different subcellular distribution. According to some reports, Lo-FGF-2 is predominantly cytosolic, while Hi-FGF-2 isoforms are mainly nuclear (Bikfalvi *et al.*, 1997; Arese *et al.*, 1999; Delrieu, 2000), due to the presence of putative nuclear localization sequence (NLS) at the N-terminal extension of Hi-FGF-2. However, Lo-FGF-2 is also present in the nucleus, and nuclear matrix (Bouche *et al.*, 1987; Sheng *et al.*, 2004). Also, ectopically expressed Lo-FGF-2 localized in the nucleus of mouse fibroblast NIH 3T3 and human HEK 293 cells (Foletti *et al.*, 2003), baby hamster kidney (BHK-21) cells (Tessler *et al.*, 1990), rat cardiomyocytes (Pasumarthi *et al.*, 1994; Pasumarthi *et al.*, 1996), and rat Schwann cell (Claus *et al.*, 2003); Claus and colleagues showed that nuclear Lo-FGF-2 localized to different sub-nuclear

domains compared to Hi-FGF-2. Presence of Lo-FGF-2 in the nucleus can be attributed to another NLS composed of 17 amino acid sequence located at the C-terminal end of Lo-FGF-2 (Sheng *et al.*, 2004). In particular within the C-terminal NLS sequence are two arginines (Arg149 and Arg151), which play a crucial role in FGF-2 nuclear localization.

Hi-FGF-2 levels also vary in a tissue specific manner. Within the adult brain, Hi-FGF-2 is the predominant species (Delrieu, 2000), while 18 kDa Lo-FGF-2 isoform is more predominant in the adult rat heart (Liu *et al.*, 1993). These early studies need to be re-evaluated, due to Hi-FGF-2-to-Lo-FGF-2 conversion that can happen during handling, which can lead to underestimation of Hi-FGF-2 contribution. In hyperglycemia, the IRES-dependent Hi-FGF-2 expression was reported to be upregulated in mouse aorta but not in brain tissue (Teshima-Kondo *et al.*, 2004).

FGF-2 also accumulates at the extracellular space, associated with heparan sulfate proteoglycans or HSPGs (Moscatelli *et al.*, 1987). The HSPGs in the matrix and basement membrane are considered to act as a reservoir that retains FGF-2 and facilitates bindings to its plasma membrane receptors (FGFR1-4) (Vlodavsky *et al.*, 1991). Also, HSPGs in the matrix are proposed to act as a molecular trap that helps export intracellular FGF-2 during in an unconventional transport process across the plasma membrane (Zehe *et al.*, 2006). HSPGs can also protect FGF-2 from proteolytic degradation by proteases also present within the extracellular matrix (Kardami *et al.*, 2007).

1.4 Export mechanisms of FGF-2

The mechanism by which FGF-2 is transported to the extracellular space is incompletely understood. In general, secreted proteins contain signal peptides for secretion (5-30 amino acids long) and are transported through the conventional secretory pathway via the endoplasmic reticulum (ER)-Golgi apparatus. Upon translation, nascent proteins enter the endoplasmic reticulum through the signal peptide recognition site (Nickel *et al.*, 2009). The newly synthesized proteins exit the ER via ER exit sites (tER sites) from which cargo-containing coat protein complex II (COPII)-coated vesicles engulf the proteins for transport to the Golgi apparatus, where they are processed and directed towards their final destination of secretion (Nickel *et al.*, 2009).

Because FGF-2 does not contain a conventional signal peptide sequence, it is not secreted through the conventional ER-Golgi apparatus (Szebenyi *et al.*, 1999). FGF-2 can be released via sub-lethal plasma membrane disruptions. For example adult cardiomyocytes secrete FGF-2 on a beat to beat basis via mechanically-induced transient disruptions of the sarcolemma (Clarke *et al.*, 1995). Furthermore, increased FGF-2 release was observed when cardiomyocytes undergo vigorous activity. Cardiac fibroblasts, a major source of FGF-2 and a major cardiac cell type that exists in close proximity to cardiomyocytes, would be expected to be stretched passively by myocyte contraction, and thus also release FGF-2 to the extracellular environment via passive stretching. Cell death or injury by endotoxins and/or irradiation also leads to the release of FGF-2 into the extracellular environment (Yu *et al.*, 2007). In

non-small cell lung cancer, cisplatin induced-apoptosis or heat-induced necrosis resulted in increased levels of FGF-2 within the extracellular environment (Kuhn *et al.*, 2005). The Na⁺/K⁺ ATPase α -subunit at the plasma membrane is implicated in FGF-2 export by viable cells, because ouabain mediated inhibition of ion transport also inhibits FGF-2 secretion; the process is facilitated by 27 kDa heat shock protein acting as a chaperone (Piotrowicz *et al.*, 1997). Viable cells have also been reported to export FGF-2 (both Hi- and Lo-FGF-2 isoforms) inside membrane-shed vesicles (Taverna *et al.*, 2003).

Caspase-1, a protease activated by the inflammasome and part of the innate inflammation response to stress signals, has also been implicated in the release of FGF-2 (of unknown isoform composition) and several other unconventionally secreted cytokines such as the interleukins (IL-1 β and IL-1 α) (Keller *et al.*, 2008). The direct mechanism of translocation of Lo-FGF-2 through the plasma membrane has been studied extensively by Nickel and colleagues. According to their recent findings, Lo-FGF-2 is first recruited to the inner leaflet of the plasma membrane by mechanism mediated by phosphatidylinositol-4,5-bisphosphate (PI(4,5)P₂) as well as heparin sulfate proteoglycans (HSPGs) at the outer leaflet of plasma membrane acting as a molecular trap for FGF-2 release (Zehe *et al.*, 2007; Temmerman *et al.*, 2008). Upon recruitment to the plasma membrane, Tec-kinase, a novel factor involved in the export machinery of Lo-FGF-2, binds to Lo-FGF-2 and forms a heterodimeric complex. Lo-FGF-2, which remains in a folded confirmation, is phosphorylated at tyrosine 82 by Tec-kinase, a post-translational modification shown to be essential for Lo-FGF-2

membrane translocation to the cell surfaces (Ebert *et al.*, 2010). There have been no studies addressing the possibility that Hi-FGF-2 may also be secreted by as similar Tec-kinase mediated pathway. At this point, there is no evidence that different mechanisms may exist for export of different FGF-2 isoforms.

Once released into extracellular space, FGF-2 is bound to heparan sulfate proteoglycans at the basal lamina as well as extracellular matrix. These pools of FGF-2 can be released via the action of heparinases (Kardami *et al.*, 2007). Liberated FGF-2 can then bind to plasma-membrane bound FGFR for an acute cellular response. It is important to note that many of the studies on FGF-2 release have been based on cells that overexpress either Hi- or Lo-FGF-2 through transient or stable gene transfer, therefore, their physiological relevance should be re-evaluated. Studies presented here have focused on the mechanisms controlling the production of Hi-FGF-2 (accumulation and release) using primary, non-transformed cells under physiological and pathophysiological conditions, and on the biological activities associated with the secreted Hi-FGF-2.

1.5 Biological effects of extracellular-acting FGF-2

Extracellular-acting FGF-2, operating in autocrine or paracrine pathways, plays a major role in various physiological and pathophysiological conditions including vascular remodeling, angiogenesis, hypertrophy, and tumor growth (Yu *et al.*, 2007). The biological activities of Hi- and Lo-FGF-2 isoforms remain to be fully described, although there is clear evidence for FGF-2 isoform specific-effects.

In vitro studies comparing the effects of added recombinant Hi-FGF-2 versus Lo-FGF-2 have shown that Hi-FGF-2, but not Lo-FGF-2 inhibited cell migration of bovine arterial of endothelial cells (Piotrowicz *et al.*, 2001). In addition, Hi-FGF-2 was shown to inhibit IGF-1-induced migration of mammary carcinoma cells (MCF-7). The inhibitory effect of Hi-FGF-2 on migration is via FGFR1-mediated estrogen receptor activation (Piotrowicz *et al.*, 2001). However, Lo-FGF-2, which also binds FGFR1, was not able to activate estrogen receptor in similar fashion as Hi-FGF-2. The ability of Hi-FGF-2 to inhibit cell migration has been attributed to an 86 amino-acid Hi-FGF-2-specific N-terminal extension of the FGF-2 molecule, and appears to require the membrane co-receptor neuropilin-1 (Zhang *et al.*, 2013).

Piotrowicz and colleagues have reported that Lo-FGF-2, but not Hi-FGF-2, stimulated endothelial cell proliferation (Piotrowicz *et al.*, 2001). In our laboratory, recombinant rat Hi-FGF-2 but not Lo-FGF-2, stimulated neonatal rat cardiomyocyte hypertrophy *in vitro* and *in vivo* (Jiang *et al.*, 2007). However, the related signaling transduction pathways that differentiate the effects of Hi- and Lo-FGF-2 remain elusive.

In terms of *in vivo* studies, administration of Lo-FGF-2 into coronary arteries caused transient beneficial effects by promoting revascularization in ischemic regions in patients with myocardial infarction (Simons *et al.*, 2003). Furthermore, administration of Lo-FGF-2 pre-, during, and post-ischemic conditions exerted acute cardioprotective effects in the rat heart (Kardami *et al.*, 2007).

1.5.1 FGF-2 isoforms in knock out mouse models

Transgenic mice engineered to express only Hi- or only Lo-FGF-2 have shown that Hi-FGF-2 expression promoted increased susceptibility to ischemia and reperfusion injury (Liao *et al.*, 2010). FGF-2 knockout mice were created by replacing the exon 1 of the *FGF-2* gene with hypoxanthine guanine phosphoribosyl transferase (*HPRT*) minigene, resulting in the removal of the first 59 amino acids of FGF-2 protein, which have been shown to be involved in heparin and receptor binding, thus preventing mitogenic activities (Zhou *et al.*, 1998). FGF-2 knockout mice displayed a decreased vascular tone and low blood pressure with decreased vascular smooth muscle contractility (Zhou *et al.*, 1998). Otherwise, these mice had no behavioral or morphological defects with normal lifespan and fecundity. In the case of mice expressing only Hi-FGF-2 isoforms, a construct encoding the *FGF-2* gene, where the AUG methionine start codon was replaced with alanine to prevent the production of the Lo-FGF-2 isoform, was knocked-in into the previously described FGF-2 knockout mice. The mice only expressing Hi-FGF-2 are viable and fertile with no abnormalities in endothelial cell migration and proliferation (Liao *et al.*, 2009). However, these mice have been shown to have significantly impaired response to ischemia/reperfusion injury (Liao *et al.*, 2010). In the case of mice expressing only Lo-FGF-2 isoform, a 14 bp oligonucleotide sequence was inserted into the first exon of the *FGF-2* gene between the canonical methionine start codon and upstream of the CUG start codon. The 14 bp oligonucleotide was designed to introduce stop codons preventing the production of the Hi-FGF-2 isoforms. This

construct was knocked-in into the FGF-2 knockout mice. The mice expressing only Lo-FGF-2 are viable and fertile with no abnormalities. In ischemia-reperfusion injury, these mice showed improvement in cardiac contractile function (Liao *et al.*, 2010).

Doetschman and colleagues recently reported distinct developmental and physiological roles of FGF-2 isoforms in the cardiovascular system, effects that were also modulated by gender (Nusayr *et al.*, 2013). They have indicated that Lo-FGF-2 signaling is necessary in the female heart only for normal growth, but is required by both female and male hearts for normal diastolic function. These authors concluded that Hi-FGF-2 is necessary only in male hearts for modulating systolic function and appears to play no obvious physiological role in female hearts (Nusayr *et al.*, 2013). In addition, these transgenic mice were exposed to daily injections of isoproterenol (up to 4 days). The results indicated that post-isoproterenol treatment in female Hi-FGF-2 expressing mice did not exhibit significant differences in hypertrophic and fibrotic response compared to wildtype control (where both isoforms are present), while Lo-FGF-2 expressing mice displayed a blunted hypertrophic response (Nusayr *et al.*, 2013). In male hearts, post-isoproterenol treatment in Hi-FGF-2 expressing mice displayed an exacerbated fibrotic response with increased α -smooth muscle actin levels, whereas the Lo-FGF-2 expressing mice had a blunted fibrotic response (Nusayr *et al.*, 2013).

1.6 FGF-2 signal transduction pathways

The different FGF-2 isoforms are capable of signaling from the outside-in, by activating plasma membrane receptors, in both autocrine and paracrine pathways. They are also present within the cell where they trigger intracrine signaling pathways. The biological effects of extracellular-acting FGF-2 are mediated by binding to high affinity FGF receptors (FGFR1-4) and low affinity heparan sulfate proteoglycans or HSPGs (Galvez-Contreras *et al.*, 2012). Four types of FGFRs have been isolated and studied, however, a fifth receptor (FGFR5 or FGFR1) has been identified with high homology to the other four (Kim *et al.*, 2001; Sleeman *et al.*, 2001). Hi- and Lo-FGF-2 can bind and activate FGFR1-3 in a similar manner and therefore different outcomes likely represent contributions from signaling triggered by internalized FGF-2 (unpublished observations).

FGFR5 has been described in vertebrates (Bertrand *et al.*, 2009) is devoid of an intracellular kinase domain and binds neither FGF-2 nor FGF-1 (Kim *et al.*, 2001; Sleeman *et al.*, 2001). Unlike the canonical FGFRs that signal via tyrosine kinase domains, the short intracellular sequence of FGFR5 consists of a putative Src homology domain-2 (SH2)-binding motif (Silva *et al.*, 2013). The same group has shown at least in part using beta-cells, that FGFR5 enhances ERK1/2 signaling through association of SHP-1 phosphatase with the receptor's intracellular SH-2 binding motif at insulin secretory granules. Splice variants of the FGFR also exist (Wuechner *et al.*, 1996). The significance of FGFR splice variants is not well understood, but studies have shown that splicing changes the receptor affinities for the different FGF-2 isoforms and appears to be tissue-

specific (Yeh *et al.*, 1993). Whether splicing variants plays a critical role in Lo-FGF-2 versus Hi-FGF-2 signaling is yet to be determined.

FGFR1 is considered to be the most abundant FGFR in embryonic, neonatal, and adult cardiomyocytes (Kardami *et al.*, 2007; Cilvik *et al.*, 2013). The FGF-2 ligand binding to FGFR causes the receptor to dimerize and become autophosphorylated at tyrosine residues within the C-terminal tail (Klint *et al.*, 1999). Activated FGFRs are then able to recruit and phosphorylate other signaling molecules, and result in the activation of all branches of the mitogen activated protein kinase (MAPK) pathways, phospholipase C-protein kinase C (PKC), and Src-dependent pathways as reviewed in (Kardami *et al.*, 2007). Studies have also shown that binding of FGF-2 to HSPGs on its own can also lead to the activation of extracellular signal-regulated kinases 1 and 2 (ERK1/2) (Chua *et a.*, 2004).

Extracellular-acting FGF-2 signaling includes FGF-2-FGFR1 internalization to the cytosol and nucleus of cells (Maher *et al.*, 1996; Malecki *et al.*, 2004). Internalization and the subsequent nuclear translocation of FGF-2-FGFR1 complex is mediated by β -importin (Stachowiak *et al.*, 2003). This process is reported to be required for Lo-FGF-2 to stimulate mitosis (Bossard *et al.*, 2003). While nuclear translocation of Lo-FGF-2 is mediated by binding to translokin, this is not the case for Hi-FGF-2 (Bossard *et al.*, 2003). Hi-FGF-2 is transported to the nucleus by its N-terminal extension containing nuclear localization sequences (Delrieu, 2000). It is important to emphasize that the end-effects of extracellular-acting FGF-2 are a combination of signals activated

downstream of the plasma membrane FGFR as well as by signals triggered by internalized FGF-2 and FGF-2/FGFR complexes that translocate to the nucleus and affect gene expression directly, as reviewed in (Kardami *et al.*, 2004); see also (Dunham-Ems *et al.*, 2009).

In cardiomyocytes, overexpression of Hi-FGF-2 (but not Lo-FGF-2) by transient gene transfer increased cell binucleation and chromatin compaction via an intracrine-only mode of action (Pasumarthi *et al.*, 1996). The nuclear Hi-FGF-2-induced chromatin compaction was shown to represent a cell death pathway with mitochondrial engagement and apoptotic features (Hirst *et al.*, 2003). Intracrine-acting Hi-FGF-2 required ERK activation as well as nuclear localization to promote cell death (Ma *et al.*, 2007). Microarray studies, by Quarto *et al.* (2005), reported FGF-2-isoform specific gene expression; Hi-FGF-2 expression was associated with cell cycle inhibition and tumor suppression.

1.6.1 Angiotensin II signaling transduction pathways

Angiotensin II (Ang II) is a major bioactive octapeptide in the renin-angiotensin system (RAS). Hepatic-derived angiotensinogen is cleaved by the renin enzyme made in the kidneys to produce a decapeptide Angiotensin I, which is converted into Ang II mediated by angiotensin-converting enzymes or ACEs (Berry *et al.*, 2001). Besides the systemic production of Ang II, it can also be produced locally via tissue RAS (Kaschina *et al.*, 2003). Generally, Ang II functions by modulating blood pressure but it has also been implicated in inflammation, endothelial dysfunction, atherosclerosis, hypertension, and

congestive heart failure (Mehta *et al.*, 2007). In cultures of rat myocytes, Ang II has been shown to stimulate protein synthesis but not DNA synthesis, in contrast, Ang II was shown to induce mitogenic activities in rat cardiac fibroblasts (Sadoshima *et al.*, 1993). Ang II was also shown to induce secretion of paracrine factors that can act on cardiac myocytes stimulating hypertrophy (Gray *et al.*, 1998).

Various signaling pathways have been implicated in the activation of the hypertrophic response of the heart in the presence to chronic stress. One of the major signaling transduction pathways that is activated involves the Ang II binding to G-protein coupled receptors (GPCRs), leading to the activation of G α q, a small GTP-binding protein (Sadoshima *et al.*, 1993). Multiple downstream signaling cascades follows which include mitogen activated protein kinases, p38, ERK, c-jun N-terminal kinase (JNK), and JAK/STAT pathways that lead to the expression of cardiac gene program manifesting into a hypertrophic phenotype (Mehta *et al.*, 2007). The major actions of Ang II are mediated by two trans-membrane glycoprotein, AT-1R and AT-2R GPCRs. In rodents, there are two sub-types of AT-1R (AT-1Ra and AT-1Rb), whereas humans possess a single AT-1 receptor (Kaschina *et al.*, 2003). AT-1 receptor is involved in the classical physiological actions of Ang II via activation of the PLC pathways and AT-2 receptor may oppose the effects of AT-1R by activating phosphatases (Kaschina *et al.*, 2003).

In addition to activating G-protein dependent pathways, Ang II also cross-talks with several tyrosine kinases such as epidermal growth factor receptor

(EGFR) leading to the activation of mitogen activated protein kinases and ERK1/2 (Mehta *et al.*, 2007). The Ang II-induced upregulation of MMP-2 activity has also been shown to be dependent on ERK1/2. The role of ERK 1/2 and MMP-2 activities in FGF-2 expression by human cardiac myofibroblasts has not been investigated. A complete detailed summary of Angiotensin II signaling pathways in the cardiovascular system is extensively reviewed in Mehta *et al.* (2007).

1.7 FGF-2 isoforms in heart disease

The heart can undergo physiological or pathological remodeling, consisting of changes in cardiac shape, size, connective tissue and function. Physiological remodeling is compensatory in nature and occurs in athletes (Mihl *et al.*, 2008). Maladaptive cardiac remodeling includes pathological cardiac and cardiomyocyte hypertrophy, increased inflammation and fibrosis. It can lead to heart failure and can occur under various pathological conditions, for example during the repair process after a heart attack, in hearts subjected to chronic pressure and/or volume overload and in diseases such as idiopathic dilated cardiomyopathy (Frey *et al.*, 2003).

Adaptive hypertrophy is encountered when increased functional demands are within a physiological range, for example during exercise. Maladaptive hypertrophy occurs under chronic and excess exposure to pathophysiological states such hypertension and/or aortic stenosis, and in familial cardiomyopathy (Opie *et al.*, 2006). The compensatory state is considered beneficial and helps

enhance cardiac performance as needed (Dorn *et al.*, 2007). However, if the stress stimulus persists, cardiac hypertrophy becomes pathological and decompensatory, characterized by progressive systolic dysfunction leading to heart failure (Hunter *et al.*, 1999). In fact, pathological hypertrophy is a risk factor for development of heart failure. (Frey *et al.*, 2003). Cardiac hypertrophy is described as concentric or eccentric. The first is accompanied by increased thickness of myocytes in response to increase in pressure, and the second by increased myocyte length in response to volume overload (Opie *et al.*, 2006). Hypertrophy is accompanied by re-induction of fetal genes including β -type Natriuretic Peptide (BNP), Atrial Natriuretic Peptide (ANP), and β -Myosin Heavy Chain (β -MHC) (Kohli *et al.*, 2011).

Molecular triggers of cardiac hypertrophy include bioactive peptides such as angiotensin II (Ang II), endothelin-1 (ET-1), interleukin-6 (IL-6), insulin-like growth factor-1, and FGF-2; these exert effects on cardiomyocytes as well as cardiac non-myocytes, as reviewed in (Kardami *et al.*, 2004).

Multiple intracellular signaling cascades have been implicated in the induction of hypertrophic gene expression, including all three branches of the mitogen-activated protein kinase (MAPK) pathway via Ras activation (Kardami *et al.*, 2004), PI3 Kinase signaling, calcium-calcineurin-NFAT pathway, and G-Protein Coupled Receptor (GPCR) pathway (Kohli *et al.*, 2011). Studies have shown that these pathways can act in concert with each other. For example, calcineurin-NFAT signaling regulates the cardiac hypertrophic response in coordination with MAPKs (Molkentin, 2004). Upon activation of these pathways

by hypertrophic stimuli, downstream signals such as NFAT and ERK1/2 translocate into the nucleus to activate transcription factors, which further regulate the expression of hypertrophic genes. For detailed summary of the signaling pathways leading to the activation of transcription factors that regulate hypertrophy-associated genes, readers are referred to (Kardami *et al.*, 2004; Kohli *et al.*, 2011).

FGF-2 and cardiac hypertrophy. The use of FGF-2-depleted mice demonstrated that FGF-2 expression is required for the development of hypertrophy in response to Ang II, or aortic stenosis (Schultz *et al.*, 1999; Pellieux *et al.*, 2001). These knock-out studies did not discriminate between the different FGF-2 isoforms. Work in my supervisor's laboratory has shown that direct injection of Hi-FGF-2 to the infarcted heart caused cardiac and cardiomyocyte hypertrophy, increased scarring, and decreased contractile function. Injection of Lo-FGF-2 on the other hand has the opposite effects (Jiang *et al.*, 2007). In other studies, relative cardiac Hi-FGF-2 levels showed a positive correlation with the degree of hypertrophy and fibrosis observed in a mouse model subjected to trans-aortic constriction-induced pressure overload. Maladaptive remodeling in this model was exacerbated by high fat diet, and this was paralleled by increases in Hi-FGF-2 in the heart (Ahmadie *et al.*, 2010).

FGF-2 and fibrosis: Increased deposition of extracellular matrix proteins, most predominantly collagen, by cardiac fibroblasts and myofibroblasts results in fibrosis. Aberrant accumulation of collagen results in ventricular stiffness, which then causes inadequate diastolic function (Biernacka *et al.*, 2011). Fibrosis can

also interfere with the electrical coupling of cardiomyocytes (Swynghedauw *et al.*, 1999); can lead to reduced capillary density; and increase oxygen diffusion distance resulting in hypoxic cardiomyocytes (Sabbah *et al.*, 1995). The term reactive fibrosis describes the increase of cardiac interstitium without cardiomyocyte loss, while reparative fibrosis describes the scar formation following myocardial infarction (Anderson *et al.*, 1979; Weber, 1989). In animal models of left ventricular pressure overload, reactive fibrosis is observed first and accompanied by cardiomyocyte hypertrophy as part of an adaptive response; and eventually, reparative fibrosis follows as cardiomyocytes undergo necrosis and apoptosis (Isoyama *et al.*, 2002). A different scenario of events occur in acute setting of myocardial infarction, whereby the death of a large number of cardiomyocytes triggers an inflammatory reaction that is rapidly followed by reparative fibrosis (Hasenfuss, 1998). Transforming growth factor (TGF β) is considered a major trigger of the fibrotic response (Biernacka *et al.*, 2011). However, more recently, FGF-2 has also been implicated in the fibrotic response of the heart. Fibrosis in a transgenic mouse model of cardiac failure was strongly linked to an upregulation of FGF-2 (of unknown isoform composition) specifically in cardiac fibroblasts (Thum *et al.*, 2008). However, Lo-FGF-2 has been associated with anti-fibrotic activities (Fedak *et al.*, 2012), and is considered to antagonize the profibrotic effects of TGF β (Narine *et al.*, 2006). Thus, it is possible that the effects reported by Thum *et al.* represent those of Hi-FGF-2 isoforms.

FGF-2 and inflammation: Inflammation plays a key role in the remodeling process of the heart. Cardiac fibroblasts have been well-documented to be pro-inflammatory (Heim *et al.*, 2000; Lafontant *et al.*, 2006), however, their relative contribution in the activation of the post-infarction inflammatory cascade *in vitro* and *in vivo* remains unknown due to the absence of specific and reliable markers for cardiac fibroblasts. There is also limited information as to the role of FGF-2 isoforms in tissue inflammation. Thus far, Dr. Kardami's group has documented that increased cellular infiltration in isoproterenol-induced cardiac lesions was associated with increased Hi-FGF-2 (Padua *et al.*, 1993). Chronic heart-specific Lo-FGF-2 overexpression in a mouse transgenic model (FGF-2-TG) also augmented endogenous Hi-FGF-2, due to the ability of FGF-2 to stimulate its own gene expression (Meij *et al.*, 2002). Isoproterenol-induced cardiac lesions in the FGF-2-TG model were characterized by high levels of lymphocyte infiltration, suggesting the possibility that Hi-FGF-2 may be a pro-inflammatory molecule (Meij *et al.*, 2002). Furthermore, the requirement for caspase-1 activity in FGF-2 secretion indicated a potential involvement with the innate inflammatory response (Keller *et al.*, 2008).

1.8 Myofibroblasts and FGF-2

Fibroblasts represent the largest cardiac cell population in terms of numbers, provide mechanical support, and are found in connective tissue throughout the normal heart (Camelliti *et al.*, 2004). Fibroblasts produce extracellular matrix proteins including structural component collagens, proteoglycans, glycoproteins, as well as matricellular proteins that play signaling

and supportive functions. Fibroblasts become activated following injury, differentiating into myofibroblasts and participating in scar formation (Shinde *et al.*, 2014). Myofibroblasts are not present in the healthy, non-stressed heart, but they appear soon after injury and are central agents of the remodeling process (Davis *et al.*, 2014). During cardiac remodeling, fibroblasts migrate and infiltrate the injured area, phenotypically converting into hypersecretory and hypercontractile myofibroblasts. At the end of the repair process, myofibroblasts would be expected to return to a fibroblastic quiescent state, or undergo apoptosis, however due to unknown mechanisms; myofibroblasts remain in a hypersecretory mode producing excessive collagen, and matrix, thus resulting in fibrosis (Tomasek *et al.*, 2002). Persistent myofibroblasts continue to secrete cytokines and growth factors that can initiate and sustain a maladaptive response during cardiac remodeling.

It is now believed that myofibroblasts can be derived from transdifferentiation of several cell types. As reviewed recently (Davis *et al.*, 2014), sources of myofibroblasts in the acute repair response can be, in addition to resident fibroblasts, smooth muscle cells, and vascular pericytes. During chronic injury hematopoietic cells, fibrocytes, and even epithelial cells, undergoing epithelial-to-mesenchymal transition, can acquire a myofibroblast phenotype.

Transformation of fibroblast to myofibroblast is believed to occur gradually, in a continuum process. Upon stimulation, fibroblasts differentiate into “protomyofibroblasts” and then into more fully mature myofibroblasts in the

stressed pathologically hypertrophied myocardium (Tomasek *et al.*, 2002). The first stage is characterized by small adhesion complexes that allow cell migration into the area of damage; the mature stage is characterized by expression of alpha smooth muscle actin, forming the stress fibers mediating contractility of the myofibroblast (Hinz *et al.*, 2007; Hinz *et al.*, 2010).

TGF β is a major stimulant of myofibroblast differentiation, and fibrosis, by both canonical and non-canonical pathways (Davis *et al.*, 2014). In addition, the neuroendocrine agent Ang II which is upregulated during chronic heart disease is strongly implicated in the induction of myofibroblast differentiation and fibrosis, likely by upregulating TGF β signal transduction (Campbell *et al.*, 1997). Another bioactive peptide, which is produced during cardiac injury, endothelin-1 (ET-1), is also implicated in myofibroblast differentiation and fibrosis (Shi-Wen *et al.*, 2004). Both Ang II and ET-1 upregulate total and Hi-FGF-2 in cardiac myofibroblasts (Santiago *et al.*, 2011).

Fibroblasts are a major source of FGF-2 in the heart (Santiago *et al.*, 2011) pointing to the possibility that cardiac fibroblast-derived FGF-2 may be one of the factors contributing to the remodeling process via paracrine or autocrine fashion. FGF-2 levels increase in both fibroblasts and myofibroblasts during the process of scar formation (Galzie *et al.*, 1997; Hoerstrup *et al.*, 2000) and once secreted can stimulate cardiac hypertrophy (Jiang *et al.*, 2007). The mechanism and isoform specific effects of FGF-2 in the process of remodeling are not well understood and merit further investigation. A major component of my work in this

thesis addressed the paracrine and autocrine effects of secreted cardiac fibroblast-derived Hi-FGF-2.

1.8.1 Matricellular proteins and myofibroblasts

Matricellular proteins are a family of proteins that are rapidly turned over, highly expressed, and secreted into the extracellular matrix. They do not directly play any roles in tissue architecture or structural properties of the matrix (Bornstein *et al.*, 2002). Distinguishing characteristics of matricellular proteins include the high levels of expression during development and in response to injury, the ability to bind to cell surface receptors and initiate cell-cell or cell-matrix interactions, and matricellular proteins generally induce de-adhesion rather than adhesion. In general, targeted disruption of matricellular genes produced a grossly normal phenotype or subtle abnormalities, however such phenotype tends to be exacerbated in the presence of stress or injury indicating a role in wound healing or remodeling (Bornstein *et al.*, 2002).

Matricellular proteins have been shown in a variety of cardiac pathophysiological conditions, including cardiac hypertrophy and fibrosis, by acting as transducers of signaling cascades in cardiac remodeling and as modulators of cell migration, proliferation, and adhesion in the presence of stress (Frangogiannis, 2012). Several of these matricellular family including thrombospondin-1 (TSP-1), thrombospondin-2 (TSP-2), osteopontin (OPN), secreted protein, acidic and rich in cysteine (SPARC), periostin, tenascin-C and cry-61, connective tissue growth factor (CTGF) are important modulators of

fibroblast phenotype and play an essential role in modulating growth factor signaling. In the presence of pressure-overload, matricellular proteins within the ECM stimulate cytokine and growth factor signaling in cardiac myocytes leading to apoptosis and hypertrophic growth, modulate matrix assembly and metabolism, and elicit the fibrogenic potential of inflammatory cells and fibroblasts (Frangogiannis, 2012). The effects of FGF-2 on matricellular protein production by fibroblasts is not known.

Periostin is a matricellular protein with important roles in cardiac development and remodeling. Periostin is a 90 kDa secreted glycoprotein with 4 repetitive fasciclin domains that play a role in promoting collagen fibrogenesis and regulating valve formation during development (Zhao *et al.*, 2014). Periostin expression is upregulated in the presence of tissue injury, repair, and remodeling (Frangogiannis, 2012). Typically, periostin upregulation is considered important to correct early tissue repair, however it becomes deleterious/profibrotic if periostin remains upregulated after the conclusion of the healing response (Conway *et al.*, 2008). Zhou and colleagues have demonstrated that in tissues collected from heart transplant recipients and control hearts from unmatched donors, that in the control human heart, low levels of mRNA expression of periostin was observed and at the protein level, periostin was not detectable (Zhou *et al.*, 2014). However, in the failing heart of transplant patients, periostin mRNA levels increased significantly and was positively associated with myocardial fibrosis as well as left ventricular diastolic dimension (Zhou *et al.*, 2014). *In vitro* studies indicated that TGF β and BMP signaling are potent

inducers of periostin in a variety of cell types including fibroblasts (Frangogiannis, 2012). Furthermore, FGFs, PDGF-BB, and Angiotensin II have also been shown to be capable of upregulating periostin expression in smooth muscle cells (Liu *et al.*, 2014). The effect of FGF-2 in periostin accumulation and secretion is not known.

1.9 *In vitro* model of cardiac myofibroblasts

Work by Thum *et al.* (2008) provided evidence that ventricular fibroblast activation is a primary event in ventricular remodeling due to pressure overload. The mechanisms mediating the transition of fibroblasts to myofibroblasts remain to be fully described. In my previous work (Master's thesis) and in collaboration with Dr. Ian Dixon (Department of Physiology), I reported that isolated neonatal and adult rat cardiac fibroblasts (at passage P0) undergo phenotypic transition to myofibroblastic cells upon passage. Phenotypic transition was marked by increased alpha-smooth muscle actin, smooth muscle embryonic myosin heavy chain, extra domain-A fibronectin, paxillin, tensin, and transforming growth factor β receptor II (Santiago *et al.*, 2010). Relative levels of Hi- and Lo-FGF-2 increased with successive passages (P1-P3) (Santiago *et al.*, 2010). My previous studies therefore established an *in vitro* model exhibiting cardiac rat myofibroblast properties. This model was used to show that Ang II upregulated Hi-FGF-2 accumulation by activating the Ang II type 1 receptor (AT-1R); and that Ang II stimulation promoted increased Hi-FGF-2 export to the extracellular space (Santiago *et al.*, 2011).

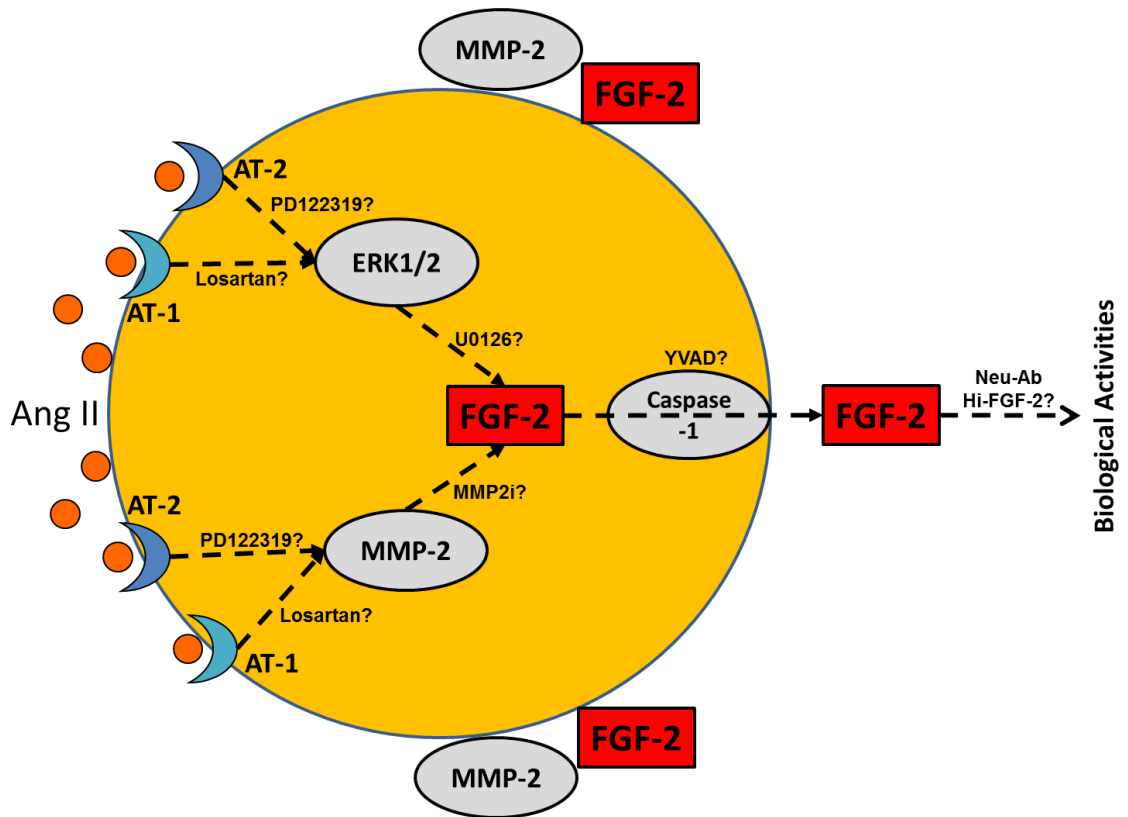
1.10 Rationale and hypotheses of the study

Previous studies (Keller *et al.*, 2008) have indicated that FGF-2 (of unknown isoform composition) requires the activity of caspase-1 for secretion by an unconventional pathway common to several inflammation-associated cytokines. It is not known if the caspase-1-mediated mechanism is FGF-2 isoform selective. I therefore investigated the **Hypothesis (#1)** that Hi-FGF-2 secretion by rat or human myofibroblasts requires caspase-1 activity.

Studies in supervisor's laboratory have shown that recombinant rat Hi-FGF-2 is pro-hypertrophic *in vitro* and *in vivo* (Jiang *et al.*, 2007). We have observed a strong correlation in upregulation of Hi-FGF-2 in a mouse model of exaggerated cardiac hypertrophy and fibrosis (Ahmadie *et al.*, 2010), suggesting that endogenously expressed Hi-FGF-2 contributes to hypertrophy and fibrosis. These previous studies have not addressed a potential paracrine pro-hypertrophic effect of myofibroblast-secreted Hi-FGF-2. Potential autocrine effects of extracellular-acting Hi-FGF-2 on cardiac myofibroblasts have not been investigated. I investigated the **Hypothesis (#2)** that extracellular-acting Hi-FGF-2 stimulates cardiomyocyte hypertrophy and production of fibrosis-related matricellular proteins by myofibroblasts.

Studies using rodent models have provided strong evidence that Hi- and Lo-FGF-2 exert distinct biological activities. For example, after myocardial infarction, rat Lo-FGF-2, but not Hi-FGF-2, promoted sustained cardioprotection and angiogenesis, while Hi-FGF-2, but not Lo-FGF-2, promoted myocardial

hypertrophy and reduced contractile function (Jiang *et al.*, 2007). Rodent Hi-FGF-2 levels were upregulated by pathological stimuli (Santiago *et al.*, 2011), upon fibroblast to myofibroblast conversion (Santiago *et al.*, 2010) and in models of cardiac hypertrophy and fibrosis (Ahmadie *et al.*, 2010). There is as yet no information regarding Hi-FGF-2 in human myocardium. To establish the translational potential of our studies on the rodent FGF-2 isoforms, I investigated **Hypothesis (#3)** that Hi-FGF-2 is expressed by human cardiac cells *in vivo*, is secreted to the extracellular space *in vitro* and *in vivo*, and is upregulated by the Angiotensin II (Ang II)/Ang II receptor/ERK pathway in human cardiac myofibroblasts. Below is the schematic diagram of targeted pathways blocked by specific inhibitors to examine the proposed objectives.



Schematic of targeted pathways in FGF-2 accumulation, secretion, and biological activities. Human cardiac myofibroblasts were incubated with Angiotensin II in the presence or absence of the following: Losartan (AT-1R blocker), PD123319 (AT-2R blocker), U0126 (MEK inhibitor), MMP2i (MMP-2 inhibitor), YVAD (Caspase-1 inhibitor), nue-Ab^{Hi-FGF-2} (neutralizing antibodies to human Hi-FGF-2). Post-treatment, relative levels of Hi- and Lo-FGF-2 isoforms in extracellular pools (cell-associated and in conditioned medium) were assessed. In addition, biological activities (induction of rat neonatal cardiomyocyte hypertrophy, effects on myofibroblasts) of 'secreted' FGF-2 were analyzed.

Material and Methods described in this section were obtained from Manuscript 1 (Santiago *et al.*, 2011) including supplementary materials, as well as from Manuscript 2 (Santiago *et al.*, 2014).

2.1 Rat primary cultures

The investigation conforms with the Guide for the Care and Use of Laboratory Animals by the US National Institutes of Health (NIH Publication No. 85-23, revised 1996). Approval was given by the Protocol Management and Review Committee of the University of Manitoba. Primary cultures of rat neonatal myofibroblasts or cardiac myocytes were obtained as in (Doble *et al.*, 1995; Doble *et al.*, 1996). Adult heart-derived rat myofibroblasts as in (Brilla *et al.*, 1994). All rat myofibroblasts studies used cells at passage P2.

One-day-old pups and adult Sprague-Dawley rats were provided by the Central Animal Care Facility at the University of Manitoba. Primary cultures of neonatal myofibroblasts or cardiomyocytes were isolated from cardiac ventricles of one-day-old Sprague-Dawley rat pups (36x pups/isolation) as we published previously (Doble *et al.*, 1995; Doble *et al.*, 1996). Briefly, the hearts were placed into a Petri dish in PBS containing 3.5 g/L of glucose and minced with scissors until the pieces were about 1 mm³ or small enough to pass through the tip of 10 mL pipette. The heart tissue was digested in a water-jacketed spinner flask at 37°C containing collagenase (740 U/digest), trypsin (370 U/digest), and DNase I (2880 U/digest). The digestion was repeated six times, and the cells were pooled

in a bottle with 10 mL of High Clone FBS (GIBCO) to inactivate the enzymes. After the 6th digestion, the cells were filtered through a nytex membrane using a syringe filter; and centrifuged at 2000 rpm for 5 minutes. The pellet was resuspended in 1x ADS buffer (6.8 g NaCl, 4.76 g HEPES, 0.14 g NaH₂PO₄•H₂O, 1.0 g glucose, 0.4 g KCl, 0.2 g MgSO₄•7H₂O, pH to 7.35 ± 0.5 with 1 N NaOH in 100 mL to make 10x ADS, then diluted to 1x ADS); and once again filtered through a nytex membrane. The cell suspension was layered onto a discontinuous Percoll gradient (Amersham Biosciences) and centrifuged at 3500 rpm for 30 minutes. The upper band of cells was removed and plated in 100 mm cell culture dish using Ham's Mixture Nutrient F-10 medium in 10% FBS and 1% penicillin/streptomycin (GIBCO); and labeled as P0 cells. The cells were passaged and rat myofibroblasts studies presented here were done using cells at passage P2. Each primary culture of neonatal rat myofibroblasts and cardiac myocytes was obtained from the hearts of 36x one day old pups, and was sufficient for one complete experimental series as described in each Figure, providing enough culture plates and cells to allow an n=3/group, for Western blot analyses. Each experiment was repeated twice in its entirety, with new cultures. A total of 10 adult (200 g) Sprague-Dawley rats were used to obtain adult cardiac myocytes and myofibroblasts.

2.2 Human tissues, primary cultures, and pericardial fluid

According to institutional policies (University of Manitoba and St. Boniface General Hospital), all surgery patients sign a consent form allowing tissue

materials and fluids (removed and discarded as a normal part of surgery) to be used for research purposes. Based on this, the Research Ethics Board of the University of Manitoba waived the need for individualized informed consent by donors, and granted permission for use of human tissue and pericardial fluid from cardiac surgery patients (#H2007:004). Data were analyzed anonymously.

Human atrial tissue fragments, of approximately 0.5 cm³ in size, were obtained from patients undergoing coronary artery bypass grafting and placed in basal medium on ice. One-half of each tissue fragment was stored in liquid nitrogen, and used to obtain tissue protein extracts. The other half was either placed in 10% formalin followed by embedding in paraffin, or used to obtain primary cultures of mobile fibroblastic cells. In the latter case, tissue was minced finely and placed in a 60 mm plastic dish with basal medium plus 10% fetal bovine serum (FBS), 100 units/ml penicillin, and 100 µg/ml streptomycin (GIBCO). Cells migrating from the explants and allowed to grow for up to 2 weeks were passaged two more times before use. These cells (at P2-P3) represent human cardiac myofibroblasts (hMFs). Pericardial fluid was obtained from patients (n=10) undergoing routine cardiac surgical procedures, through aspiration of fluid from the pericardium prior to systemic heparinization, avoiding contamination with blood. Human adult atrial or ventricular fibroblast primary cultures (NHCF-A, NHCF-V) obtained from healthy individuals were purchased from Lonza.

2.3 Adult rat cardiomyocytes isolation

Adult rat ventricular cardiomyocytes were isolated according to (Netticadan *et al.*, 1999). Briefly, hearts were excised and perfused with Ca^{2+} free buffer containing 90 mM NaCl, 10 mM KCl, 1.2 mM KH_2PO_4 , 5 mM $\text{MgSO}_4 \cdot 7\text{H}_2\text{O}$, 15mM NaHCO_3 , 30 mM taurine, and 20 mM glucose for 5 min, followed by perfusion with buffer containing 0.05% collagenase and 0.2% bovine serum albumin for 30 mins. Then, ventricles were minced and pipetted several times to allow separation of individual cardiomyocytes. Cells were suspended in a buffer containing 200 μmol Ca^{2+} and were allowed to settle. The buffer was changed from 0.5 mM to 1 mM to 1.5 mM in increasing Ca^{2+} concentration (stepwise). Cardiomyocytes were then transferred into laminin-coated dish, incubated with medium-199 containing 10% fetal bovine serum at 37°C for 2 hours. After the incubation period, the medium was replaced with serum free medium-199 supplemented with 5 mM taurine, 2 mM carnitine, 1 mM creatine, and 1 μmol insulin for another 24 hours prior to treatment.

2.4 Mouse embryonic fibroblasts (MEFs)

FGF-2 transgenic mice were purchased from The Jackson Laboratory. Three lines were obtained: FGF-2 knockout, only expressing Hi-FGF-2, and only expressing Lo-FGF-2 isoform (K01, K02, and K03; respectively) mice. All mice are fertile, exhibit no observable behavioral defects, and have normal life span. Gene ablation in targeting specific allele to disrupt FGF-2 expression and specific isoforms is described as in (Azhar *et al.*, 2009). The different FGF-2 transgenic mice, as well as wild type mice were used to prepare MEFs. Timed mouse

pregnancies were set up and fetuses removed at E12.5 – 14.5 days. The fetuses were counted after dissection of the pregnant dams. The embryos were washed individually in 1-2 mL of sterile CMF-PBS to remove all of the blood clots; then placed into a 60 mm dish and minced with scissors until the pieces were about 1 mm³. After mincing, the fetal tissues were vigorously pipetted until small enough to pass through the tip of 10 mL pipette. The fetal tissues/explants from each embryo were placed in a 60 mm plastic dish with Ham's Mixture Nutrient F10 basal medium plus 10% fetal bovine serum (FBS), 100 µg/mL streptomycin, and 100 units/mL penicillin; purchased from GIBCO. Migratory cells from the explants were allowed to grow; passaged into 100 mm plastic dish; and frozen in basal medium with 40% FBS and 10% DMSO for future studies.

2.5 Reagents

Rat recombinant histidine-tagged His^{Hi}- and His^{Lo}-FGF-2 were obtained as in (Jiang *et al.*, 2004; Jiang *et al.*, 2007). Losartan (Merck Frost), PD123319 (Tocris Bioscience), and YVAD (Ac-YVAD-CMK; Alexis Biochemicals) were used, respectively, at 10⁻⁶, 10⁻⁶, and 10⁻⁵ M. Angiotensin II (Ang II) was purchased from Sigma or Bachem. Due to variation in potency of various batches of Ang II, this reagent was used at 10⁻⁶ M, as this concentration gave consistent results with all batches. ERK1/2 inhibitor, U0126, (Millipore) was used at 10⁻⁵ M, while matrix metalloprotease 2 (MMP-2) inhibitor-1 (MMP2 I1, cis-9-Octadecenoyl-N-hydroxylamide, Oleoyl-N-hydroxylamide, OA-Hy; Millipore) was

used at 3×10^{-5} M. Protease (PIC) and phosphatase (PPIC II and PPIC IV) inhibitor cocktails were from Sigma and Calbiochem, respectively.

2.6 Antibodies

Monoclonal anti-FGF-2 antibodies for Western blot detection (#05-118, clone bFM-2, Millipore) and for activity neutralization (#05-117, clone bFM1, Cedarlane) have been validated in previous studies (Kardami *et al.*, 1990; Anderson *et al.*, 1991; Pasumarthi *et al.*, 1996; Sun *et al.*, 2001). Rabbit polyclonal antibodies specific for human Hi-FGF-2 were custom made (Sigma Genosys) against a sequence (GRGRGRAPERVG) present in the N-terminal extension of human Hi-FGF-2, using the same strategy as in (Ding *et al.*, 2002); they were affinity-purified, and used at 10-20 $\mu\text{g/ml}$. Mouse monoclonal antibodies to pro-collagen (sp1D8), striated muscle myosin (MF-20), and cardiac troponin T (TnT; CT3), were developed by Dr. Heinz Furthmayr, Dr. Donald A. Fischman, and Dr. Jim Jung-Ching Lin, respectively, and obtained from the Developmental Studies Hybridoma Bank developed under the auspices of the NICHD and maintained by the University of Iowa, Department of Biological Sciences, Iowa City, IA 52242. Antibodies to extra-domain fibronectin (EDA-FN; MAB 1940), embryonic smooth muscle myosin heavy chain (SMemb), and α -smooth muscle actin (α -SMA), were from Chemicon. Antibodies to desmin, α -actinin, and vimentin were from Sigma, while N-cadherin was from Abcam. Antibodies for phospho ERK and total ERK were from Cell Signaling. Antibodies for Ang II Type-1 (goat; AT-1R) and Type-2 (rabbit; AT-2R) receptors, as well as

plasminogen activator inhibitor-1 (PAI-1) and pro-interleukin 1- β (IL-1 β) were obtained from Santa Cruz Biotechnology Inc. For loading control, mouse monoclonal anti-GAPDH, used at 1:4000 was from Abcam (ab8245). Pan-actin antibodies purchased from Sigma (A 2066) were used at 1:2000 dilution and β -Tubulin purchased from Santa Cruz (sc-9104) was used at 1:400 dilution. Secondary antibodies for Western blotting (anti-mouse and anti-rabbit immunoglobulin conjugated to horseradish peroxidase) were purchased from BioRad (1:10000).

2.7 Expression of human FGF-2 isoforms by gene transfer

This work was done by Dr. Xin Ma in supervisor's laboratory and is described in detail in Santiago *et al.*, 2014 (*PLoS One*) and in (Jiang *et al.*, 2007).

2.8 Isolation of anti-human Hi-FGF-2 antibodies by affinity chromatography

This work was done by Dr. Xin Ma in supervisor's laboratory and is described in detail in Santiago *et al.*, 2014 (*PLoS One*).

2.9 Immunoprecipitation with anti-human Hi-FGF-2 antibodies

This was done in collaboration with Dr. Xin Ma in supervisor's laboratory. Human embryonic cardiac fibroblasts (obtained commercially from Cell Applications Inc.), grown to confluency, were scraped and sonicated briefly into RIPA buffer (150 mM NaCl, 1% (v/v) NP-40, 0.25% (w/v) deoxycholate, 0.1% (w/v) SDS, 50 mM Tris-HCl pH 8.0, 1 mM EGTA, 1 mM EDTA, 1 mM Na₃VO₄),

supplemented with protease inhibitors. For immunoprecipitation, 900 μg total extract protein were pre-absorbed with protein A-Sepharose (GE Health care), and then incubated with 9 μg of either purified anti-Hi-FGF-2 IgG, or non-specific IgG. Immunocomplexes were collected with 40 μL protein A-Sepharose slurry, washed extensively with RIPA buffer, and eluted by boiling into twice-concentrated SDS/PAGE sample buffer.

2.10 Cell treatments

Confluent cardiac fibroblasts were placed for 24 h in Ham's F-10 medium supplemented with 0.5% foetal bovine serum (FBS) and 10 $\mu\text{g}/\text{mL}$ each of insulin, transferrin, and selenium; 20 $\mu\text{g}/\text{mL}$ ascorbic acid; and 0.2% bovine serum albumin (BSA). Cells were then subjected to various treatments such as Angiotensin II in the presence or absence of Losartan, PD123319, YVAD, U0126, and MMP2i for 24 h unless stated otherwise. For measurements of cell injury during treatments, lactic dehydrogenase activity (LDH) was measured using a commercially available kit, as described in the manufacturer's instruction manual (Roche Diagnostics). Briefly, 200 μL of reaction mixture was added to 100 μL of sample (in triplicate) using a 96-well plate and incubated for 30 minutes at room temperature in the dark. Standard concentration of LDH was included to determine the amount of LDH release. Quantification of LDH release was done by colorimetric assay at 490 nm.

2.11 High salt elution of extracellular, cell associated human FGF-2

After aspiration of conditioned medium, rat or human myofibroblasts were gently washed with 2 mL (per 100 mm dish) of 2 M NaCl in 10 mM Tris-HCl, pH 7.2 (Khalil *et al.*, 2005), supplemented with 0.5% BSA. High salt washes were diluted to 0.5M NaCl with 10 mM Tris-HCl pH 7.2 supplemented with PIC, before being used to obtain the heparin-bound fraction. High salt or phosphate-buffered saline (PBS) -'washed' cells were scraped and sonicated into SDS/PAGE sample buffer supplemented with protease inhibitor cocktail (PIC: 1 mM PMSF, 5 µg/mL pepstatin, and 5 µg/mL leupeptin).

2.12 Heparin–Sepharose fractions

Conditioned media (pooled; 30 – 60 mL, as indicated), or the high salt washes (pooled; 6 mL), were either brought up to or diluted down to 0.5 M NaCl in the presence of 10 mM Tris-HCl (pH 7.2) with PIC. Pericardial fluid (0.5 mL) was diluted to 10 mg protein/mL and made up to 0.6 M NaCl before incubation with heparin-Sepharose. Each sample was incubated with a heparin–Sepharose CL-6B slurry (100 µL unpacked beads) and left at room temperature for 2 h with gentle agitation. Sepharose beads were pelleted and washed with PIC-supplemented PBS. Washed pellets were boiled in 35 µL of 2x SDS/PAGE sample buffer (final concentration: 125 mmol/L Tris-HCl pH 6.8, 2% SDS, 20% glycerol, 0.010% bromophenol blue, 10% β-mercaptoethanol) to elute heparin-bound proteins which were analysed by Western blotting.

2.13 Tissue/cell extraction for analysis by Western blotting

Total protein extraction from cardiac tissue or cells was performed as we previously described (Srisakuldee *et al.*, 2009). All buffers were supplemented with protease inhibitor cocktail (PIC) as well as phosphatase inhibitor cocktails (PPIC II, IV). For FGF-2 detection by Western blotting, tissue or cell lysates, at respectively, 50-100 or 10-50 μg protein/lane, were analyzed in 15% SDS/PAGE gels. Protein concentrations were measured using BCA assay (Bicinchoninic acid; Sigma). Antigen-antibody complexes were developed and visualized on film by chemiluminescence using ECL Plus (Amersham BioSciences).

2.14 Western blotting

Cell lysates (10-50 μg protein/lane), or proteins eluted from heparin-Sepharose beads were analyzed in 15% SDS-PAGE gels, followed by transfer to 0.45 μM polyvinylidene difluoride (Roche) as we described (Sun *et al.*, 2001; Hirst *et al.*, 2003). With constant agitation, the membranes were blocked in a TBS-T solution containing 10% dried non-fat (skim) milk powder for a period of 1 hour at room temperature. The blots were then incubated with primary antibody in 1% non-fat skim milk powder in TBS-T overnight at 4°C or for one hour at room temperature. Then the membranes were washed again for 15 minutes once, followed by 3 washes for 5 minutes at room temperature. Secondary antibody in TBS-T containing 1% skim milk was applied and incubated for 1 hour at room temperature. Following the secondary antibody, the membranes were washed in TBS-T only. Protein bands on Western blots were visualized by ECL Plus (Amersham BioSciences) according to the manufacturer's instructions, and

developed on film. Blots were stripped and re-probed with anti-GAPDH, pan-actin, and β -tubulin antibodies or stained for Ponceau Red to confirm even protein loading.

2.15 Hypertrophy *in vitro*

Cell surface area of neonatal cardiac myocytes was determined as in (Jiang *et al.*, 2007). Conditioned medium from Ang II treated rat or human cardiac myofibroblasts was collected under sterile conditions and used to stimulate neonatal cardiomyocyte hypertrophy. Neonatal cardiac myocytes were plated on collagen-coated coverslips at 10^5 cells/35 mm dish in the presence of 10% FBS. The next day cells were switched to a low-serum (0.5% FBS) medium for 24 h. They were then subjected to various treatments for 48 h. These included incubation with non-conditioned or conditioned medium obtained from Ang II (10^{-6} M)-stimulated myofibroblasts, supplemented with either anti-FGF-2 neutralizing antibodies (10 μ g/mL) or neutralizing antibodies to human Hi-FGF-2 (20 μ g/mL) or generic mouse IgG (10 μ g/mL); direct stimulation with Ang II (10^{-6} M) or Hi-FGF-2 (10 ng/mL). At the end of the experiment cells were fixed in 4% paraformaldehyde in PBS for 15 minutes, rinsed, and then permeabilized with 0.1% Triton-X-100 in PBS for another 15 minutes. After rinsing with chilled PBS, cells were incubated with anti-N-Cadherin (Sigma; sc-7939) and anti- α -Actinin (Sigma; A-5044) at 1:100 and 1:500 dilutions, respectively, in PBS containing 1% BSA overnight. Coverslips were washed in PBS and then incubated with secondary antibodies for immunofluorescence for 90 minutes at room

temperature. After rinsing sections were mounted with ProLong Gold antifade reagent (Invitrogen; P36931) and observed in a Zeiss LSM 5 fluorescence microscope. Cell surface area was measured by morphometry using NIH ImageJ program. A total of n=320-660 cells, from randomly selected, non-overlapping visual fields, were measured per group.

Protein synthesis (^3H -leucine incorporation) was determined as previously described (Jiang *et al.*, 2007). Briefly, cardiomyocyte in 35 mm dishes (n=5 dishes/group) were placed in leucine-free media that had been conditioned by either Ang II-stimulated, or non-stimulated human cardiac myofibroblasts, incubated in the presence or absence of neu-Ab^{Hi-FGF-2} (20 $\mu\text{g}/\text{mL}$) and followed by addition of ^3H -leucine (5 $\mu\text{Ci}/\text{well}$). Cells were processed for scintillation counting 24 h later.

2.16 qRT-PCR

Analysis of brain natriuretic peptide (BNP) and cardiac β -myosin heavy chain (MHC) gene expression were done in collaboration with Dr. Hope Anderson (CCARM, St. Boniface Research Centre). Total RNA was isolated from neonatal rat cardiac myocytes using RNase RNA kit (Qiagen). First-strand cDNA was synthesized from 1 μg of RNA sample with oligo(dT) primers using Moloney murine leukemia virus reverse transcriptase (Invitrogen). The real-time PCR primers for rat BNP were 5'-CAGCTCTCAAAGGACCAAGG-3' and 5'-CGATCCGGTCTATCTTCTGC-3'. The primers for β -MHC were 5'-CAGCTCTCAAAGGACCAAGG-3' and 5'-CGATCCGGTCTATCTTCTGC-3'. The

primers for rat GAPDH were 5'-CTCATGACCACAGTCCATGC-3' and 5'-TTCAGCTCTGGGATGACCTT-3' (Sigma). The total volume of each reaction was 50 μ L, including 25 μ L iQ SYBR Green Supermix (Bio-Rad), 1 μ L of each primer and 2 μ L of DNA template. Amplification was performed at 95°C at 5min followed by 42 cycles of 95°C for 30s, 57°C for 30' and 72°C for 30s. The relative change in BNP mRNA expression was determined by the fold change analysis in which the degree of change= $2^{-\Delta\Delta Ct}$, where $Ct=(Ct_{BNP} - Ct_{GAPDH})_{treatment} - (Ct_{BNP} - Ct_{GAPDH})_{control}$. Ct was the cycle number at which the fluorescence signal crossed the threshold, which was determined by iQ5 Optical System software (version 2; Bio-Rad). The same equation was applied for β -MHC.

2.17 Immunolocalization

Immunohistochemistry of paraffin sections (4 μ m) of human atrial tissue samples were used for immunohistochemical detection of human Hi-FGF-2, as described in (Wu *et al.*, 2007). The Vectastain® ABC kit (rabbit IgG) from Vector laboratories was used. Sections were incubated with anti-human-Hi-FGF-2 rabbit polyclonal antibodies (20 μ g/mL in blocking solution), followed by horseradish peroxidase (HRP)-labeled secondary antibodies and diaminobenzidine (Sigma). Sections were counterstained with haematoxylin (Vector Laboratories Inc.). Atrial tissue paraffin sections were also subjected to immunofluorescence, following de-paraffinization with successive washes in xylene, and decreasing concentrations of ethanol. Antigen-unmasking of sections was achieved by

immersion in 1:100 dilution of 'antigen unmasking solution' (Vector Laboratories, H-3300), as per manufacturer's instructions. Tissue sections were also treated with the autofluorescence eliminator reagent as per manufacturer's instructions (Millipore). Immunofluorescence of cells in culture was done exactly as we described previously (Doble *et al.*, 2004; Ma *et al.*, 2007).

2.18 Secretome analysis by LC-MS/MS

This work was done in collaboration with Dr. Vincent Chen (UBC) who conducted the MS/MS analysis. Conditioned media used for secretome analysis were obtained as follows. Neonatal rat cardiac myofibroblasts in 3x15cm plates were grown to 80-90% confluency followed by incubation in serum-free medium in the absence or presence of 10 ng/mL of recombinant rat Hi- or Lo-FGF-2 for 24 h. Conditioned media were collected in 50mL tubes supplemented with broad-spectrum protease inhibitors (CompleteTM, Roche), ice chilled, and subjected to centrifugation (1000 rpm) for debris removal. The supernatants were used to obtain protein precipitates by adding 1:4 (v/v) of concentrated aqueous trichloroacetic acid (1:1 w/w TCA: water, Thermofisher Scientific), followed by centrifugation (14,000 rpm, 5 min, 4°C) and protein pellet collection. Supernatants were discarded and proteins neutralized by repeated acetone washes (2 x 10mL). Isolated pellets were air dried and stored at -80°C prior to processing for HPLC-MS measurement and fragmentation analysis. Here, protein pellets were resuspended in 200 µL of 1% deoxycholate in 50 mM ammonium bicarbonate (pH 8.0), and heated for 5 mins at 100°C.

Concentrations of each of these samples were determined by BCA (Pierce) and normalized (absolute amount and concentration) prior to reduction/alkylation (DTT, iodoacetamide) and digestion (trypsin, 50:1 w/w %, Promega, sequence grade, 16 h, 37°C). The following day, digestion was halted and samples were acidified with 50 µL of aqueous HPLC sample buffer (1% trifluoroacetic acid, 0.5% acetic acid) followed by a brief centrifugation to remove precipitated deoxycholic acid. Samples then underwent solid phase extraction (SPE) using C18 stage-tip backfilled with 5 µL of chromatographic support (Bakerbond C18, JT baker). Isolated peptides were then vacuum dried (Savant, Speed-vac) and samples originating from control, Lo-, and Hi-FGF-2 were respectively encoded by covalent modification (a.k.a. peptide dimethylation) using either light, medium and heavy isotopologues of formaldehyde (CH₂O, CD₂O, ¹³CD₂O Cambridge Isotopes, >98% purity), in the presence of deuterated (>99%) cyanoborohydride or reagent of natural isotopic abundance (Sigma) as previously described (Chen *et al.*, 2012). Light, medium and heavy-modified peptides within each replicate set were then thoroughly mixed and subjected to a second round of SPE prior to nanoflow HPLC separation using Agilent 1100 series chromatograph housing a autosampler & chiller (4°C) that were interfaced to an LTQ-OrbitrapXL mass spectrometer (ThermoFisher, Bremen, Germany) via a Proxeon/ThermoFisher nanospray source. Methods for data handling, protein, identification, and searches were conducted using rat IPI v.3.68 using a false-discover cut off 1% and 2 or more peptides. Relative quantifications were achieved by integrating extracted ion chromatograms using the MaxQuant software package as

previously described (Chen *et al.*, 2012). Proteins and ratios reported are the average of 3 biological replicates and qualified for reporting only after observations were made 2 or more times.

2.19 Zymography

As in (Wu *et al.*, 2007). Briefly, hMF conditioned medium (2 mL) was concentrated to 0.1 mL with Nanosep 10K Omega concentrators (PALL). Concentrated conditioned medium (20 μ L) was mixed with sample buffer containing 20% glycerol, 4% SDS, 0.13 M Tris-HCl, pH 6.8, and resolved on a 7.5% polyacrylamide gel containing 1 mg/mL porcine gelatin (Sigma). Purified human MMP-2 (Chemicon) was used as a positive control. After electrophoresis, gels were washed twice with 2.5% Triton X-100 for 30 min at room temperature to remove SDS, and placed in 50 mM Tris-HCl, 5 mM CaCl₂, 0.2 M NaCl, pH 7.6, at 37°C for 48 h. Gels were then stained with Coomassie blue and de-stained with 40% methanol and 10% acetic acid.

2.20 Statistical analysis

Densitometric quantitation of each Western blot band was done using Quantity One 1-D Analysis Software, connected to a GS-800 Calibrated Densitometer. Values were expressed as means \pm SEM; n = 3 (for Western blot analyses). Statistical comparisons between two groups was done using t-test. One-way analysis of variance (ANOVA) followed by the Tukey–Kramer multiple comparisons test was used for comparing differences among multiple groups,

with GraphPad InStat 3.0. Two-way ANOVA followed by the Holm–Sidak comparison test (SigmaStat 3.5) was also used. Differences among groups were defined as significant at $P < 0.05$.

3.1 Production of Hi-FGF-2 by rat cardiac myofibroblasts

Please note that we have used a dual listing system for the Figures. The first listing (Figures 1,2, etc.) numbers Figures as they appear in this thesis. The second listing represents the corresponding Figure number within the published manuscripts (Manuscript 1; Santiago *et al.*, 2011 and Manuscript 2; Santiago *et al.*, 2014). For example, Figure 1 in this thesis is described as Figure 1/M1-Fig.1A. In this section, cardiac myofibroblasts are referred to as CNMs (cardiac non-myocytes) (and cardiac myocytes as CMs, otherwise the type of cells are stated

3.1.1 FGF-2 isoforms in cardiac cells

Relative content of Hi- and Lo-FGF-2 isoforms was determined in cardiac myofibroblasts and myocytes. Myofibroblasts accumulated predominantly (93% of total) Hi-FGF-2 (as 22 and 23 kDa immunoreactive bands), products of translation of the rat mRNA from CUG sites (Sorensen *et al.*, 2006; Liao *et al.*, 2009). The 18 kDa Lo-FGF-2, translated from the AUG start codon, was also detected (Figure 1/M1-Fig.1A). We have shown (Santiago *et al.*, 2011), that the antibodies used here strongly recognize our positive controls (recombinant Hi- and Lo-FGF-2) and detect no other band in total cell lysates.

Cardiac myofibroblasts accumulated significantly higher (approximately five-fold) levels of Hi-FGF-2 per μg extracted protein compared to myocytes and

there was also a significant difference between Lo-FGF-2 levels for the two cell types but to a significantly lesser extent than Hi-FGF-2, Figure 1/M1-Fig.1. The distinct identity of myofibroblasts versus myocyte cultures, as judged by expression of cell-type-specific markers, is illustrated in Figure 1/M1-Fig.1B. Cardiomyocytes express cardiac myofibrillar proteins troponin-T (TnT) and striated myosin, whereas myofibroblasts (but not myocytes) express extra-domain A (EDA)-Fibronectin. Vimentin was more prominently expressed by myofibroblasts but was also present in immature myocytes, as previously shown (Kim, 1996). Lysates from adult heart myofibroblasts, but not adult cardiomyocytes, elicited a strong anti-FGF-2 signal, composed mainly of Hi-FGF-2 (Figure 2/M1-Fig.2A). In adult heart (ventricle)-derived tissue sections, strong anti-FGF-2 staining was observed mainly in association with the cardiomyocyte periphery and with non-myocytes located in the vicinity of cardiomyocytes (Figure 2/M1-Fig.2B). These non-myocytes stained positive for vimentin, indicating that they were, for the most part, fibroblasts.

3.1.2 Hi-FGF-2 export and caspase-1

We asked whether Hi-FGF-2 export by cardiac myofibroblasts would be affected by caspase-1, as reported recently for several unconventionally secreted proteins including 'FGF-2' of undetermined isoform composition (Keller *et al.*, 2008). We have recently shown that Ang II significantly increases relative levels of exported Hi-FGF-2 (Santiago *et al.*, 2011). We therefore examined the effect of YVAD, a caspase-1 inhibitor, on baseline and Ang II-stimulated Hi-FGF-2

present in the extracellular pools including conditioned medium and in association with the extracellular surface and matrix. As shown in Figure 3/M1-Fig.6A, the Ang II-induced Hi-FGF-2 increase in conditioned medium was prevented in cells treated with YVAD. This experiment was done twice with similar results. YVAD prevented the Ang II-induced Hi-FGF-2 up-regulation in the 2M NaCl wash of the cell monolayer, which contains FGF-2 from the cell surface/matrix (Figure 3/M1-Fig.6B). This experiment was done twice with similar results. YVAD had no significant effect on the Ang II-induced up-regulation in total (intracellular and cell-bound) cell-extracted Hi-FGF-2 (Figure 3/M1-Fig.6C).

3.1.3 Secreted rat Hi-FGF-2 is pro-hypertrophic

Conditioned medium from Ang II-treated cardiac myofibroblasts (*Medium), which contains secreted Hi-FGF-2, promoted a significant 20% increase in cardiomyocyte cell surface area, compared with cells incubated with non-conditioned medium (Medium; Figure 4/M1-Fig.7 A and B). This increase was completely abolished by treatment with anti-FGF-2-neutralizing antibodies, indicating that Hi-FGF-2, secreted by fibroblasts, played a major role in the pro-hypertrophic effect (Figure 4/M1-Fig.7 A and B). The pro-hypertrophic effect of *Medium was not due to residual Ang II. Direct stimulation of cardiomyocytes with Ang II elicited, compared with unstimulated cells, a small 7.5% increase in cell size which was significantly less potent than that of *Medium. Interestingly, the direct effect of Ang II on cardiomyocyte size was not altered in the presence of anti-FGF-2-neutralizing antibodies. Direct stimulation with recombinant rat Hi-

FGF-2 (10 ng/mL) elicited a 27% increase in cell size compared with unstimulated cells, confirming its pro-hypertrophic effect (Jiang *et al.*, 2007).

Cardiac hypertrophy is characterized by increased expression of the genes for brain natriuretic peptide (BNP) and β -myosin heavy chain (β -MHC) (Krenz *et al.*, 2004; Mahadavan *et al.*, 2014). We compared the effects of recombinant rat Hi- or Lo-FGF-2 on the expression of these genes in neonatal cardiomyocytes. Recombinant Hi-FGF-2 but not Lo-FGF-2 stimulated a significant increase in expression of BNP when compared to unstimulated cardiomyocytes. Although not statistically significant, we have also observed a trend towards increased β -MHC expression as well in the Hi-FGF-2-stimulated cells (Figure 5).

To validate our findings from neonatal cardiomyocytes in the adult rat ventricular cardiomyocyte model, these cells were stimulated with recombinant Hi- and Lo-FGF-2 and their size measured morphometrically one day later. Each group (control, Hi-FGF-2-stimulated, Lo-FGF-2-stimulated) consisted of myocytes in 3x35 mm plates. The size of 200 myocytes per plates was measured and results from each individual plate are shown in Figure 6. The size of myocytes in all plates treated with Hi-FGF-2 (but not Lo-FGF-2) was significantly larger than the size of myocytes in any of the control plates.

3.1.4 Autocrine effects of Hi-FGF-2

Very little is known about potential autocrine effects of extracellular-acting Hi-FGF-2 on cardiac fibroblasts. Previous studies in my supervisor's laboratory

indicated that Hi-FGF-2 upregulated expression of cardiotrophin-1, a cytokine belonging to the interleukin-6 family, in cardiac fibroblasts but not myocytes (Jiang *et al.*, 2007). This suggested that Hi-FGF-2 may have distinct effects on the secretome profile of myofibroblasts. As a first step in addressing this issue, we used LC-MS/MS proteomics analysis of proteins secreted by myofibroblasts in response to Hi- or Lo-FGF-2 stimulation. As shown in the thermal map of Figure 7, the secretome profile in response to Hi-FGF-2 was quite different to that by Lo-FGF-2 in regards to several proteins. The MS/MS data suggested that Hi-FGF-2 was more potent, compared to Lo-FGF-2, in stimulating secretion of several extracellular matrix-associated proteins including periostin, tenascin, plasminogen activator inhibitor-1 (PAI-1), and follistatin-like protein 1 (FSTL-1). Our preliminary secretome data led us to examine further these top four most abundant extracellular matrix proteins.

To validate the MS/MS data, we used Western blot-based detection of the above mentioned extracellular matrix proteins in conditioned media (Figure 8) and cell lysates (Figure 9) from rat neonatal fibroblasts stimulated with Hi- or Lo-FGF-2. Western blotting of conditioned media showed that Hi-FGF-2 elicited robust up-regulation of secreted periostin (Figure 8A), PAI-1 (Figure 8B), FSTL 1 (Figure 8C) and tenascin C (Figure 8D), compared to unstimulated cells. Lo-FGF-2 elicited no changes compared to unstimulated cells. These data agree with the MS/MS data.

Cardiac myofibroblast lysates were examined for cell-associated accumulation of the above extracellular matrix proteins. Western blotting of total cell

lysates showed that Hi-FGF-2 elicited a significant increase in the accumulation of periostin (Figure 9A), PAI-1 (Figure 9B), tenascin C (Figure 9D), but not FSTL1 (Figure 9C) compared to controls. Lo-FGF-2 also stimulated significant cell-associated periostin accumulation, but had no effect on the other matricellular proteins.

The effect of endogenous expression of exclusively Hi- or Lo-FGF-2 on cell-associated accumulation of matricellular proteins was examined. We used primary mouse embryonic fibroblasts (MEFs) isolated from mice lacking all FGF-2 isoforms (K01), and from mice expressing only Hi-FGF-2 (K02), or only Lo-FGF-2 (K03); these mice have been described in (Schultz *et al.*, 1999; Azhar *et al.*, 2009; Nusayr *et al.*, 2013). Results are shown in Figure 10. Of the four matricellular proteins examined in the preceding studies, the expression of only periostin was significantly elevated in K02 MEFs as compared to either K01 or K03 (Figure 10A).

We next examined if endogenous expression of exclusively Hi- or Lo-FGF-2 would affect the myofibroblast phenotype in MEFs, assessed by expression of specific protein markers such as α -SMA, procollagen 1, SMemb, and EDA-Fibronectin; Figure 11. Accumulation of α -SMA did not differ between MEFs from K01, K02 or K03 mice; Figure 11A. Procollagen 1 was significantly elevated in the K02 MEFs compared to the other groups; Figure 11B. Relative SMemb levels were significantly higher in the K01-derived MEFs, compared to the K02- or K03-MEFs; Figure 11C. Finally, relative EDA-Fibronectin levels were significantly higher in the K02-derived MEFs compared to the other groups; Figure 11D.

Thus exclusive endogenous expression of Hi-FGF-2 (in the K02-derived MEFs) upregulated two (out of four) protein markers associated with the myofibroblast phenotype.

Figure 1

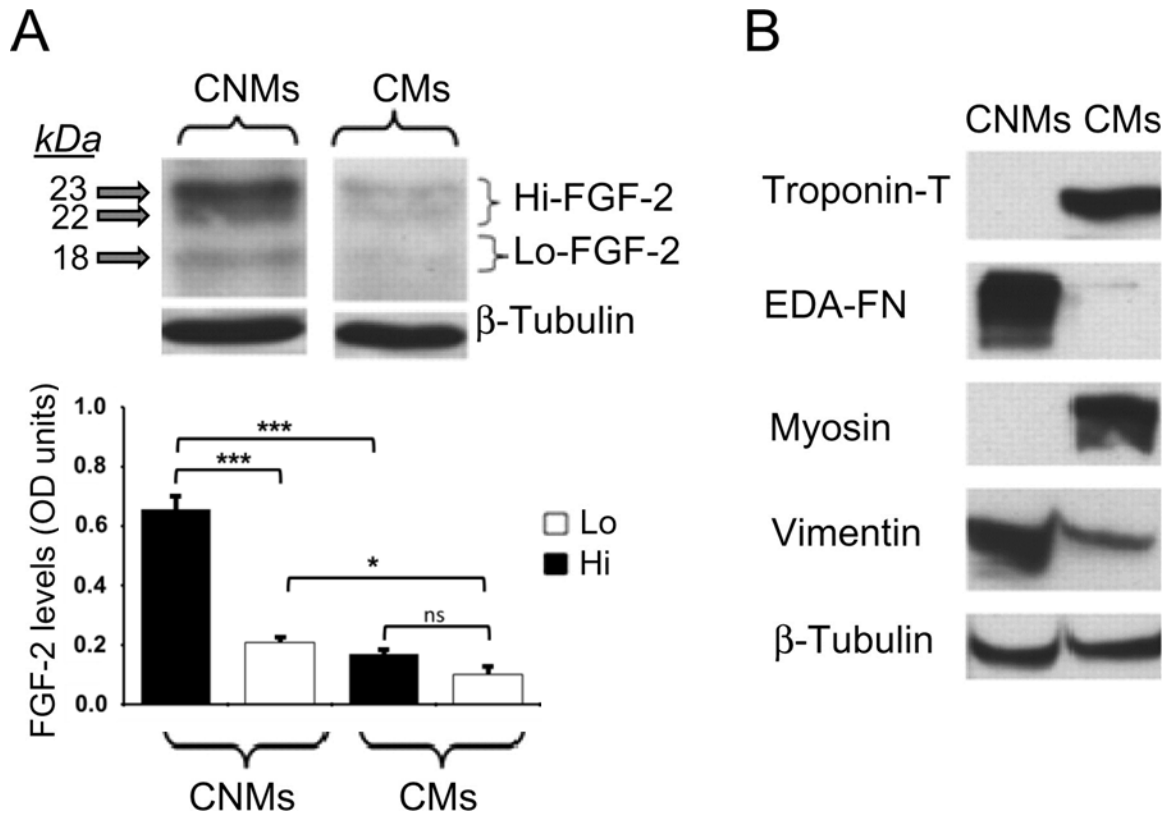


Figure 1. Expression of Hi-FGF-2 by neonatal heart-derived non-myocytes (CNMs, or myofibroblasts) and cardiomyocytes (CMs). (A) Representative Western blot probed for FGF-2 and corresponding quantitative data for relative Hi- and Lo-FGF-2 levels (as indicated, in black or white columns, respectively) in lysates (50 μ g/lane) from CNMs and CMs ($n = 3$). Brackets point to comparisons between groups. *** $P < 0.001$; NS, non-significant. (B) Representative ($n = 2$) Western blot images showing appropriate expression of cell-specific markers in CMs and CNMs, as indicated. TnT, cardiac troponin T; EDA-FN, extra-domain A fibronectin; myosin, striated muscle myosin. Reactivity for β -tubulin is used to indicate even protein loading. This Figure is the same as Fig.1 in M1

Figure 2/M1-Fig.2

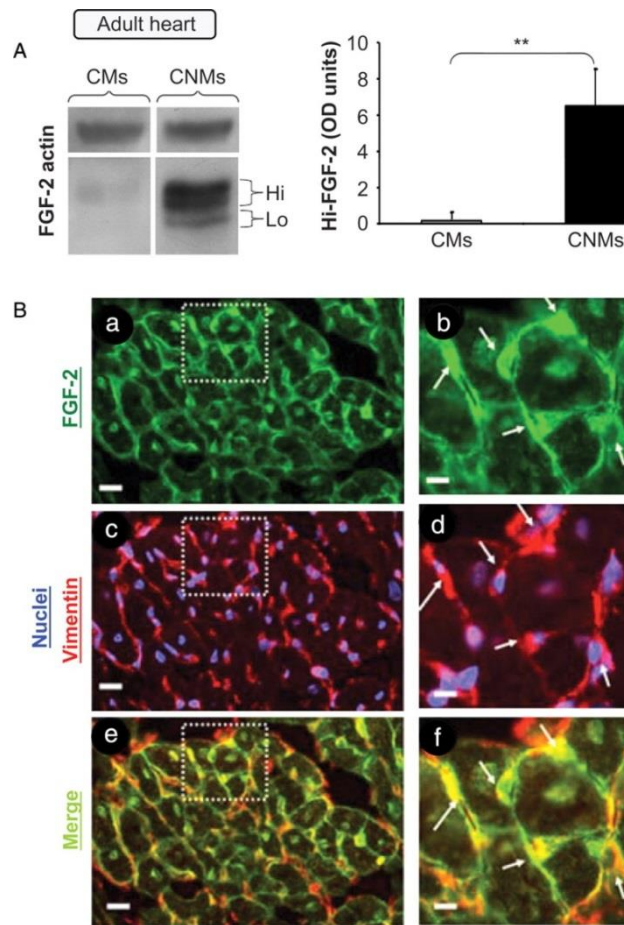


Figure 2/M1-Fig.2. Expression of FGF-2 by adult heart cells. (A) *In vitro*: representative Western blot probed for FGF-2 and corresponding quantitative data for relative Hi-FGF-2 levels in adult heart-derived CNMs (myofibroblasts) and cardiomyocytes, CMs. **** $P < 0.01$ ($n = 3$).** **(B) *In vivo*:** predominant FGF-2 localization in adult rat heart non-myocytes. Adult rat heart ventricular sections were stained for FGF-2 (green), vimentin (red), and nuclei (blue), as indicated. Images a, c, and e show the same field stained for: a, FGF-2; b, vimentin as well as nuclei; and c, FGF-2 and vimentin. The region enclosed within the dotted-line square in a, c, and e is shown at higher magnification in, respectively, b, d, and f. White arrows point at fibroblastic cells (vimentin-positive) surrounding CMs. Sizing bars in a, c, and e or b, d, and f correspond to 50 or 20 μ M, respectively.

Figure 3/M1-Fig.6

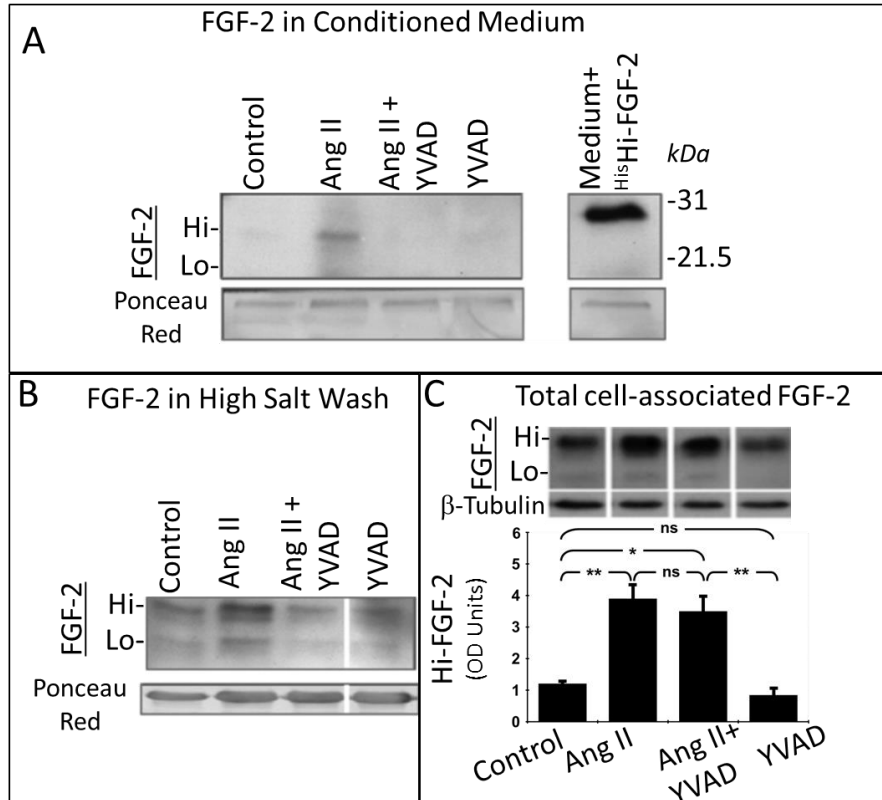


Figure 3/M1-Fig.6. Caspase-1 inhibition prevents Hi-FGF-2 export. (A) YVAD prevents Hi-FGF-2 release to the conditioned medium. Representative Western blot of heparin–Sepharose-bound fractions from (pooled; 60 mL per sample) conditioned media derived from unstimulated myofibroblasts (CNMs; Control); CNMs stimulated with 10^{-7} M Ang II in the absence or presence of YVAD (Ang II and Ang II + YVAD, respectively); YVAD alone (YVAD), and probed for FGF-2. Lane labelled ^{His}Hi-FGF-2' shows immunoreactivity of 0.5 ng recombinant ^{His}Hi-FGF-2 used as a positive control. Ponceau Red staining of the same blot (as indicated) shows a protein band present in all heparin–Sepharose fractions in equivalent amounts. **(B)** YVAD down-regulates exported and cell/matrix-bound Hi-FGF-2. Representative Western blot of heparin–Sepharose-bound fractions from 2 M NaCl washes (pooled; 6 mL per sample) of the CNM monolayer following the same treatments as in (A), as indicated, and probed for FGF-2. Ponceau Red staining of the same blot (as indicated) shows a protein band present in all heparin–Sepharose fractions in equivalent amounts. **(C)** YVAD has no effect on the Ang II-induced up-regulation of cell-associated Hi-FGF-2. Representative Western blot and corresponding cumulative data ($n = 3$) of cell lysates from neonatal CNMs treated with Ang II, Ang II plus YVAD, YVAD, and probed for FGF-2 or β -tubulin. Brackets point to comparisons between groups; *, **, and NS denote $P < 0.05$, $P < 0.01$, and $P > 0.05$, respectively.

Figure 4/M1-Fig.7

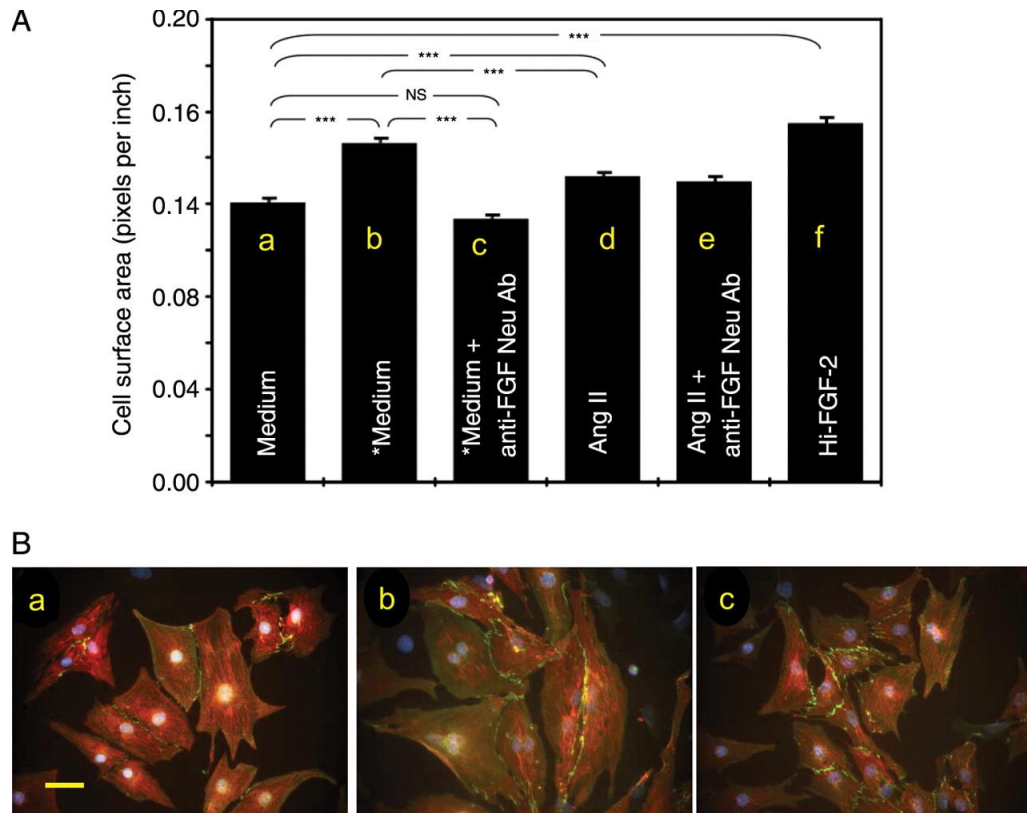
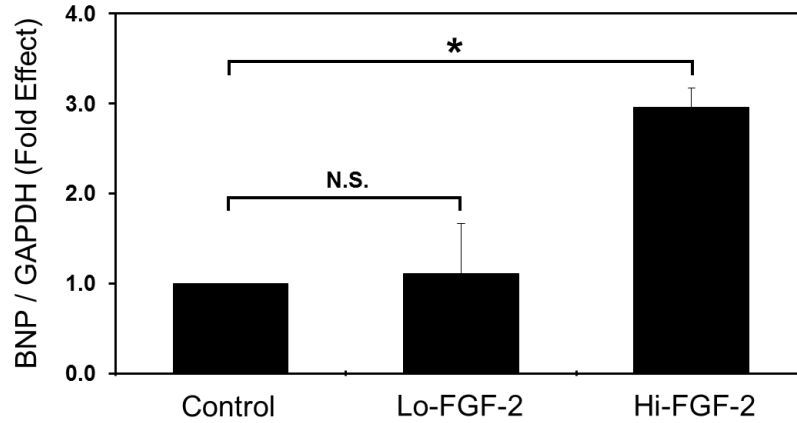


Figure 4/M1-Fig.7. Secreted Hi-FGF-2 is pro-hypertrophic. (A) Cardiomyocyte size (CM; cell surface area) is shown as a function of incubation under several conditions for 2 days: a, 'Medium' (non-conditioned medium); b, '*Medium' (conditioned medium from Ang II-treated neonatal CNMs); c, '*Medium + anti-FGF Neu Abs' (conditioned medium from Ang II-treated CNMs supplemented with 10 $\mu\text{g}/\text{mL}$ anti-FGF-2-neutralizing antibodies); d, 'Ang II' (10^{-7} M Ang II); e, 'Ang II + anti-FGF Neu Abs' (10^{-7} M Ang II + 10 $\mu\text{g}/\text{mL}$ anti-FGF-2-neutralizing antibodies); f, Hi-FGF-2 (10 ng/mL recombinant Hi-FGF-2). Culture media in a, b, d, and f included 10 $\mu\text{g}/\text{mL}$ of mouse IgG. Brackets denote comparisons between groups, where *** is extremely significant ($P < 0.001$); $n = 960$ myocytes/group. **(B)** Representative CM images from the first three groups (a–c) shown in (A). These images cover the full range of myocytes sizes observed in all experimental groups. Myocytes are stained for α -actinin (red), N-cadherin (green), and nuclei (DAPI; blue). Bar corresponds to 50 μM .

Figure 5

A.



B.

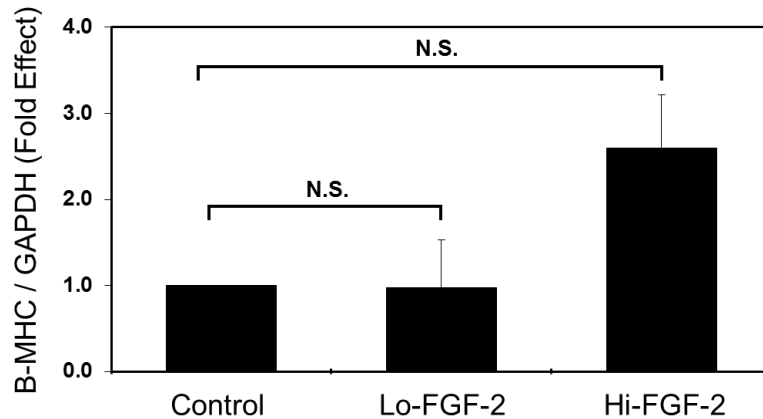


Figure 5. Hi-FGF-2 stimulates expression of BNP in neonatal cardiomyocytes. Rat neonatal cardiomyocytes were kept in medium (no serum) for 24 hours and were treated with Hi- or Lo-FGF-2 at 10 ng per mL for another 24 hours. **Panel (A)** expression of BNP; and **Panel (B)** expression of β -MHC were determined by qRT-PCR. Data were expressed as mean \pm SEM. GAPDH expression was used as a normalizing control. * denotes $P < 0.05$ and NS denotes $P > 0.05$ considered not significant ($n = 3$). A trend towards increasing β -MHC expression is observed upon Hi-FGF-2 treatment.

Figure 6

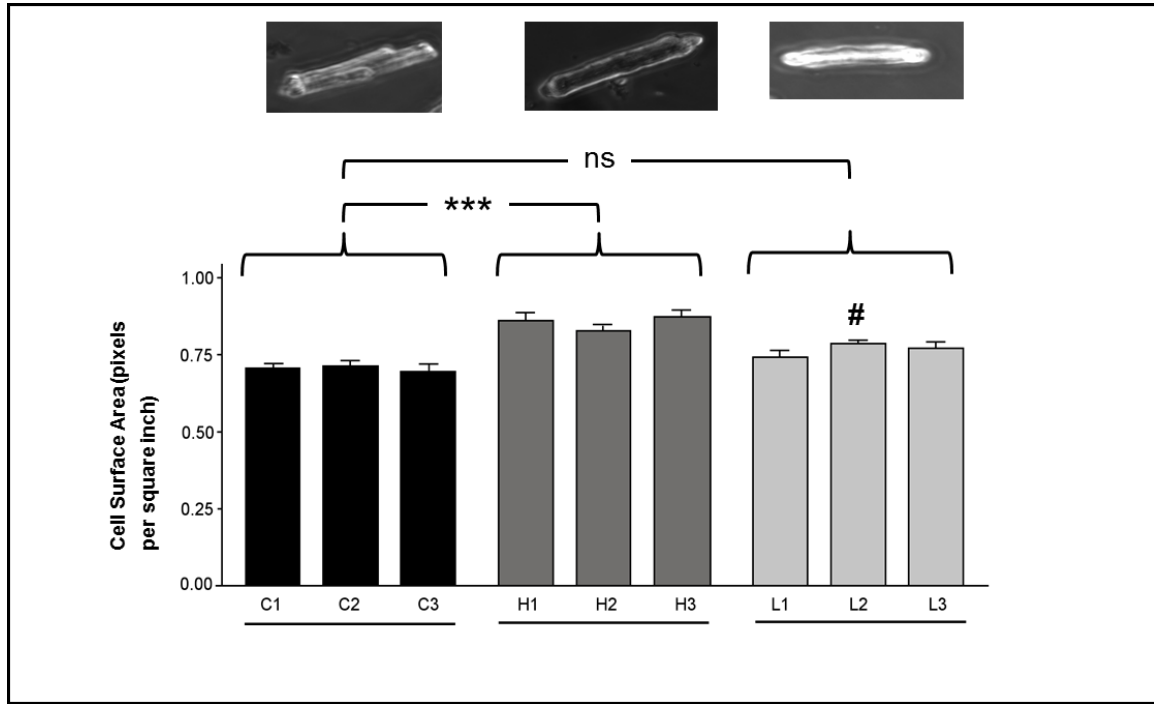


Figure 6: Hi-FGF2 increases adult rat cardiomyocyte cell size Isolated adult rat cardiomyocytes were plated on laminin-coated coverslips (n=3 per treatment) in the presence of serum for 4 h, and then kept in the absence of serum (medium M199) for 24 h. They were then left untreated (controls, C1, C2, C3); treated (10 ng/ml each) with Hi-FGF-2 (H1, H2, H3); or Lo-FGF-2 (L1, L2, L3), for another 24 hours. Cell size (surface area) was measured morphometrically for randomly chosen 200 cells per coverslip, and the mean \pm SEM is shown for each individual coverslip. All Hi-FGF2 (H) values were significantly, ***P<001, higher to all Control (C) values. There were no significant differences between the Lo-FGF2 and Control values with the exception of L2 which was significantly, #P<0.05, higher than C3.

Figure 7

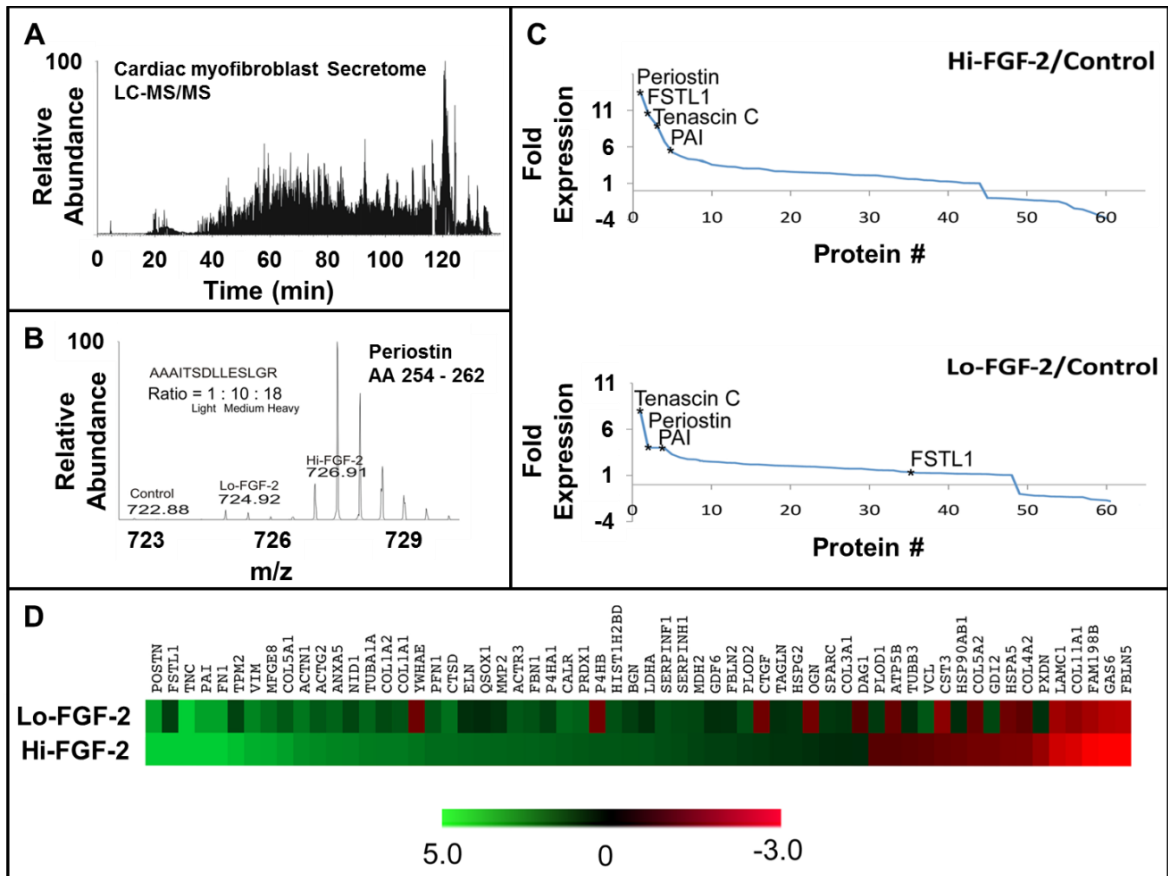


Figure 7. The effect of Hi- and Lo-FGF-2 stimulation on the secretome profile of rat cardiac myofibroblasts analyzed by LC-MS/MS. In collaboration with Dr. Vincent Chen, UBC. **(A)** Total ion chromatogram of dimethylated peptides found within the conditioned media of cultured rat cardiac myofibroblastic cells. **(B)** High-resolution MS scan of triplex dimethylated periostin peptide. Signals originating from control, Lo-FGF-2 and Hi-FGF-2 experimental condition are as indicated. **(C)** Relative expression of periostin, follistatin-like protein-1 (FSTL-1), plasminogen activator inhibitor (PAI or Serpin E1) and tenascin-C show abundance changes with Hi-FGF-2 over control compared to Lo-FGF-2 over control. **(D)** Heat map representation of all proteins derived from these experiments that were found to have similar and differential abundances within the condition media of FGF-2 treated cardiac myofibroblasts. A total of three runs (n=3 per run) were processed, averaged, and analyzed by LC-MS/MS.

Figure 8

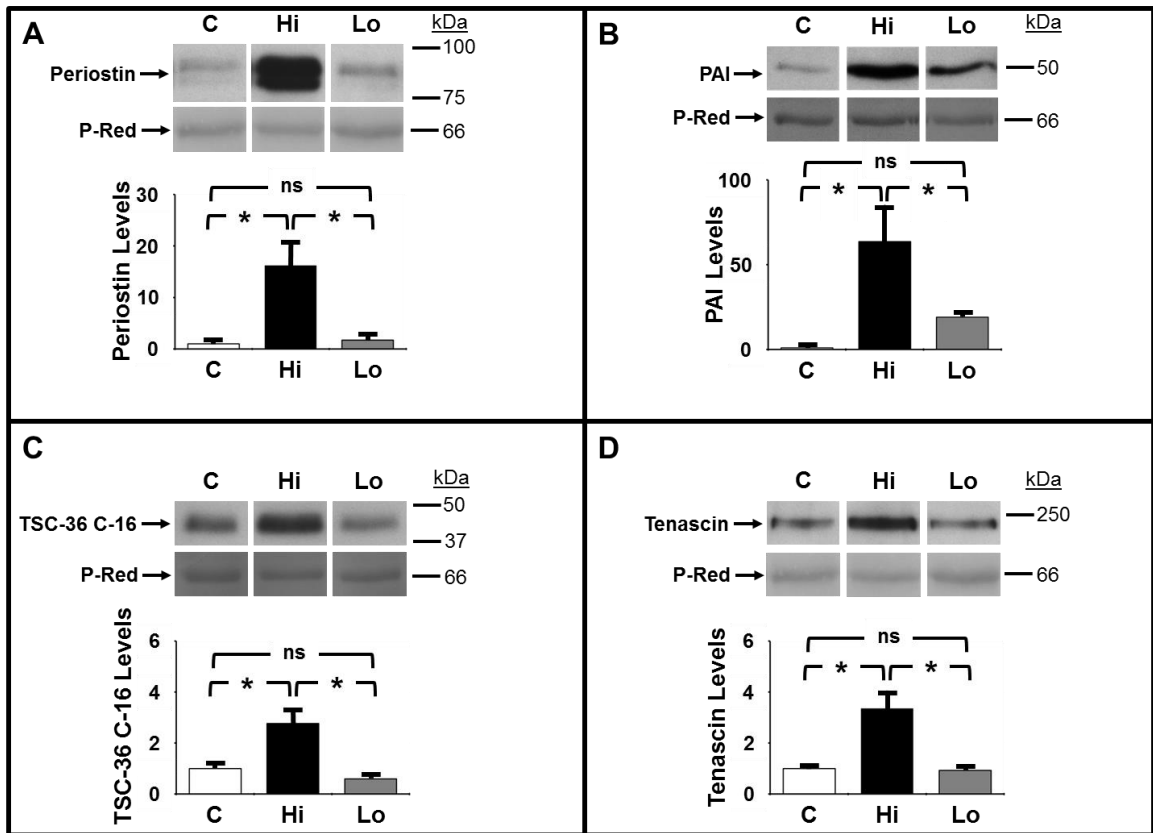


Figure 8. Hi-FGF-2, but not Lo-FGF-2 stimulates significant upregulation of matricellular proteins secreted in conditioned medium by cardiac myofibroblasts. Panels A, B,C and D show representative Western blots, and corresponding quantitative data, for, respectively, periostin, plasminogen activator inhibitor 1 (PAI), follistatin-like protein 1 (FSTL1) and tenascin C. Each lane contains concentrated conditioned medium from neonatal cardiac fibroblasts subjected to no treatment (C, control), treatment with Hi-FGF-2 (Hi) or treatment with Lo-FGF-2 (Lo), as indicated. Ponceau Red staining of an unknown band is used as loading control. NS, and * denotes P>0.05 and P<0.05; where 'C' is Control Group, 'Hi' is Hi-FGF-2 treated group, and 'Lo' is Lo-FGF-2 treated group (n=3 per group).

Figure 9

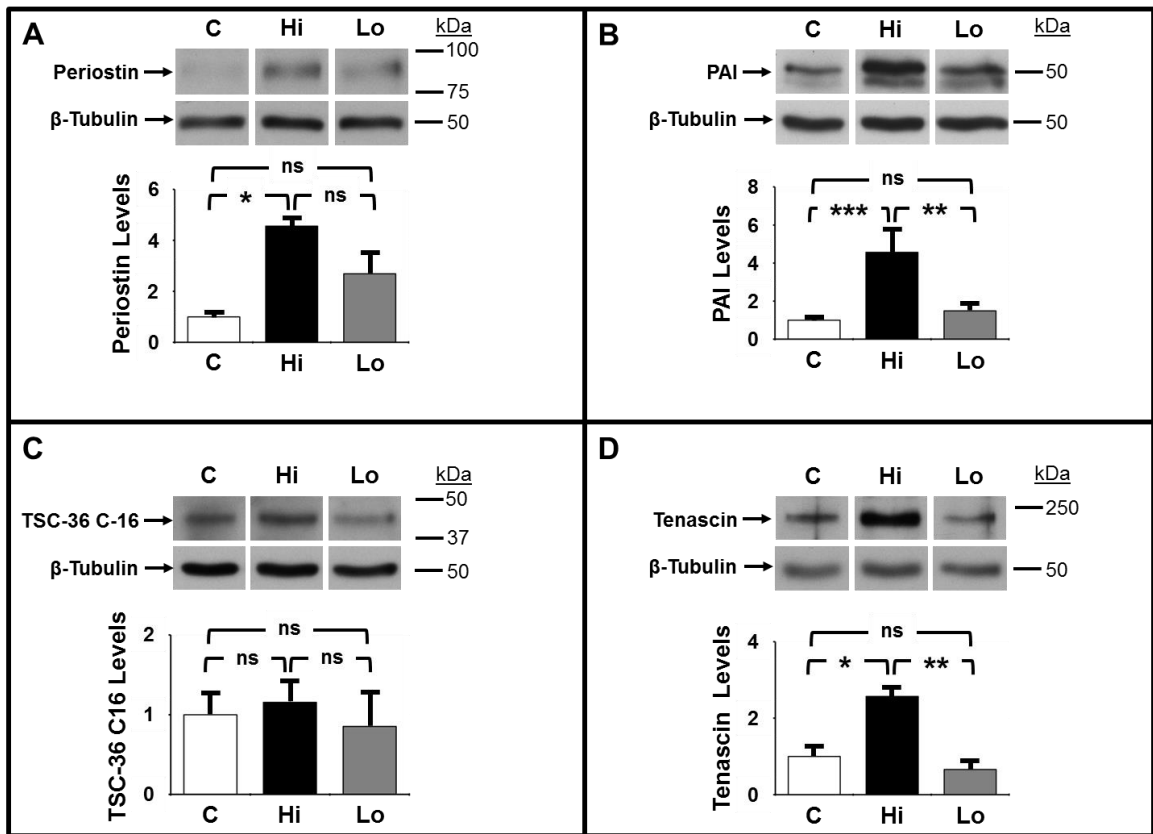


Figure 9. The effect of Hi-FGF-2 versus Lo-FGF-2 stimulation on matricellular protein accumulation in cardiac myofibroblast extracts. Panels A, B, C and D show representative Western blots, and corresponding quantitative data, for, respectively, periostin, PAI, FSTL1 and tenascin C. Each lane contains cell lysate from neonatal cardiac fibroblasts subjected to no treatment (C, control), treatment with Hi-FGF-2 (Hi) or treatment with Lo-FGF-2 (Lo), as indicated. Staining for β tubulin is used as loading control. NS, *, **, * denotes $P > 0.05$, $P < 0.05$, $P < 0.01$, $P < 0.001$; where 'C' is Control Group, 'Hi' is Hi-FGF-2 treated group, and 'Lo' is Lo-FGF-2 treated group (n=3 per group).**

Figure 10

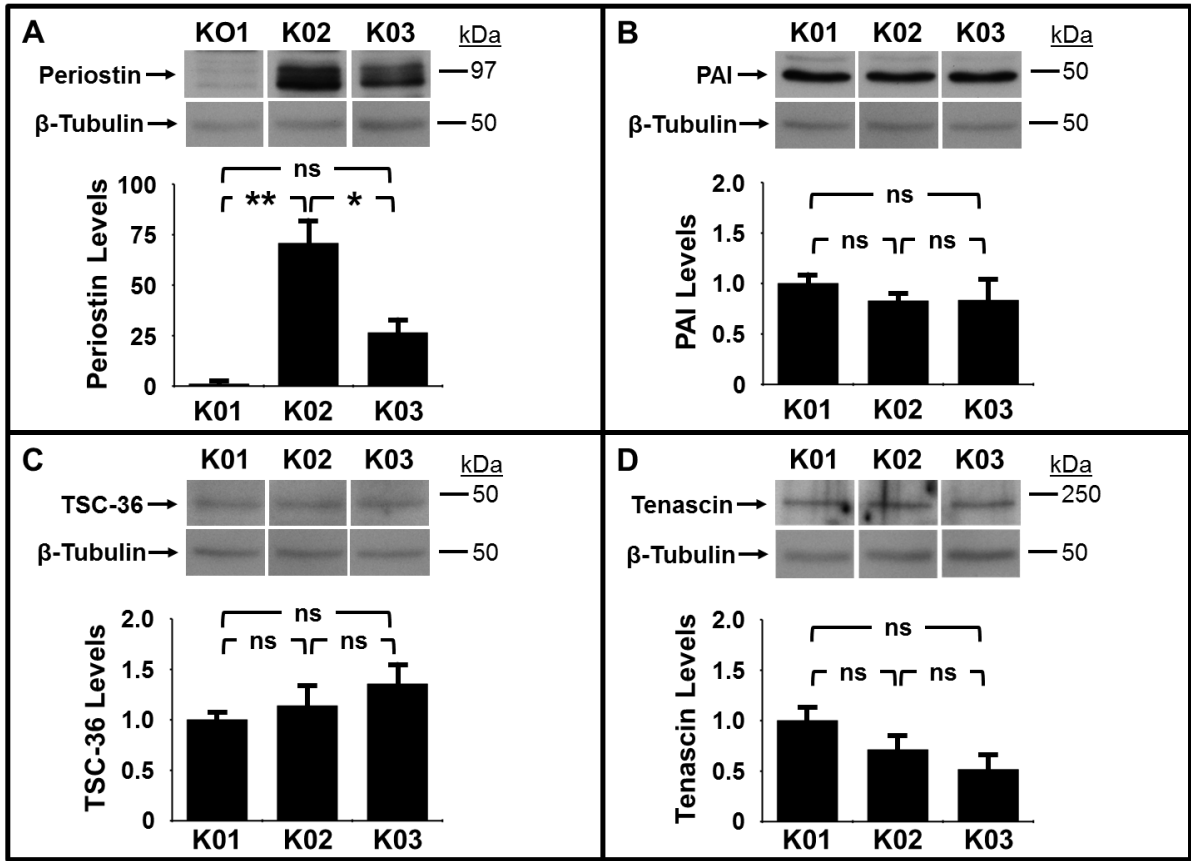


Figure 10. The effect of endogenous expression of Hi- or Lo-FGF-2 on the accumulation of selected matricellular proteins in MEFs. K01-derived MEFs do not express any FGF-2 isoforms. K02 and K03 MEFs express, respectively, only Hi-FGF-2, and only Lo-FGF-2. **Panels A, B, C, D** show relative cell-associated accumulation of, respectively, periostin, PAI, FSTL1, and tenascin C. NS, *, and **, denotes $P > 0.05$, $P < 0.05$, and $P < 0.01$; ($n = 3$ per group). Periostin was significantly upregulated in both K02 and K03 MEFs, but the effect was more pronounced in the K02 cells.

Figure 11

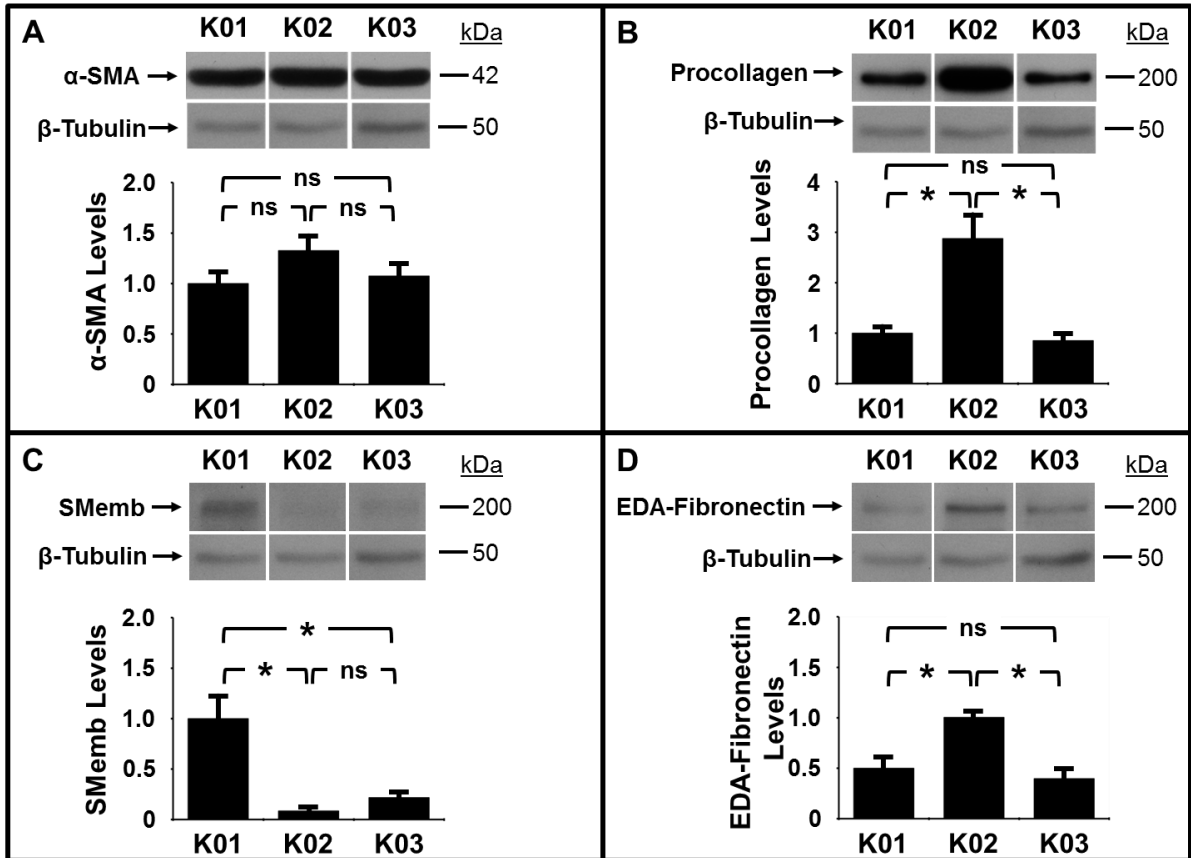


Figure 11. The effect of endogenous expression of Hi- or Lo-FGF-2 on the accumulation of myofibroblast marker proteins by MEFs. K01-derived MEFs do not express any FGF-2 isoforms. K02 and K03 MEFs express, respectively, only Hi-FGF-2, and only Lo-FGF-2. **Panels A, B, C, D** show relative accumulation of, respectively, alpha smooth muscle actin (α -SMA), procollagen I, Smooth muscle embryonic myosin (SMemb) and extra domain A (EDA-) fibronectin. Procollagen and EDA-Fibronectin were significantly higher in K02 MEFs compared to K01, and K03 MEFs. NS, *, and **, denotes $P > 0.05$, $P < 0.05$, and $P < 0.01$; ($n = 3$ per group).

3.2 Expression and role of human Hi-FGF-2

All of the results presented in this section were derived from Manuscript M2 (Santiago *et al.*, 2014). The term hMFs is used to refer to human myofibroblasts. The numbering of figures was changed similar to the previous section; please refer to the List of Figures. Thesis figures are numbered sequentially as they first appear in the text.

3.2.1 Human FGF-2 isoform expression in human cardiac tissue

As a first step towards investigating potential relevance of our findings with rodent heart cells in the adult human heart, we asked if Hi-FGF-2 isoforms were present in the human myocardium. According to the literature, FGF-2, of uncertain isoform composition, is present in mammalian atria and ventricles; relative FGF-2 levels are especially high in atrial tissue (Corda *et al.*, 1997). We therefore used human atrial tissue in order to maximize the ability to detect all FGF-2 isoforms by Western blotting analysis of unfractionated lysates. Use of unfractionated lysates from freshly obtained atrial tissue was crucial in order to prevent partial proteolytic conversion of Hi-FGF-2 isoforms to Lo-FGF-2-like proteins during handling (Doble *et al.*, 1990; Yu *et al.*, 2008). An additional argument in favor of using atrial tissue for these initial studies is that, unlike human ventricular tissue, it was possible for us to obtain a relatively large number of small tissue fragments (n=60) from patients undergoing routine cardiac surgery and thus obtain a more comprehensive picture regarding the relative expression of Hi- versus Lo-FGF-2.

Tissue lysates were analyzed for FGF-2 isoform composition by Western blotting and densitometry. Representative Western blot images labeled as hA1 and hA2, derived from small 15% polyacrylamide gels, are shown in Figure 12A. Immunoreactive bands were detected at 18 kDa (Lo-FGF-2), as well as at 22 and 24 kDa (Hi-FGF-2). The 22 kDa band resolved into a doublet (22 and 22.5 kDa Hi-FGF-2 isoforms) when samples were analyzed in large 15% polyacrylamide gels, and a typical pattern is shown in Figure 12A, labeled as hA3. The 18, 22-22.5 and 24 kDa bands compose, respectively, 47%, 39% and 14 % of total atrial tissue-derived FGF-2 (Figure 12A). Hi-FGF-2 constituted 53% (± 20 SD, n=45) of total tissue FGF-2. Using a recombinant FGF-2 standard curve and densitometry, we estimated that human atrial extracts contained 1.78 (± 0.09 SEM) pg total FGF-2 per μ g of extracted protein. Figure 13 shows a Western blot of recombinant FGF-2 (12.5-200 pg/lane) side-by side with selected representative human atrial extract samples (50 μ g/lane), to illustrate that the intensity of immunoreactive signals in human tissue samples was within range shown by the recombinant FGF-2 samples.

To determine cellular and subcellular distribution of Hi-FGF-2 in human atrial tissue we used immunocytochemistry with affinity-purified anti-human Hi-FGF-2 antibodies. Figure 12 (B, C) shows atrial serial sections incubated in the presence (Figure 12B) or absence (Figure 12C) of anti-Hi-FGF-2 antibodies. Staining of antigen-antibody complexes generated a brown color, while counterstaining with haematoxylin, in Figure 12 (B, C) elicited a blue color, visualizing nuclei. Relatively extensive brown staining was seen only in Figure 12B

consistent with a specific reaction for Hi-FGF-2. Cells present near the epicardium and staining positive for Hi-FGF-2 are indicated by arrows in Figure 12 B. Higher magnification images of the anti-Hi-FGF-2 staining patterns are shown in Figure 12 (D, E). Hi-FGF-2 was localized in both the nuclei (yellow arrows) and cytosol (pink arrows) of atrial cardiomyocytes. Cardiomyocytes were recognized by their relatively large size, long cylindrical shape, prevalence in tissue, and presence of striations (see inset in Figure 12D). Hi-FGF-2 was also localized in non-cardiomyocytes, including the endothelial blood vessel lining (green arrows in E), and small connective tissue cells with fibroblastic appearance (blue arrows in D). Double-immunofluorescence staining of human atrial tissue sections for Hi-FGF-2 (green) and the muscle cytoskeletal protein desmin (red), Figure 12F, confirmed presence of Hi-FGF-2 within cardiomyocytes, in both the nuclei and cytosol. Simultaneous fluorescence staining for nuclei confirmed nuclear localization of Hi-FGF-2 in atrial cardiomyocytes and is shown in higher magnification in Figure 14A, B. As in Figure 12B, Hi-FGF-2 was localized in cells near the epicardium that were also positive for the mesenchymal/fibroblastic marker vimentin (Figure 12G). A higher magnification image of these cells is included in Figure 14C. Tissue sections were obtained from 5 patients and all displayed similar patterns of Hi-FGF-2 localization as shown in Figure 12B (patient 1), and Figure 12D, E (patient 2). Commercially available atrial sections from a healthy individual were also examined, and again displayed an immunostaining pattern similar to that shown in Figure 12B, D, E; included in Figure 14D. Taken together, experimental data

included in Figure 12 show that Hi-FGF-2 is indeed present in human atrial tissue, constituting, on average, about half of total FGF-2, and that it is expressed by cardiomyocytes as well as non-myocytes including connective tissue cells. Cardiomyocytes and extracellular space constitute 45% and 49% of human atrial volume, with non-cardiomyocytes such as endothelial cells and connective tissue cells making up the rest (Hinescu *et al.*, 2006). The bulk of tissue lysate-extracted FGF-2 therefore is likely to be dominated by cardiomyocyte-FGF-2, as well as extracellular matrix-bound FGF-2, secreted or released by cardiac cells.

Characterization of the anti-human Hi-FGF-2 antibodies used here is included in Figures 15 and 16. Firstly, we asked if anti-Hi-FGF-2 could detect human Hi-FGF-2 in cells *in situ* by immunofluorescence. We used transient gene transfer to introduce cDNAs modified to express human Hi-FGF-2 only, or Lo-FGF-2 only, in a transformed cell line with relatively low levels of endogenous FGF-2, the human embryonic kidney (HEK293) cells, as we have done in previous studies (Ma *et al.*, 2007). We then probed, by dual immunofluorescence, for Hi- or total FGF-2 expression, using affinity purified anti-human Hi-FGF-2 antibodies, or commercially available monoclonal antibodies recognizing all FGF-2 isoforms. The latter antibody served to document total FGF-2 (Hi- or Lo-) overexpression. As seen in Figure 15, anti-Hi-FGF-2 antibodies detected overexpressing cells only in cultures transfected with the cDNA for human Hi-FGF-2. By Western blotting of denatured proteins, we found that anti-Hi-FGF-2 could only detect purified recombinant human Hi-FGF-

2, but not recombinant rat Hi-FGF-2 or rat Lo-FGF-2 (Figure 16A). In a third experiment we asked if the anti-human Hi-FGF-2 antibodies could interact with and immunoprecipitate native human Hi-FGF-2, but not Lo-FGF-2, from non-transfected cell extracts. We used extracts from commercially available primary human embryonic cardiac cells, and found that anti-Hi-FGF-2 could indeed immunoprecipitate the 22-24 kDa human Hi-FGF-2, but not the 18 kDa Lo-FGF-2 from these extracts (Figure 16C).

3.2.2 FGF-2 isoform expression in human atria-derived myofibroblasts

Fibroblasts and myofibroblasts are considered to be important sources of secreted FGF-2 in various tissues. We have shown that in the rat, heart ventricle-derived myofibroblasts express, and secrete, predominantly Hi-FGF-2 (Santiago *et al.*, 2011). There is as yet no information as to the relative FGF-2 isoform expression and/or secretion by adult human cardiac myofibroblasts, atrial or ventricular. To address this issue we used patient-derived atrial explants to isolate migratory, proliferative cells that were identified as 'activated fibroblasts', or myofibroblasts (hMFs). Identification was based on fibroblastic morphology, presence of stress-fibers, and expression of fibroblast and/or myofibroblastic marker proteins including co-expression of vimentin and α -smooth muscle actin (α -SMA), expression of embryonic smooth muscle myosin (SMemb) as well as expression of extracellular matrix proteins, such as collagen (in its procollagen form), and extra domain A (EDA)-Fibronectin (Porter *et al.*, 2009; Santiago *et al.*, 2010), shown in Figure 17. Use of readily available patient-derived atrial tissue

gave us an ongoing tissue source for preparation of primary cultures, providing sufficient cellular material at early passages (P2-P4) for completion of our studies. Having access to both the originating tissue and hMFs from that tissue, furthermore, enabled us to compare FGF-2 content and isoform composition between tissue-, and tissue-derived cell lysates, to examine the possibility that the isolated cells might carry a tissue 'signature' regarding FGF-2 expression. Figure 18A shows FGF-2 isoform detection in primary cultures, arbitrarily labeled as C11-20, derived from 10 different patients (patients 11-20); also included in the figure is a Western blot showing the FGF-2 signal from lysates of the originating tissues (T11-20). The anti-FGF-2 signal in hMF lysates represents cell-associated (intracellular as well as cell surface-bound externalized protein) FGF-2 isoforms. All hMF cultures expressed all five human FGF-2 isoforms (Arnaud *et al.*, 1999) at 18, 22+22.5, 24, 34 kDa, Figure 18A. The 34 kDa FGF-2 was not detectable in the originating tissue lysates (Figure 12 and Figure 18). All hMF cultures accumulated predominantly Hi-FGF-2 (from 76-91% of the total), with a mean value of 83 ± 4 (SD)% of total FGF-2; n=10. In comparison, the Hi-FGF-2 percentage in the ten originating tissues used for this experiment ranged from 25-76% of total FGF-2, with a mean value of 55 ± 14 (SD)%, n=10. Please note that this determination was not significantly different to the value obtained from the first group of samples (n=45) shown in Figure 12. In hMFs, the 22-22.5 kDa FGF-2 (the bulk of Hi-FGF-2 isoforms) was significantly (4-fold) higher than the 18 kDa Lo-FGF-2. The relative contribution of the 34 kDa FGF-2 displayed a high degree of variability between cultures compared to the other FGF-2

isoforms, with cultures C11 and C19 presenting a relatively strong signal. Regardless of whether the originating tissue contained predominantly Hi- or Lo-FGF-2, primary myofibroblast cultures from that tissue accumulated predominantly Hi-FGF-2, thus there was no correlation between tissue and hMF FGF-2 isoform composition (correlation coefficient, Pearson $r=0.23$; $P>0.05$). This is illustrated clearly in Figure 18B, where selected tissues lysates (T11, T15, T17), are analyzed side by side with lysates from hMFs derived from these tissues (C11, C15, C17) and compared for their relative FGF-2 content and isoform composition. To obtain anti-FGF-2 signals of near-equivalent intensity it was necessary to load 5-fold more tissue- (compared to cell-) lysate protein/lane. Hi-FGF-2 in lysates from T11, T15 and T17 was at 76%, 43% and 25% of the total FGF-2 signal while that for corresponding hMFs was at 91%, 81% and 83% of the total. Relative levels of hMF-associated FGF-2 were about 15-fold higher than in tissue lysates, as shown in Figure 18B. There was no correlation regarding total FGF-2 content between tissue- and hMF-lysates (correlation coefficient, Pearson $r=0.24$; $P>0.05$). Total FGF-2 content as well as isoform composition in tissue lysates is likely to be dominated by cardiomyocyte-associated FGF-2, with smaller contributions from fibroblasts and other non-myocytes, and influenced by patient pathology and drug treatments. The FGF-2 content and isoform composition in our primary cultures reflects the properties of a hyper-synthetic, hyper-contractile and hyper-secretory myofibroblast state, and supports the notion that the conversion of endogenous cells to such a

myofibroblast phenotype *in vivo* would result in potent local production of Hi-FGF-2.

Immunofluorescence staining was used to examine the subcellular localization of Hi-FGF-2 in hMFs: staining with anti-Hi-FGF-2 antibodies indicated that Hi-FGF-2 localized not only to the nucleus and nucleoli, as expected from previous reports (Claus *et al.*, 2003; Chlebova *et al.*, 2009), but also to the cytosol. The cytosolic anti-Hi-FGF-2 staining presented as a granular and thread-like appearance (Figure 18C, D).

We asked whether the predominant accumulation of Hi-FGF-2 isoforms was a common characteristic between hMFs from various sources. FGF-2 isoform composition was determined in myofibroblasts from healthy human atrial tissue (adult), healthy human ventricular tissue (adult), and human embryonic ventricular tissue. Rat ventricular myofibroblasts were also analyzed for comparison. All of these different hMFs expressed Hi-FGF-2, including the 22-22.5, 24 and 34 kDa Hi-FGF-2 isoforms, comprising over 80% of total cell-associated FGF-2; Figure 19A. Rat MFs expressed, as expected from our previous report (Santiago *et al.*, 2011), the 21.5, 20 and 18 kDa FGF-2 isoforms (Shimasaki *et al.*, 1988). Relative total FGF-2 levels in human adult ventricular or atrial hMFs were significantly (4-fold, $P < 0.05$, $n = 3$) higher than those in adult rat ventricular MFs. Overall the FGF-2 isoform composition was similar between adult patient-derived atrial fibroblasts, adult normal heart-derived atrial or ventricular hMFs, as well as embryonic ventricular hMFs. Thus regardless of atrial versus ventricular origin, or adult versus embryonic stage, cardiac tissue-

derived myofibroblasts accumulate predominantly Hi-FGF-2. It should be noted that atrial fibroblasts have been shown to exhibit a heightened reactivity to various growth factors, and an enhanced profibrotic potential compared to their ventricular counterparts (Burstein *et al.*, 2008). Although our studies show no differences regarding the ability to express and secrete Hi-FGF-2 between human atria and ventricular myofibroblasts, a systematic study would be required to determine whether there are differences in the regulation of Hi-FGF-2 expression and secretion between these two cellular populations.

In addition to myofibroblasts, endothelial cells produce growth factors contributing to tissue remodeling (Zhang *et al.*, 1999); sublethal oxidative damage of endothelial cells is reported to result in the release of both Hi- and Lo-FGF-2 isoforms to the extracellular space (Yu *et al.*, 2008). We compared cell-associated Hi-, and Lo-FGF-2 levels between human primary endothelial cells (lymphatic and aortic) and atrial hMFs. Atrial hMFs accumulated over 20-fold more FGF-2 (both Hi- and Lo- isoforms) compared to either lymphatic or aortic endothelial cells; the 34 kDa Hi-FGF-2, furthermore was not detectable in the endothelial cells tested; Figure 19B. Our data suggest that, (a), compared to endothelial cells, hMFs are likely to be a more significant source of Hi-FGF-2 in cardiac interstitium, and (b), accumulation of high levels of Hi-FGF-2 by human myofibroblasts is not likely to be an artifact caused by conditions *in vitro*, but rather it represents a physiologically relevant cell type (myofibroblast)-related property.

3.2.3 Regulation of human FGF-2 isoform production by Angiotensin II, *in vitro*

Several chronic cardiovascular diseases characterized by myofibroblast-induced maladaptive remodeling, including hypertension, coronary heart disease, atherosclerosis, heart failure, fibrosis are linked to elevated levels of Angiotensin II (Ang II), and activation of Ang II receptors (Ferrario, 2006; Lemarie *et al.*, 2010). We next investigated the effect of the Ang II on hMF Hi-FGF-2 accumulation and secretion, *in vitro*. Figure 20A shows that stimulation with Ang II for 24 h elicited significantly increased in cell-associated 22-34 kDa Hi-FGF-2. The Ang II-induced increase in Hi-FGF-2 was significantly reduced in the presence of either losartan (AT-1R inhibitor), or PD123319 (AT-2R inhibitor), by 50% and 46%, respectively. In cells stimulated with Ang II in the presence of either inhibitor alone, Hi-FGF-2 levels remained significantly higher than those of the non-stimulated controls; Figure 20A. Hi-FGF-2 levels in cells stimulated with Ang II in the presence of both inhibitors were not significantly different than those of unstimulated cells, Figure 20B, suggesting that AT-1R and AT-2R may promote Hi-FGF-2 accumulation in an additive manner. Western blot analysis confirmed that both AT-1R and AT-2R were expressed by hMFs and that stimulation with Ang II for 24 h resulted in down-regulation of the AT-1R but not AT-2R. AT-1R and AT-2R were detected, by Western blotting, in patient atrial tissue lysates (Figure 20E), suggesting that these receptors may be mediating human FGF-2 and Hi-FGF-2 production *in vivo*.

Expression of the FGF-2 gene, as well as total FGF-2 protein accumulation, are regulated by ERK (extracellular signal activated kinase) (Thum *et al.*, 2008), as well as matrix metalloproteinase (MMP-2) activities (Tholozan *et al.*, 2007), although there is no information about the role of these signals on Hi-FGF-2 accumulation. We asked if the Ang II-induced upregulation of cell-associated Hi-FGF-2 required the activity of the ERK pathway, and/or MMP-2. Inhibition of the ERK activating pathway (with UO126), or MMP-2 activity (with MMP-2 Inhibitor) prevented the Ang II-induced increase in 22-34 kDa Hi-FGF-2 (Figure 21A). The ability of Ang II to stimulate ERK activity in hMFs was confirmed, and shown in Figure 21-M2-Fig.4B. Ang II increased ERK activity at 10 and 30 min from stimulation, without affecting total ERK levels. Ang II also elicited a small increase in MMP-2 activity, becoming significant at 6 and 24 hours after stimulation (Figure 21C).

To address Ang II receptor involvement in Ang II-induced ERK activation, hMFs were stimulated with Ang II for 30 minutes in the absence or presence of AT-1R and/or AT-2R inhibitors. Losartan elicited a 23% decrease in ERK activity, measured as the ratio of pERK/ERK, Figure 22. PD123319 did not exert a statistically significant effect although a trend towards decreasing ERK activity (by about 17%) was observed. Inhibition of ERK activity in the presence of both inhibitors, by 42%, was significantly lower than that by losartan alone, suggesting an additive effect of AT-1R and AT-2R mediated pathways to ERK activation. The same experiment was conducted in the presence of neutralizing antibodies (neu-Ab^{FGF-2}, 20 µg/mL), to block the effect of extracellular-acting FGF-2 on ERK

activity. ERK activity in hMFs stimulated with Ang II in the presence of neu-Ab^{FGF-2} decreased to about 62% in the absence of neutralizing antibodies. In the presence of neu-Ab^{FGF-2}, PD123319 elicited a very significant decrease in Ang II-induced ERK activity, by 70% of the value in the absence of the inhibitor. Losartan also decreased ERK activity, by 17%. In the presence of both inhibitors, ERK activity was decreased to the same extent as with PD123319 alone. Taken together these experiments indicate that both AT-1R and AT-2R are mediating ERK activation in response to Ang II stimulation, and suggest that the AT-1R-mediated activation of ERK may be partially dependent on the contribution of extracellular-acting FGF-2.

Levels of MMP activity in conditioned media of hMFs stimulated with Ang II for 30 min remained unchanged in the presence of losartan, PD123319, or neu-Ab^{FGF-2}; Figure 23.

3.2.4 Human Hi-FGF-2 export

To consider human Hi-FGF-2 as a potential trigger of paracrine, autocrine signaling it is important to examine if this protein can be externalized/secreted, if it is accumulating in the extracellular environment *in vitro* and/or *in vivo*, and if extracellular levels become upregulated by pathology-associated stimuli such as Ang II. We looked for presence of FGF-2 isoforms in hMF conditioned medium, as well as in cell 'eluates' containing proteins bound to the cell surface and the extracellular matrix. As seen in Figure 24A, cells exported Hi-FGF-2, detectable in both the conditioned medium as well as in the cell-surface/matrix-bound

fraction. Lo-FGF-2 was below the threshold of detection in conditioned medium, but was detectable in the cell-surface associated fraction (Figure 24B). Very similar findings were obtained when using human ventricle-derived myofibroblasts, as shown in Figure 25. Thus both atria- or ventricle-derived hMFs export FGF-2, consisting predominantly of Hi-FGF-2.

Stimulation of atria-derived hMFs with Ang II elicited a significant, 4-fold increase in Hi-FGF-2 present in conditioned medium, representing 75% of total FGF-2 (Figure 24A). A clear increase in exported FGF-2 was seen in the cell-associated fraction, again composed predominantly of Hi-FGF-2 (Figure 24B). The 22-22.5 kDa FGF-2 isoform was the predominant Hi-FGF-2 isoform present in the exported FGF-2 pools. The experiments shown in Figure 24 do not specifically address whether Ang II actively promotes the FGF-2/Hi-FGF-2 export process in hMFs, although they do suggest a positive correlation between levels of cell-associated FGF-2 and FGF-2 detected in both conditioned medium and in association with cell surface/matrix. The export of FGF-2 and rat Hi-FGF-2 has been found to require caspase-1 activity (Keller *et al.*, 2008; Santiago *et al.*, 2011), and a similar mechanism is likely mediating export of human Hi-FGF-2, as indicated by pilot experiments: incubation of either control or Ang II-stimulated hMFs with the caspase-1 inhibitor YVAD reduced levels of exported Hi-FGF-2, without affecting total levels of cell-associated Hi-FGF-2; Figure 26. The baseline levels of exported human Hi-FGF-2 observed in myofibroblasts that are not stimulated with added Ang II, are likely a reflection of baseline levels of caspase-1 activity (allowing export), as well as baseline levels of activation of the Ang II-

related signaling pathway, promoting baseline FGF-2 gene expression and protein accumulation.

Detection of Hi-FGF-2 in human atrial tissue, in combination with our *in vitro* experiments showing that human Hi-FGF-2 is exported to the extracellular environment, raised the possibility that Hi-FGF-2 may be present in biological fluids *in vivo*. We tested for presence of FGF-2 isoforms in human pericardial fluid, in a pilot study including samples from 10 cardiac surgery patients. As seen in Figure 24C, Hi-FGF-2 (22-34 kDa) as well as Lo-FGF-2 were detected in the pericardial fluid of all patients. On average, Hi-FGF-2 comprised 68 (± 25 SD) % of total FGF-2, significantly higher than Lo-FGF-2; Figure 24C. Using an FGF-2 standard curve we estimated the average total FGF-2 concentration in pericardial fluid to be at 578 pg/ml (± 354 SD), which is within the 260-770 pg/ml range reported by others (Iwakura *et al.*, 2000).

3.2.5 Biological activity of human Hi-FGF-2

Presence in the extracellular environment supports the hypothesis that human Hi-FGF-2 can exert autocrine or paracrine biological effects, by activating “outside-in” signal transduction. Maladaptive tissue remodeling in chronic heart disease includes paracrine stimulation of cardiomyocyte hypertrophy, conversion of non-myocytes to a myofibroblast phenotype promoting fibrosis (Porter *et al.*, 2009), and an increased innate inflammation response (Turner, 2013). We therefore examined the effects of extracellular-acting human Hi-FGF-2 on the

myofibroblast phenotype, on the expression of proteins linked to inflammation, and on cardiomyocyte hypertrophy.

Cells (hMFs) were incubated with antibodies specific for Hi-FGF-2 (Neu-Ab^{Hi-FGF-2}), aimed at neutralizing the effects of endogenously produced and externalized Hi-FGF-2. Control cultures were incubated with non-specific immunoglobulin. As shown in Figure 27, hMFs incubated with Neu-Ab^{Hi-FGF-2} displayed, as compared to controls, significantly decreased levels of α -SMA, EDA-Fibronectin, SMemb, and procollagen, all protein markers of a myofibroblast pro-fibrotic phenotype. Treatment with Neu-Ab^{Hi-FGF-2} did not change expression of housekeeping proteins such as β -tubulin or GAPDH. Incubation with Neu-Ab^{Hi-FGF-2} was also effective in decreasing cell-associated periostin levels compared to controls, as shown in Figure 28. Overall our data indicated that extracellular-acting endogenous Hi-FGF-2 promotes or sustains the activated fibroblast state, and promotes accumulation of matricellular proteins such as periostin.

Cells (hMFs) were treated with preparations of recombinant human Hi- or Lo- FGF-2 at 10ng/mL each and examined for accumulation of pro-interleukin-1 β (pro-IL-1 β) as well as plasminogen activator inhibitor 1 (PAI-1), proteins linked to inflammation. As seen in Figure 29A, Hi-FGF-2 elicited a robust upregulation of pro-interleukin-1 β (pro-IL-1 β), compared to unstimulated cells. Lo-FGF-2 also stimulated pro-IL-1 β expression, but was significantly less potent (by 5-fold) as compared to Hi-FGF-2; Figure 29A. Hi-FGF-2 also promoted PAI-1 upregulation while Lo-FGF-2 had no effect; Figure 29B.

Rodent Hi-FGF-2, rather than Lo-FGF-2, has been shown to promote cardiomyocyte hypertrophy (Jiang *et al.*, 2007). To test if human Hi-FGF-2 (recombinant, or secreted in conditioned medium) is pro-hypertrophic, we used rat neonatal cardiomyocytes, a widely used *in vitro* model of hypertrophy. Stimulation of these cells with the known pro-hypertrophic agent endothelin-1 (ET-1) was used as a positive control, and elicited a significant increase in cell size (Figure 30A). A preparation of recombinant human Hi-FGF-2 (10 ng/mL) also significantly increased in cardiomyocyte cell surface area, indicating that the human protein is indeed capable of pro-hypertrophic activity. To test for the effect of secreted human Hi-FGF-2 on hypertrophy we used conditioned media from Ang II-stimulated hMFs (CM*), in comparison to those from unstimulated hMFs (CM). As has been shown in Figure 21-M2-Fig.4, the Hi-FGF-2 content of CM* is significantly higher than that of CM. Figure 30A shows that CM*, but not CM, significantly increased cardiomyocyte cell surface area. This effect was not due to residual Ang II activity, since direct stimulation with Ang II had no significant effects on cardiomyocyte cell size, Figure 30A. In a separate experiment (Figure 30B), the stimulatory effect of CM* on cell size was confirmed to be FGF-2-dependent: incubation with Neu-Ab^{FGF-2} (interacting with all FGF-2 isoforms) significantly decreased the effect of CM* to levels similar to those of CM. Incubation with antibodies selective for Hi-FGF-2 prevented the pro-hypertrophic effect of CM*: Neu-Ab^{Hi-FGF-2} reduced the ability of CM* to promote ³H-leucine incorporation (protein synthesis), Figure 30C, or to increase cell surface area, Figure 30D, to levels not significantly different to CM. The neutralizing effect of

Neu-Ab^{Hi-FGF-2} is expected to result from the ability of this antibody to bind and sequester native human Hi-FGF-2 in CM* in a manner similar to Neu-Ab^{FGF-2}. As we have shown in Figure 16C, Neu-Ab^{Hi-FGF-2} does not interact with Lo-FGF-2.

Because Hi- and Lo-FGF-2 isoforms were found to co-exist in cell and tissue extracts, we asked if Hi-FGF-2 would be able to exert a pro-hypertrophic effect in the presence of at least equivalent levels of Lo-FGF-2. Cardiomyocytes were stimulated with preparations of human recombinant Hi-FGF-2, or Lo-FGF-2 preparations, at 10 ng/mL each, or with both Hi- and Lo-FGF-2. Lo-FGF-2 did not increase cell size, confirming our previous reports (Jiang *et al.*, 2007; Santiago *et al.*, 2011), Figure 30E. Cardiomyocytes stimulated with either Hi-FGF-2 alone, or with both Hi- and Lo-FGF-2 showed a significant and similar increase in cell surface area compared to unstimulated cells or cells stimulated with Lo-FGF-2 only; Figure 30E. Representative images of neonatal cardiomyocytes treated with CM, or CM* (\pm Neu-Ab^{FGF-2}) are included in Figure 30F.

It should be noted that our preparations of human recombinant Hi-FGF-2 were found to also contain 12-16 kDa fragments from the N-terminal 'half' as well as a 14.5 kDa fragment from the C-terminal 'half' of the molecule (Figure 16A,D); thus the actual concentration of intact Hi-FGF-2 is lower than the 10 ng/mL determined for the whole preparation. The N-terminal containing fragments are not expected to exert biological effects as they do not contain the FGF-2 receptor binding site, which is located towards the C-terminal half of the molecule (Valtink *et al.*, 2012). The 14.5 kDa C-terminal fragment on the other hand may have Lo-FGF-2-like activity, as it contains most of the core Lo-FGF-2 sequence; even if

that were the case we do not think that it would interfere with the activity of the intact human Hi-FGF-2, because, as shown in Figure 30E, the Hi-FGF-2 preparation retained pro-hypertrophic activity in the presence of added Lo-FGF-2.

Figure 12/M2-Fig.1

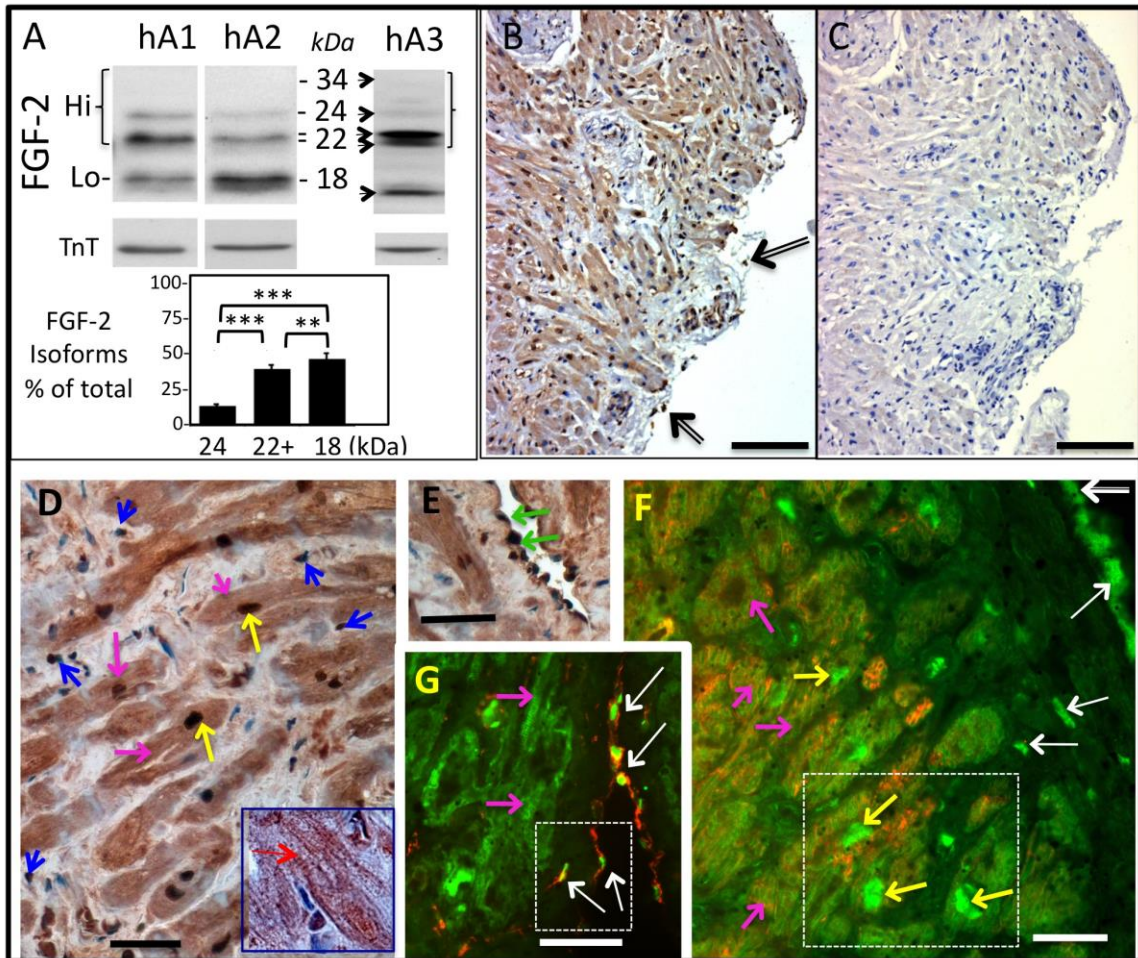


Figure 12/M2-Fig.1. Detection of Hi-FGF-2 in human atrial tissue. Panel (A) shows representative Western blot images of human atrial extracts (hA1, hA2, hA3, 50 $\mu\text{g}/\text{lane}$) probed for FGF-2 with an antibody detecting all FGF-2 isoforms. Expected migration of all human FGF-2 isoforms (34, 24, 22-22.5, and 18 kDa), corresponding to Hi- or Lo-FGF-2, is indicated by arrows; please note that the 34 kDa isoform is not detectable in tissue lysates. Western blots were also probed for cardiac troponin T (TnT) to verify equivalent loading of lanes. Samples hA1, hA2 were analyzed in small (8.3x5.5cm²) 15% polyacrylamide gels, while hA3 was analyzed in a large (16x11.5cm²) 15% polyacrylamide gel. The included graph shows percentage of each isoform over total FGF-2, where, n=45; comparisons between groups are indicated by brackets, where *** and ** denote P<0.001, and P<0.01, respectively. Panels (B) and (C) show images from patient-derived serial atrial sections, subjected to (B) incubation with purified anti-Hi-FGF-2 antibodies followed by immunohistochemical visualization of antigen-antibody complexes (brown color) as well as nuclear staining (haematoxylin, blue), and (C) similar procedures as in B but without the anti-Hi-FGF-2

antibodies. Incubation with anti-Hi-FGF-2 antibody elicits extensive immunostaining, in what appears to be nuclear as well as cytosolic sites in cardiomyocytes; staining of non-cardiomyocytes located at the epicardium is indicated by arrows. **Panels (D) and (E)** are close-up images from human atrial tissue sections stained as in (B), showing cellular and subcellular distribution of Hi-FGF-2. **Panels (G) and (F)** show human atrial sections subjected to double-immunofluorescence staining for Hi-FGF-2 (green), and either vimentin (G, red), or desmin (F, red). In all images, yellow or pink arrows point, respectively, to nuclear or cytosolic sites within cardiomyocytes. Blue arrows in (D) point to small connective tissue cells, likely fibroblasts. Green arrows in (E) point to endothelial cells, lining a vessel. White arrows in (G) and (F) point to non-myocytes, found at or near the epicardial region. These cells are positive for vimentin, but not desmin. In (F), co-staining with desmin confirms presence of Hi-FGF-2 in atrial cardiomyocytes. Sizing bars in (B) or (D,E,F,G) correspond to 250 or 100 μ M, respectively. Insets within panels G and F are shown in larger magnification in Figure 14-M2-Suppl.Fig.2.

Figure 13/M2-Fig.S1

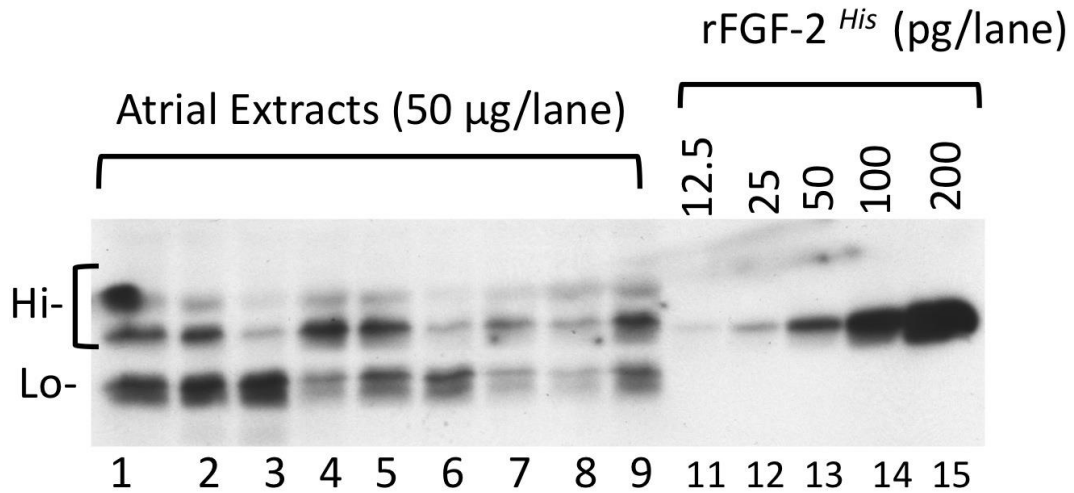


Figure 13/M2-Fig.S1. Comparison of Western blot signal for recombinant FGF-2 (12.5-200 pg/lane) with anti-FGF-2 signal in representative human atrial lysate samples. Western blot showing anti-FGF-2 immunoreactivity from 9 different patients (lanes 1-9, 50 µg/lane) in comparison to the immunoreactivity elicited by recombinant histidine (*His*)-tagged low molecular weight FGF-2 loaded at 12.5, 25, 50, 100 and 200 pg/lane. Please note that due to the *His*-tag, FGF-2 migrates near 22 kDa. The anti-FGF-2 signals in the 9 patients shown are representative of the range in total FGF-2 signal, as well as relative isoform composition, encountered in all patients analyzed ; intensity of the various anti-FGF-2 bands was within the selected recombinant FGF-2 range.

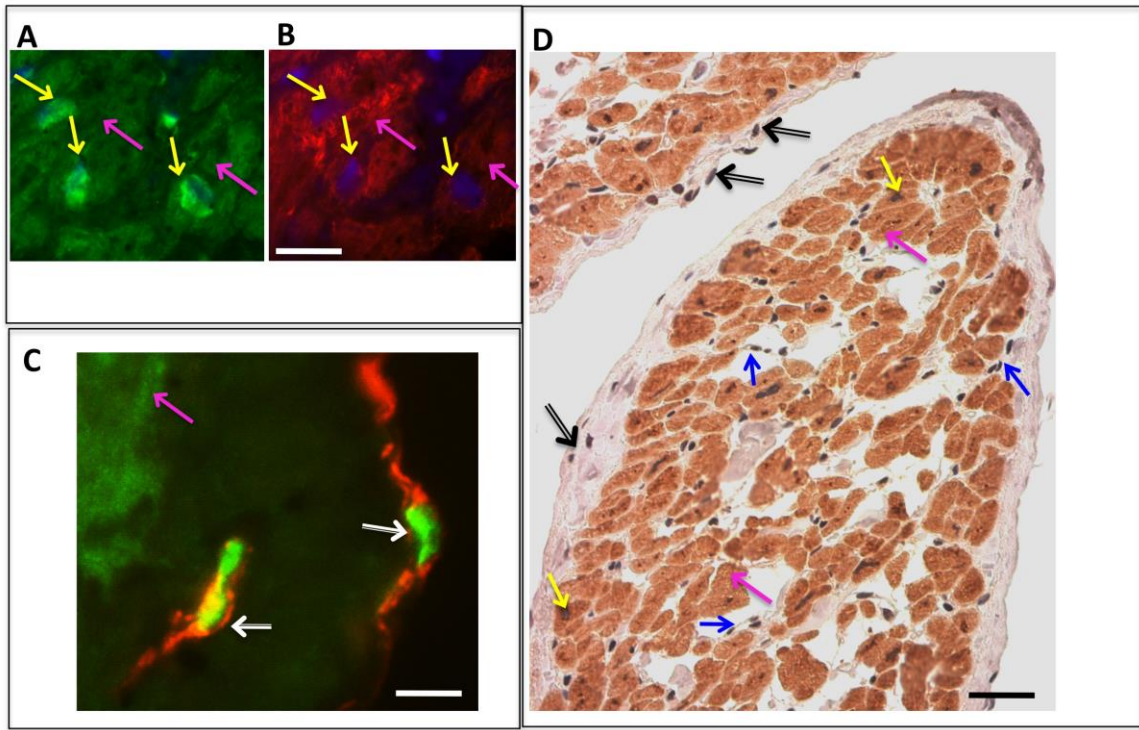


Figure 14/M2-Fig.S2. Localization of Hi-FGF-2 in cardiomyocytes and non-myocytes in human atrial tissue. Panels A and B show the area included within an inset in Figure 12/M2-Fig.1F, stained, respectively, for Hi-FGF-2 (green) and desmin (red), and counterstained with DAPI for nuclei (blue). Yellow arrows point to nuclei staining positive for Hi-FGF-2. Pink arrows point to cardiomyocyte cytosolic compartment, also staining positive for Hi-FGF-2. **Panel C** shows a larger magnification image of the inset within Figure 12/M2-Fig.1G, and represents atrial cells near the epicardial region (white arrows) staining positive for vimentin (red) and Hi-FGF-2 (green). **Panel D** shows immunohistochemical anti-Hi-FGF-2 staining of an atrial tissue section from a healthy individual. Black pointed arrows identify Hi-FGF-2-positive cells found in the epicardial lining; blue arrows identify fibroblastic connective tissue cells. Yellow arrows point to myocyte nuclei staining positive for Hi-FGF-2. Pink arrows point to cardiomyocyte cytosolic compartment, also staining positive for Hi-FGF-2. Sizing bars in B,C and D correspond, respectively to 50, 20 and 100 μ M.

Figure 15/M2-Fig.S3

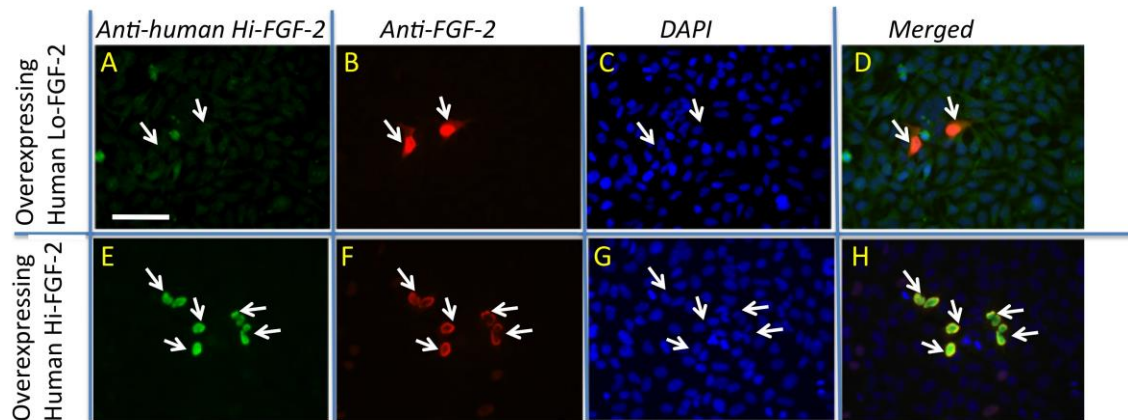


Figure 15/M2-Fig.S3. Anti-human Hi-FGF-2 antibodies detect overexpressed human Hi-FGF-2 but not human Lo-FGF-2, *in situ*. Human Hi- or Lo-FGF-2 were overexpressed in human embryonic kidney (HEK) 293 cells by transient gene transfer. HEK293 cells express low levels of endogenous FGF-2, allowing clear detection of transfected, FGF-2-overexpressing cells with appropriate antibodies. One day after gene transfer, cells were subjected to triple fluorescence staining with rabbit polyclonal anti-human Hi-FGF-2 (green), mouse monoclonal anti-FGF-2 (red), detecting both Hi- and Lo- FGF-2, and DAPI nuclear stain (blue). **A,B,C,D** panels show the same field from HEK293 cells overexpressing human Lo-FGF-2. A,B,C are stained, respectively, for Hi-FGF-2, total FGF-2 and nuclei, while D shows the merged image from A,B,C. Arrows point to cells overexpressing Lo-FGF-2, clearly identified by the monoclonal anti-FGF-2 antibodies (B, D). The overexpressing cells are not detected by anti-Hi-FGF-2 antibodies (A, D). **E,F,G,H** panels show the same field of HEK293 cells overexpressing human Hi-FGF-2 (22-24 kDa). E,F,G are stained, respectively, for Hi-FGF-2, total FGF-2, and nuclei, while H shows the merged image from E,F,G. Arrows point to overexpressing cells, clearly detected by both anti-Hi-FGF-2 antibodies (E, H), and anti-FGF-2 antibodies (F, H). Please note that panel D has been deliberately overexposed for 'green', to obtain an outline of the cell layer.

Figure 16/M2-Fig.S4

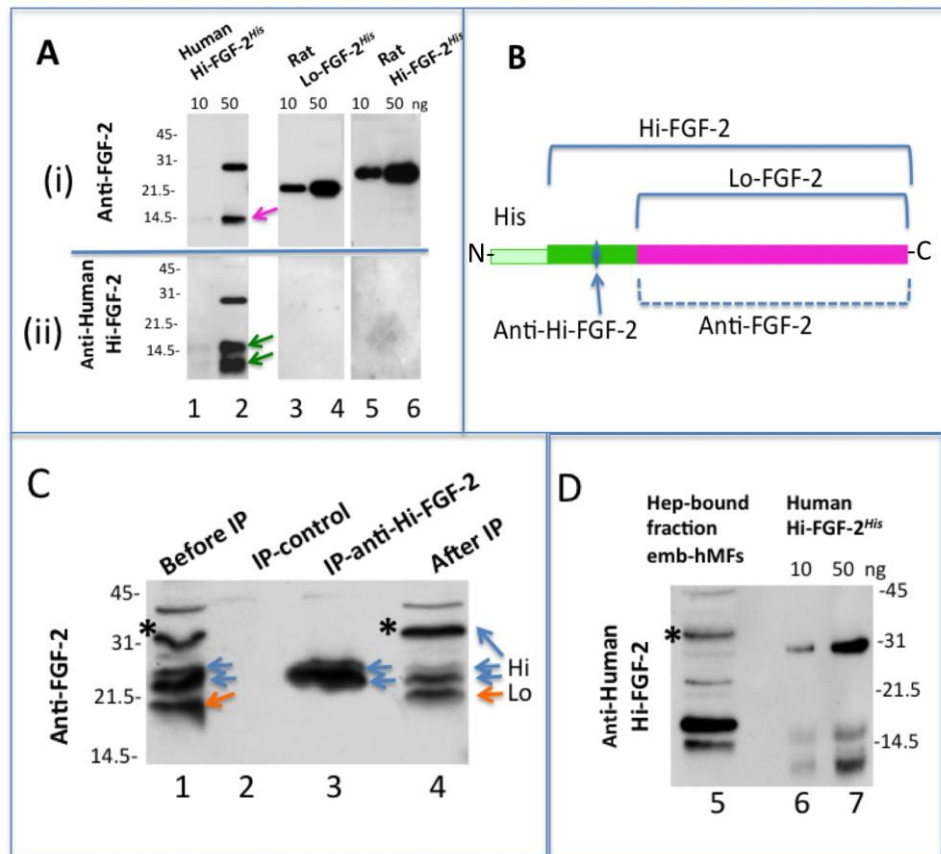


Figure 16/M2-Fig.S4. Specificity of anti-human Hi-FGF-2 antibodies for denatured and native Hi-FGF-2.

Panel A. Anti-human Hi-FGF-2 antibodies detect recombinant human Hi-FGF-2, but not Hi- or Lo-FGF-2, by Western blotting. *His*-tagged recombinant FGF-2 proteins, including human Hi-FGF-2 (24 kDa, migrating near 30 kDa due to the *His*-tag), rat Hi-FGF-2 and rat Lo-FGF-2, loaded at 10 and 50 ng/lane, were analyzed by Western blotting, and probed with monoclonal antibodies recognizing all human and rat FGF-2 isoforms (monoclonal anti-FGF-2, raised against the 18 kDa bovine Lo-FGF-2) or polyclonal antibodies raised against a sequence specific for the N-terminal of human Hi-FGF-2 (anti-Human-Hi-FGF-2), as indicated. In the gel loaded with recombinant human Hi-FGF-2 (lanes 1, 2), both antibodies recognize a band near 30 kDa representing the intact *His*-tagged human Hi-FGF-2; anti-Hi-FGF-2 antibodies also detect fragments at 15.5 and 12 kDa, containing the N-terminal of the molecule, while anti-FGF-2 antibodies recognize a 14.5 kDa fragment, containing the C-terminal of the molecule. The anti-FGF-2 antibodies detect, as expected, rat Lo-FGF-2 (lanes 3, 4) and rat Hi-FGF-2 (lanes 5, 6); these bands are not detected by the anti-human Hi-FGF-2 antibodies. **Panel B.** Schematic linear representation of

domains within the sequence of recombinant human Hi-FGF-2. N- and C- point to the N- and C-termini of the molecule. The core Lo-FGF-2 sequence is represented by pink color, while the N-terminal extension present only in Hi-FGF-2 is represented by green; the pale green edge indicates the histidine tag present in the recombinant molecule. A blue arrow points to the epitope(s) recognized by the polyclonal anti-Hi-FGF-2 antibodies. The monoclonal anti FGF-2 antibodies recognize epitopes within the Lo-FGF-2 core sequence. **Panel C. Anti-human Hi-FGF-2 antibodies interact with native endogenous human 22-24 kDa Hi- (but not Lo-) FGF-2 in solution.** This Western blot shows that anti-human Hi-FGF-2 antibodies specifically immunoprecipitate endogenously expressed human Hi-FGF-2 from embryonic human myofibroblasts. These cells express both Hi- and Lo-FGF-2 isoforms. The blot was probed for total FGF-2 with the monoclonal anti-FGF-2 antibodies. **Lane 1**, total lysate (20 μ g) from human embryonic cardiac fibroblasts, before being subjected to immunoprecipitation (IP), contains 22-24 Hi-FGF-2 (blue arrows), 34 kDa Hi-FGF-2 (asterisk) and 18 kDa Lo-FGF-2 (orange arrow). **Lane 2**, cell lysate proteins retained non-specifically by protein A-Sepharose beads (IP-control) from 900 μ g lysate show no immunoreactive signal. **Lane 3**, cell lysate proteins retained by the anti-Hi-FGF-2/protein-A-Sepharose column (IP-anti-Hi-FGF-2) from 900 μ g lysate show strong immunoreactive signal at 22-24 kDa, representing human Hi-FGF-2 isoforms. No signal for the 18 kDa FGF-2, or the 34 kDa FGF-2 is present. **Lane 4**, cell lysate (20 μ g) after being subjected to immunoprecipitation with anti-Hi-FGF-2 and protein-A-Sepharose. Blue arrows point to the signal for 22-24 kDa Hi-FGF-2 which is reduced compared to that before immunoprecipitation (lane 1), consistent with selective removal of the 22-24 kDa isoforms from the extracts by the affinity column. A 34 kDa immunoreactive band (presumably the 34 kDa human-Hi-FGF-2), marked with an asterisk, has not been depleted from the extract by the anti-Hi-FGF-2 affinity column., even though the 34 kDa human Hi-FGF-2 contains the immunoreactive epitope(s). Because, as shown next in panel D, the anti-Hi-FGF-2 antibodies can recognize denatured 34 kDa Hi-FGF-2, inability to immunoprecipitate the native protein indicates epitope masking under non-denaturing conditions. **Panel D. Anti-human Hi-FGF-2 antibodies detect 34 kDa Hi-FGF-2 in its denatured state.** The heparin-Sepharose-bound fraction from 1 mg of human embryonic fibroblast lysate was analyzed for Hi-FGF-2 by Western blotting (**lane 5**). Recombinant human *His*-tagged 24 kDa Hi-FGF-2 (**lanes 6, 7**) was used as positive control for anti-Hi-FGF-2 immunoreactivity. The anti-Hi-FGF-2 antibodies detect a 34 kDa band, indicated by an asterisk in lane 5. As expected (see panel A), in addition to detecting intact 22-34 kDa FGF-2, the anti-Hi-FGF-2 antibodies detect N-terminal containing Hi-FGF-2 fragments present in cell extracts and retained by heparin-Sepharose (lane 5), or present in recombinant Hi-FGF-2 preparations (lanes 6,7).

Figure 17/M2-Fig.S5

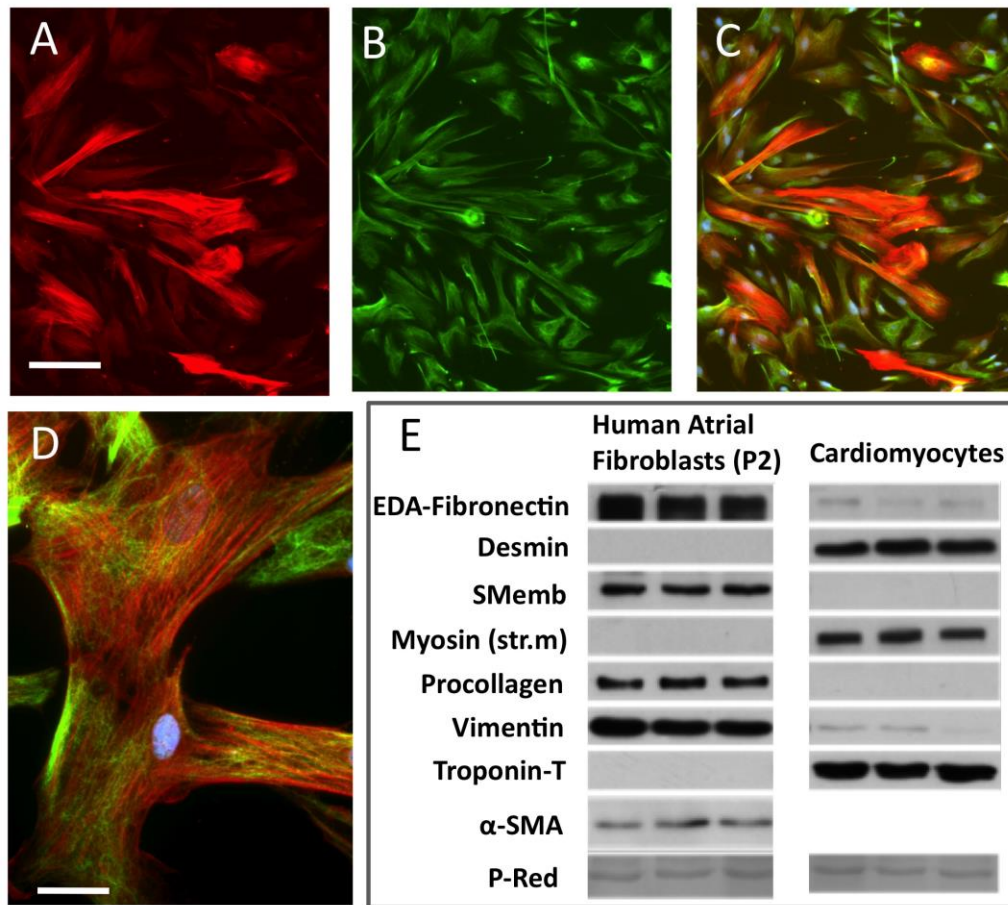


Figure 17/M2-Fig.S5. Identification of human patient atria-derived cells as myofibroblasts (hMFs).

A, B, and C. Triple fluorescence staining of cells for alpha smooth muscle actin (α -SMA, red, A, C), vimentin (green, B, C), and nuclei (blue, C). Stress fibers (α -SMA positive) are a characteristic of myofibroblasts. **D.** Close-up image of a cell subjected to triple fluorescence staining for α -SMA (red), vimentin (green), and nuclei (blue) clearly show presence of both vimentin- and α -SMA-composed filaments within the same cell, identifying it as myofibroblast. **E.** Western blot analysis of lysates from hMFs and rat neonatal cardiomyocytes (three different samples per group), probed for markers of myofibroblast phenotype (EDA-Fibronectin, SMemb, procollagen, vimentin, α -SMA) and cardiomyocyte phenotype (desmin, striated muscle myosin, Troponin-T, TnT), as indicated. Cells defined as hMFs express EDA-Fibronectin, SMemb, procollagen, vimentin, α -SMA, but not desmin, TnT, or myosin; corresponding antibodies clearly detect desmin, TnT and myosin in cardiomyocytes. Staining for Ponceau Red (P-Red) is also shown.

Figure 18/M2-Fig.2

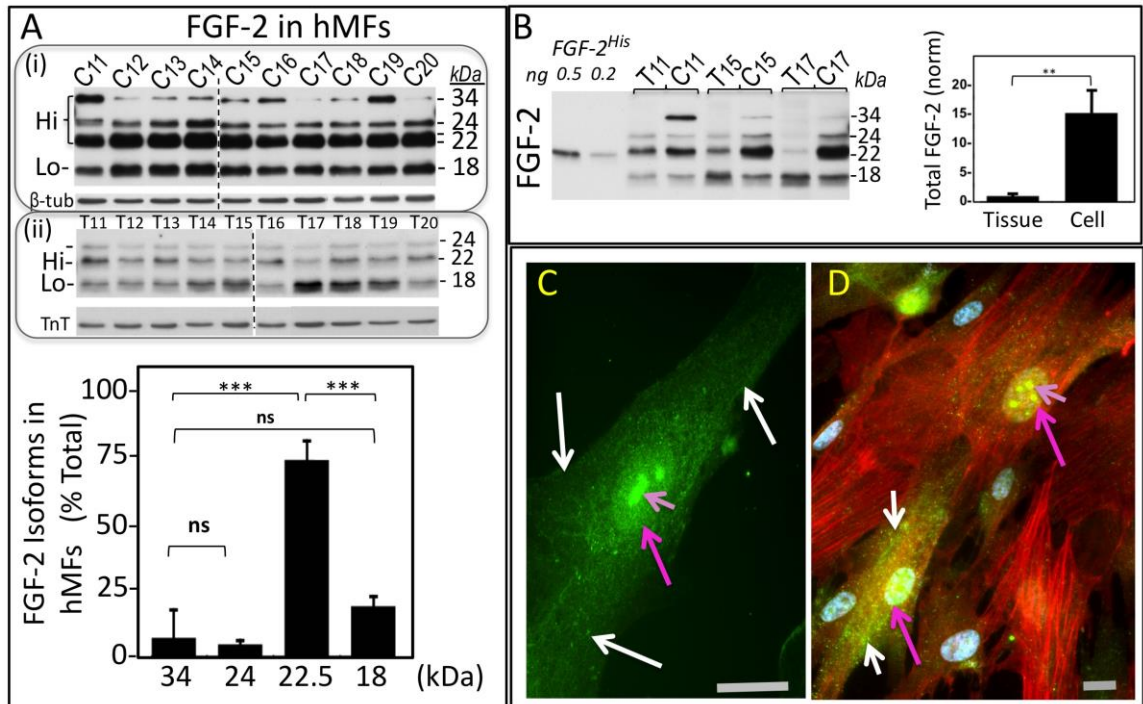


Figure 18/M2-Fig.2. Detection of Hi-FGF-2 in human atrial myofibroblasts. **Panel (A)** shows two sets of Western blots analyzing FGF-2 isoforms. The first set, (i), is a composite of two blots (separated by a broken line) and analyzes FGF-2 isoforms in hMF lysates (20 μ g/lane), from atrial myofibroblast primary cultures obtained from 10 patients (patients 11-20), and correspondingly labeled as C11-20. The second set, (ii), also a composite of two blots separated by a broken line, analyzes FGF-2 isoforms in atrial tissue lysates from patients 11-20, and labelled T11-20 (50 μ g/lane). The hMF blots or tissue blots were also probed for, respectively, β -tubulin (β -tub), or Troponin-T (TnT), as indicated. Following densitometry of the hMF blots, the % contribution of each FGF-2 isoform to the total FGF-2 signal was determined for each individual lane, and cumulative results (mean \pm SD) are included in graph form (n=10). **In Panel (B)**, a Western blot shows FGF-2 signals from 0.5 and 0.2 ng/lane of recombinant histidine tagged Lo-FGF-2 (FGF-2^{His}), atrial tissue lysates (T11, T15 and T17, loaded at 50 μ g/lane), side by side with FGF-2 signals from lysates obtained from corresponding primary hMF cultures (C11, C15 and C17, loaded at 10 μ g/lane). The graph shows comparisons between tissue and cell lysates for their relative total FGF-2 content, assessed by densitometry as optical density (O.D.) units (n=3). Measurements corresponding to cell FGF-2 were multiplied by 5, to correct for the 5-fold difference in total protein loading. In both panels, comparisons between groups are indicated by brackets, where P>0.05 is marked as ns, while P<0.001, 0.01, are marked as ***, or **, respectively. **Panels C and D** show immunofluorescence images of hMFs stained for, (C), Hi-FGF-2 (green),

as well as, (D), alpha smooth muscle actin (red) and nuclei (blue). White arrows point to cytosolic Hi-FGF-2; pink and pale- pink arrows point to nuclear and nucleolar Hi-FGF-2, respectively. Grey sizing bars correspond to 20 μm .

Figure 19/M2-Fig.S6

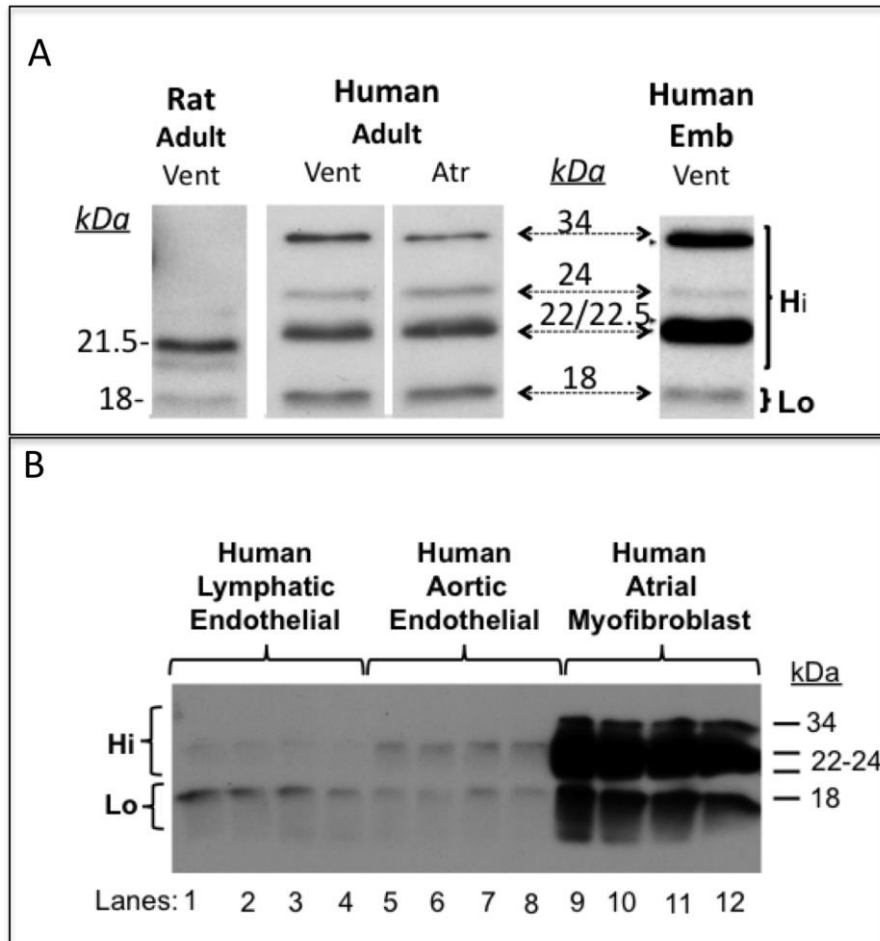


Figure 19-M2-Fig.S6. Production of Hi- and Lo- FGF-2 isoforms by cardiac myofibroblasts from different sources, and endothelial cells. Panel A. Cell-Associated FGF-2. Representative Western blot images from extracts of: rat adult ventricular myofibroblasts; human adult ventricular and atrial myofibroblasts (loaded at 10 $\mu\text{g}/\text{lane}$); human embryonic ventricular myofibroblast extract (loaded at 20 $\mu\text{g}/\text{lane}$), and probed for FGF-2, as indicated. Relative migration of FGF-2 isoforms, (18, 21, 21.5 kDa for rat, and 18, 22-22.5, 24, 34 kDa for human) is shown. **Panel B.** Western blot of total lysates isolated from human lymphatic endothelial cells (n=4, lanes 1-4), aortic endothelial cells (n=4, lanes 5-8), and atrial-derived myofibroblasts (n=4, lanes 9-12), at 50 $\mu\text{g}/\text{lane}$. The blot was probed with monoclonal anti-FGF-2 antibodies detecting all isoforms of FGF-2. Expression of all FGF-2 isoforms is shown to be substantially more pronounced (over 20-fold) in hMFs, compared to either type of endothelial cells.

Figure 20/M2-Fig.3

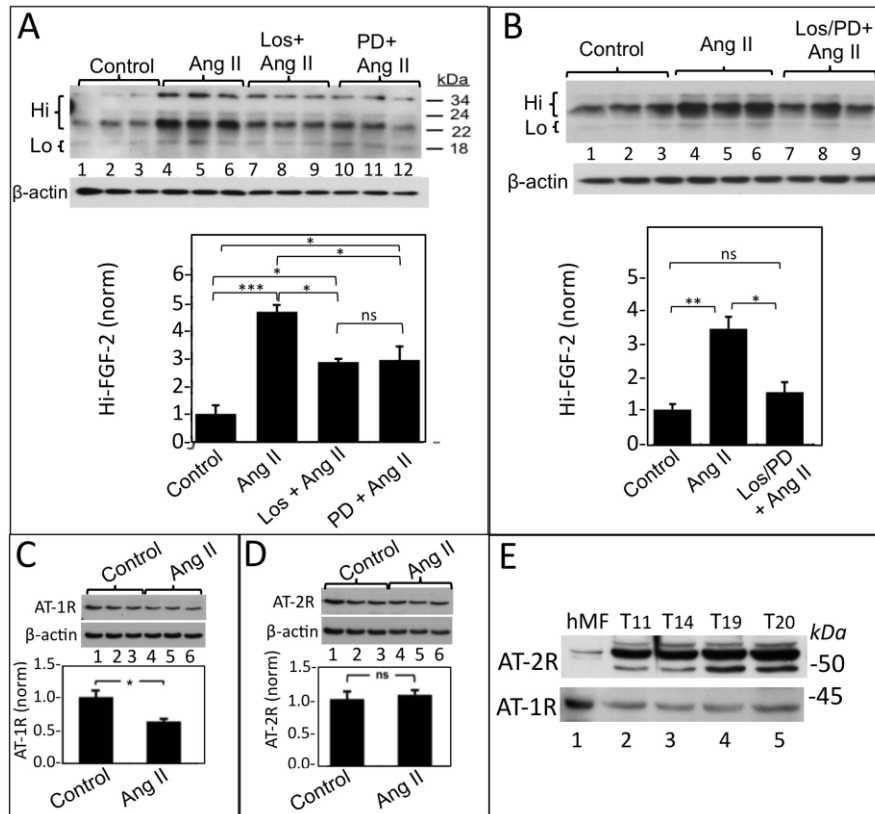


Figure 20-M2-Fig.3. Angiotensin II promotes upregulation of cell-associated human Hi-FGF-2 via AT-1R and AT-2R. **Panel A:** Western blot, and corresponding cumulative data, showing the effect of Ang II on Hi-FGF-2 accumulation by hMFs, in the absence or presence of either losartan (AT-1R inhibitor) or PD123319 (AT-2R inhibitor). Lanes 1-3; 4-6; 7-9; 10-12 correspond to lysates from, respectively, untreated (Control)-; Ang II-stimulated-; Ang II stimulated in the presence of losartan; and Ang II-stimulated in the presence of PD123319- hMFs. Ang II promotes Hi-FGF-2 upregulation, which is significantly decreased by either losartan or PD123319. **Panel B:** Western blot and cumulative densitometry data showing the effect of Ang II on Hi-FGF-2 accumulation in the absence or presence of simultaneous inhibition of both AT-1R and AT-2R. Lanes 1-3; 4-6; 7-9 correspond to lysates from, respectively, untreated (Control)-;Ang II-stimulated-; Ang II stimulated in the presence of both losartan and PD123319- hMFs. Relative levels of Hi-FGF-2 in the presence of both AT-1R and AT-2R inhibitors are not significantly different to those of unstimulated cells. **Panels C and D.** Western blots showing expression, respectively, of AT-1R or AT-2R by hMFs, and relative levels of these receptors after 24 h stimulation with Ang II. After 24 hour stimulation, levels of AT-1R, but not AT-R2, decrease compared to unstimulated cells. Signal for β -actin is also shown in A-D, serving as loading control. **E.** Western blot showing expression or

AT-1R and AT-2R in human atrial-derived tissues (Lanes 2-5) in comparison to hMFs (Lane 1). Sample size n=3 (all graphs); *, **, *** indicates $P < 0.05$, < 0.01 , < 0.001 , respectively; and ns denotes non-significance difference at $P > 0.05$.

Figure 21/M2-Fig.4

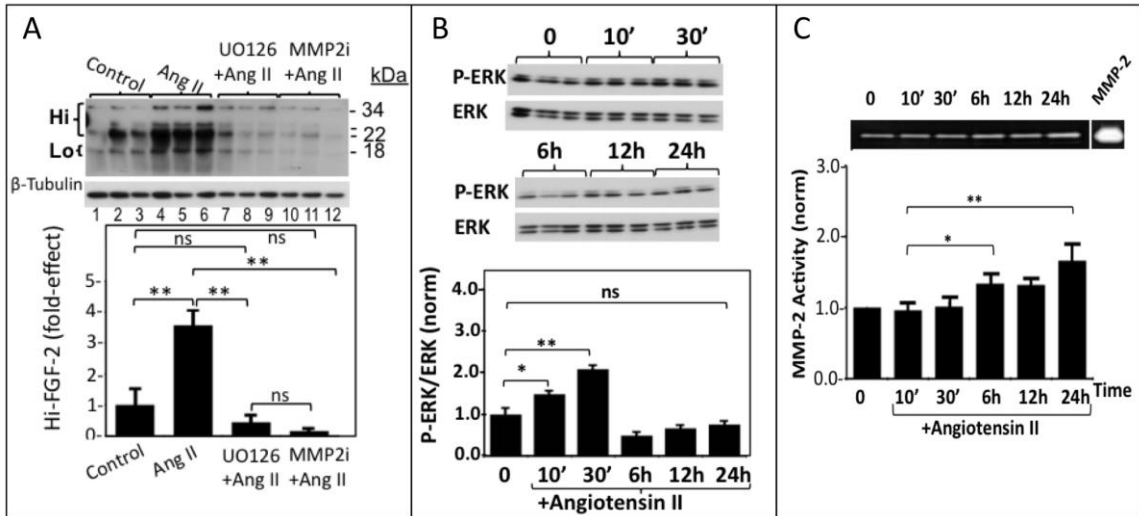


Figure 21/M2-Fig.4. ERK and MMP-2 activities mediate the Ang II-induced Hi-FGF-2 upregulation in hMFs. **Panel A.** Western blot and corresponding cumulative data showing the effect of an ERK inhibitor (UO126), or MMP-2 inhibitor (MMP2i) on the Ang II induced Hi-FGF-2 upregulation. Signal for β -tubulin is also shown, serving as loading control. **Panel B.** Western blots and corresponding cumulative data showing the effect of Ang II administration on phospho-(P)-ERK and total ERK, after 10-30 minutes and 6-24 hours of stimulation as indicated. This was done using a large gel. The graph shows cumulative data ($n=3$) of the ratio between P-ERK/ERK over time (10-30 min, 6-24 hours), in response to Ang II. Minutes and hours are indicated as ' and h. **Panel C.** Representative zymogram of MMP-2 activity in hMFs, including a positive control band (MMP-2), and corresponding cumulative data, showing relative MMP-2 activity in response to Ang II, over time (10-30 min, 6-24 hours), as indicated. For all graphs, brackets show comparisons between groups; *, **, ***, and ns correspond to $P<0.05$, $P<0.01$, $P<0.001$, and $P>0.005$, respectively.

Figure 22/M2-Fig.5

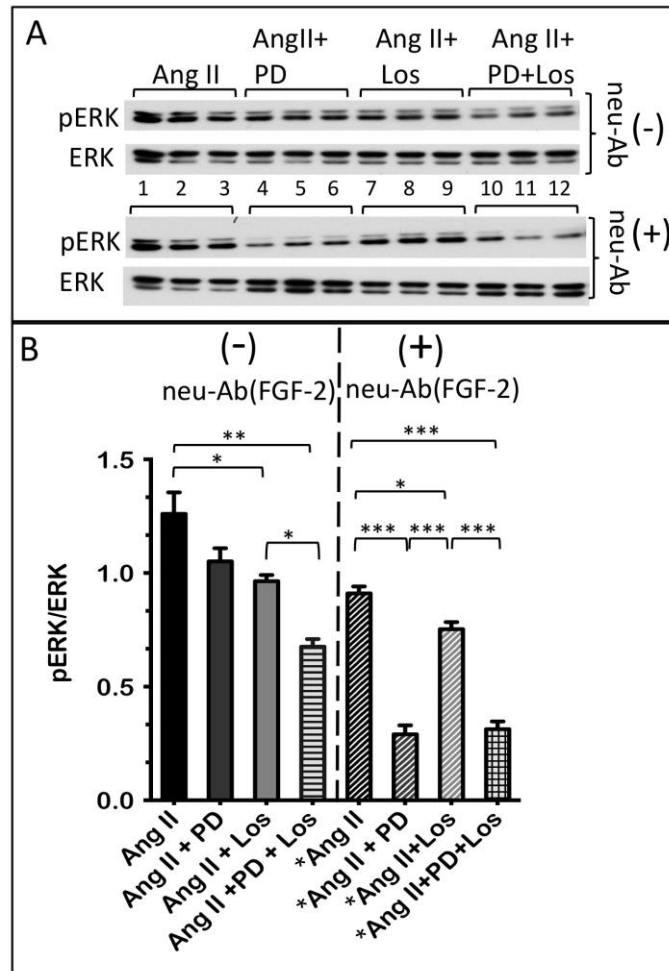


Figure 22/M2-Fig.5. Both AT-1R and AT-2R mediate the Ang II-induced ERK activation in hMFs. Panel A shows Western blot of activated (phosphorylated) pERK, and total ERK, in hMFs stimulated for 30 minutes with Ang II (lanes 1,2,3), Ang II + PD123319 (lanes 4,5,6), Ang II + Losartan (lanes 7,8,9), and Ang II +PD123319 +Losartan (lanes 10,11,12), in the absence (-) or presence (+) of neutralizing anti-FGF-2 antibodies (neu-Ab^{FGF-2}), as indicated. Please note that the Western blot for pERK in the groups incubated with neu-Ab^{FGF-2} is not directly comparable to the Western blot for pERK in the groups incubated in the absence of neu-Ab^{FGF-2} (different exposures). Panel B shows pERK/ERK ratios in the groups shown in panel A. Brackets show statistically significant differences between groups, where *, **, ***, correspond to P<0.05, 0.01, and 0.001, respectively.

Figure 23/M2-Fig.S7

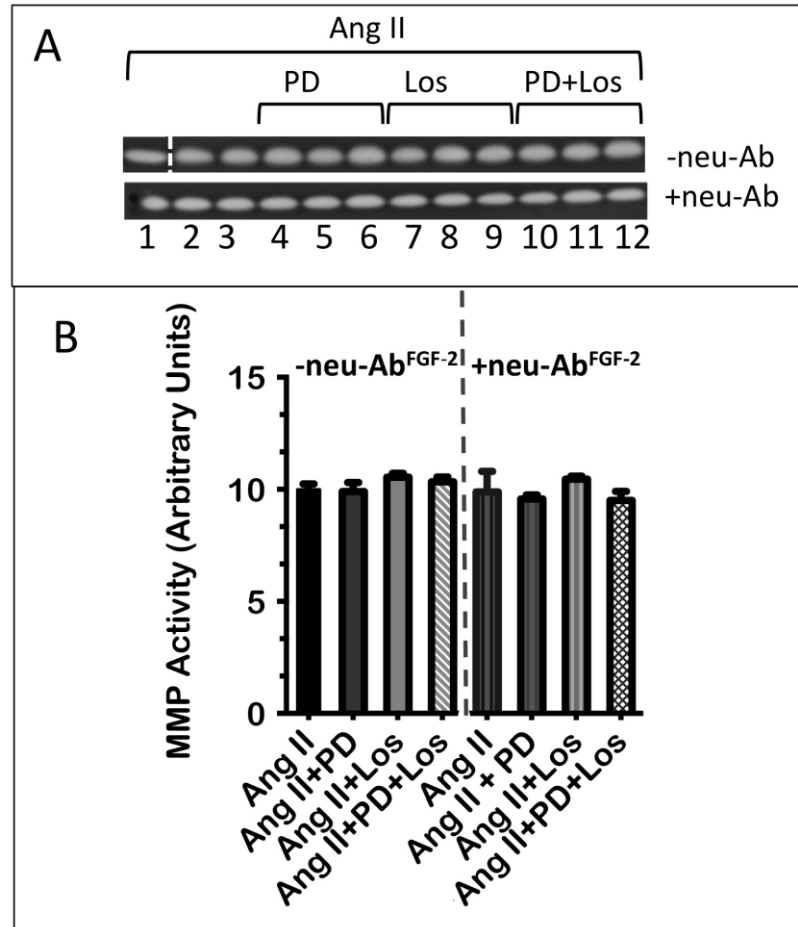


Figure 23/M2-Fig.S7. MMP activity is not affected by Ang II receptor activation nor extracellular-acting FGF-2. Panel A shows gel zymograms for MMP-2 activity detected in conditioned medium from hMFs stimulated for 30 minutes with Ang II (lanes 1,2,3), Ang II + PD123319 (lanes 4,5,6), Ang II + Losartan (lanes 7,8,9), and Ang II +PD123319 +Losartan (lanes 10,11,12), in the absence (-) or presence (+) of neutralizing anti-FGF-2 antibodies (neu-Ab^{FGF-2}), as indicated. The broken white line between lanes 1 and 2 indicates that these lanes were separated by more than one spaces on the gel. Panel B shows densitometry values (MMP Activity in arbitrary units) from the groups shown in panel A, as indicated. The vertical broken grey lines separates values obtained in the absence or presence of neu-Ab^{FGF-2} as indicated. There were no significant differences ($P>0.05$) between any of the groups.

Figure 24/M2-Fig.6

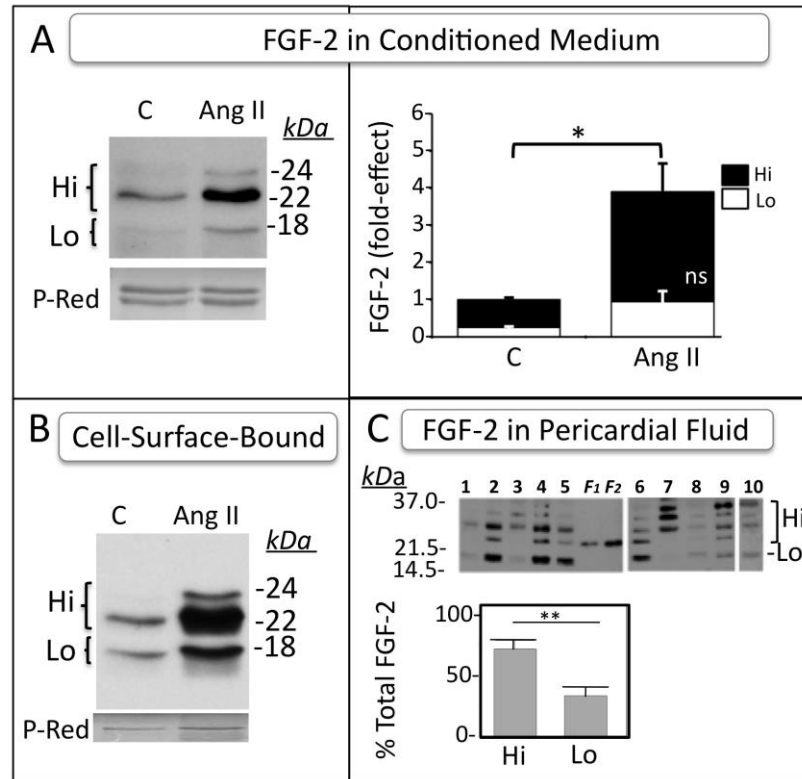


Figure 24/M2-Fig.6. Detection of Hi-FGF-2 in the extracellular environment *in vitro* and *in vivo*. **Panel (A).** Representative Western blot images of FGF-2 detection in conditioned medium from unstimulated or Ang II-stimulated hMFs. Each lane contains the heparin-Sepharose-bound fraction from 60 ml of pooled conditioned medium. **Panel (B).** Representative Western blots for FGF-2 “eluted” from the cell surface with a high salt wash, and concentrated by binding to heparin-Sepharose. Each lane contains the heparin-bound fraction from a 10 ml wash (5x100 near-confluent plates). Ponceau S Red (P-Red) staining of unidentified protein band(s) is also shown, indicative of equivalent loading. Experiments shown in A and B were repeated 2 more times, with similar results. **Panel (C).** Western blot image, and corresponding quantitative data of FGF-2 isoforms present in human pericardial fluid (n=10). Lanes 1-5 (gel 1) and 6-10 (gel 2) contain the heparin-Sepharose-bound fraction from 0.5 ml pericardial fluid of individual patients. Lanes marked as F1, F2 contain recombinant Lo-FGF-2 (histidine-tagged) loaded at 0.25 and 0.5 ng/lane respectively. Sample 10 was deliberately overexposed to increase visibility of bands. Recombinant FGF-2, used as standard, was included in the second gel as well (not shown here). The graph shows percent contribution of Hi- (22-34 kDa) or Lo-FGF-2 (18 kDa) isoforms to the total FGF-2 signal (mean \pm SEM). In all panels, brackets show comparisons between groups; * and ** correspond to $P < 0.05$ and $P < 0.01$, respectively.

FGF-2 Exported by Human Ventricular Myofibroblasts

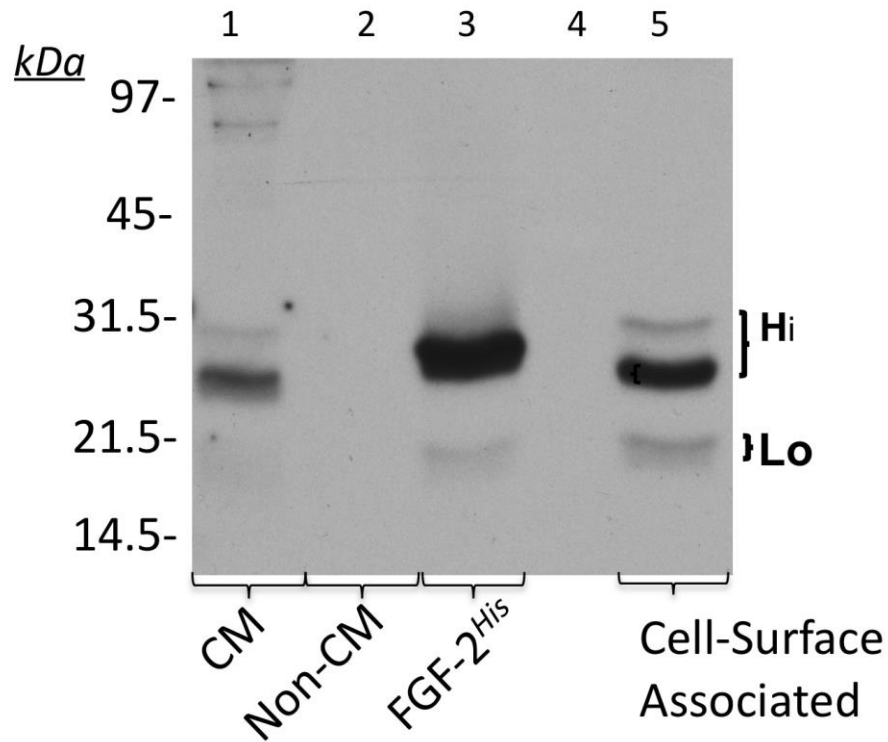


Figure 25/M2-Fig.S8. Human adult ventricular myofibroblasts export Hi-FGF-2. Western blot-based analysis of FGF-2 content in: Lane 1, heparin-bound fraction from 60 ml of pooled conditioned medium (CM) from ventricular hMFs; lane 2, heparin-bound fraction from 60 ml medium not conditioned by ventricular hMFs (Non-CM); lane 3, 2 ng of recombinant histidine-tagged Lo-FGF-2; lane 4 is left empty, lane 5, heparin-bound fraction from a 10 ml high salt eluate containing cell-surface-associated proteins. The 22-24 kDa Hi-FGF-2 is present in CM, as well as in the cell surface-associated fraction. The 18 kDa FGF-2 is detectable only in the cell-associated fraction

Figure 26

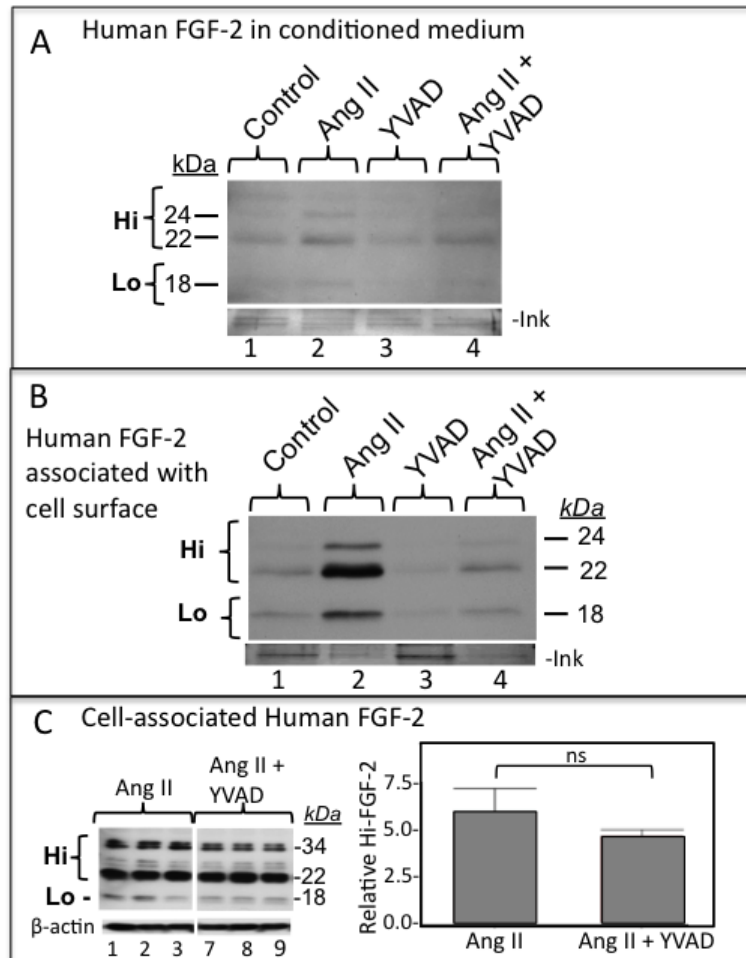


Figure 26. Exported human Hi-FGF-2 levels depend on Caspase-1 activity

Near-confluent atrial hMFs, kept for 48 hours in a low serum medium were stimulated (or not) with 10^{-6} M Ang II in the presence or absence of the Caspase-1 inhibitor (YVAD; 10 μ M) for 48 hours. Heparin-Sepharose-bound proteins from, **panel A**, conditioned media (60 ml, pooled from 6x100 mm plates), as well as, **panel B**, cell surface-bound high salt eluates (12 ml, pooled from 3x100 mm plates) from each group were analyzed for FGF-2 by Western blotting. **Panel A**. Lanes 1,2,3 and 4 show, respectively, FGF-2 signal in conditioned medium from unstimulated control cells, Ang II-stimulated cells, control cells treated with YVAD, and Ang II-stimulated cells treated with YVAD. Inclusion of YVAD appears to attenuate somewhat the FGF-2 signal from either control or Ang II treated cells. The blot was also stained with India ink (shown as -ink) to provide an evaluation of overall protein loading in these lanes. **Panel B**. Lanes 1,2,3 and 4 show, respectively, FGF-2 signal in high salt eluates from unstimulated cells, Ang II-stimulated cells, control cells treated with YVAD, and Ang II-stimulated cells treated with YVAD, representing exported, cell surface-

bound FGF-2. Inclusion of YVAD clearly decreases the FGF-2 signal from the control as well as the Ang II-stimulated group. The blot was also stained with India ink (shown as -ink) to provide an evaluation of overall protein loading. Protein loading, as assessed by a representative band, appears similar within the controls (lanes 1 and 3) and within the Ang II (lanes 2 and 4) groups. Protein loading in the Ang II groups appears reduced compared to the control groups.

Panel C. Western blot, and corresponding quantitative data, showing cell- (hMF)-associated FGF-2 in Ang II-stimulated cells, in the absence (lanes 1,2,3) or presence (lanes 7,8,9) of incubation with YVAD, as indicated. Caspase-1 inhibition had no effect on total, cell-associated FGF-2 (ns=non-significant, $P>0.05$). Signal for β -actin is also shown, used as loading control. The Western blot images shown were obtained from the same blot, where the two groups were separated by 3 lanes.

Figure 27/M2-Fig.7

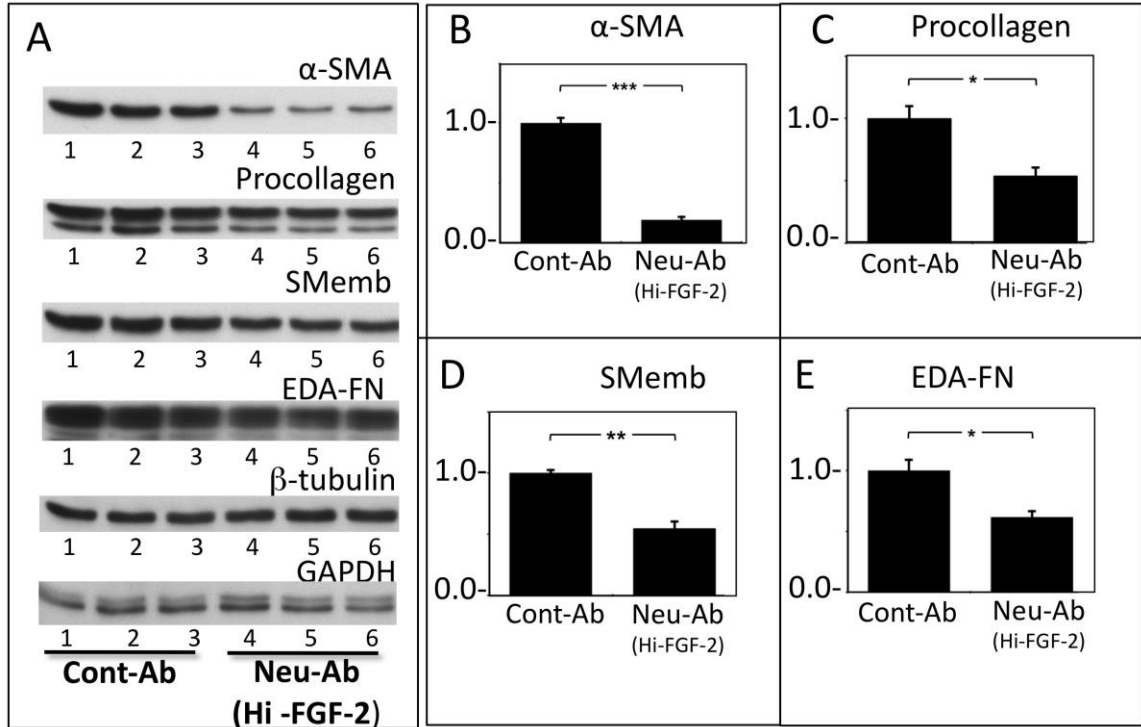


Figure 27/M2-Fig.7. Selective neutralization of extracellular human Hi-FGF-2 attenuates expression of pro-fibrotic proteins. Panel A. Western blots showing the effect of incubation with either control antibodies (Cont-Ab, 20 μ g/ml, lanes 1,2,3), or anti-Hi-FGF-2 antibodies (Neu-Ab^{Hi-FGF-2}, 20 μ g/ml, lanes 4,5,6) on the accumulation of α -SMA, procollagen, SMemb, EDA-Fibronectin (EDA-FN), β -tubulin, and GAPDH, by hMFs, as indicated. Panels B,C,D and E show corresponding quantitative (densitometry) data for α -SMA, procollagen, SMemb, EDA-Fibronectin (EDA-FN), as indicated (\pm SEM). Incubation with Neu-Ab^{Hi-FGF-2} significantly decreased expression of α -SMA, procollagen, SMemb and EDA-Fibronectin, without having any effect on GAPDH or β -tubulin. Brackets show comparisons between groups, where *, **, *** correspond to P<0.05, <0.01, <0.001; n=3/group.

Figure 28

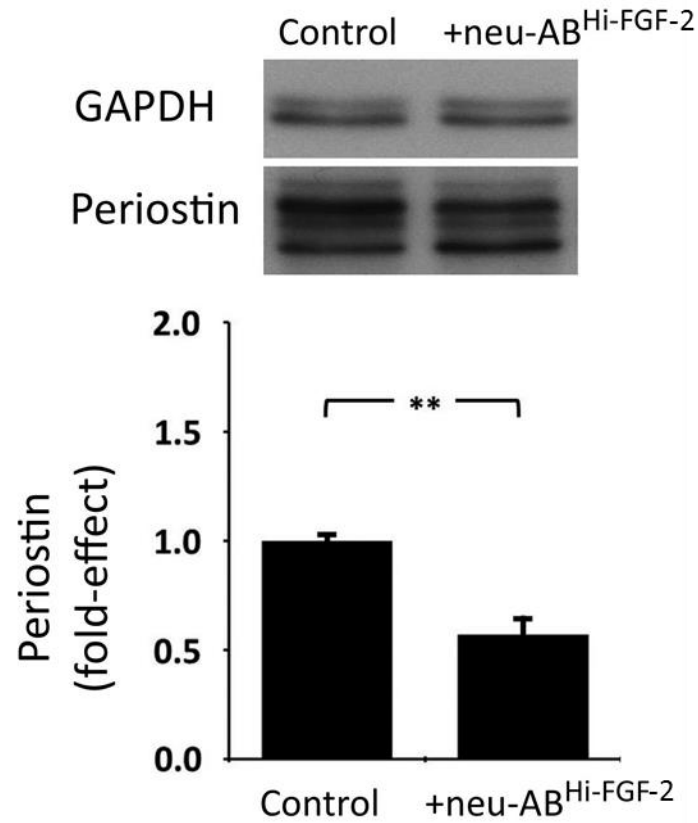


Figure 28. Neu-Ab^{Hi-FGF-2} antibodies decrease periostin accumulation. Representative Western blot cell lysates probed for periostin, a matricellular protein associated with fibrosis, and corresponding quantitative data, showing the effect of incubation with neutralizing, anti-Hi-FGF-2 antibodies on periostin accumulation by human atrial myofibroblasts compared to controls as indicated. Probing for GAPDH was used as loading control. Please note that the two GAPDH lanes shown here are the same as lanes as lanes 3 and 4 from the previous figure. ** indicate $P < 0.01$ ($n=3$)

Figure 29/M2-Fig.8

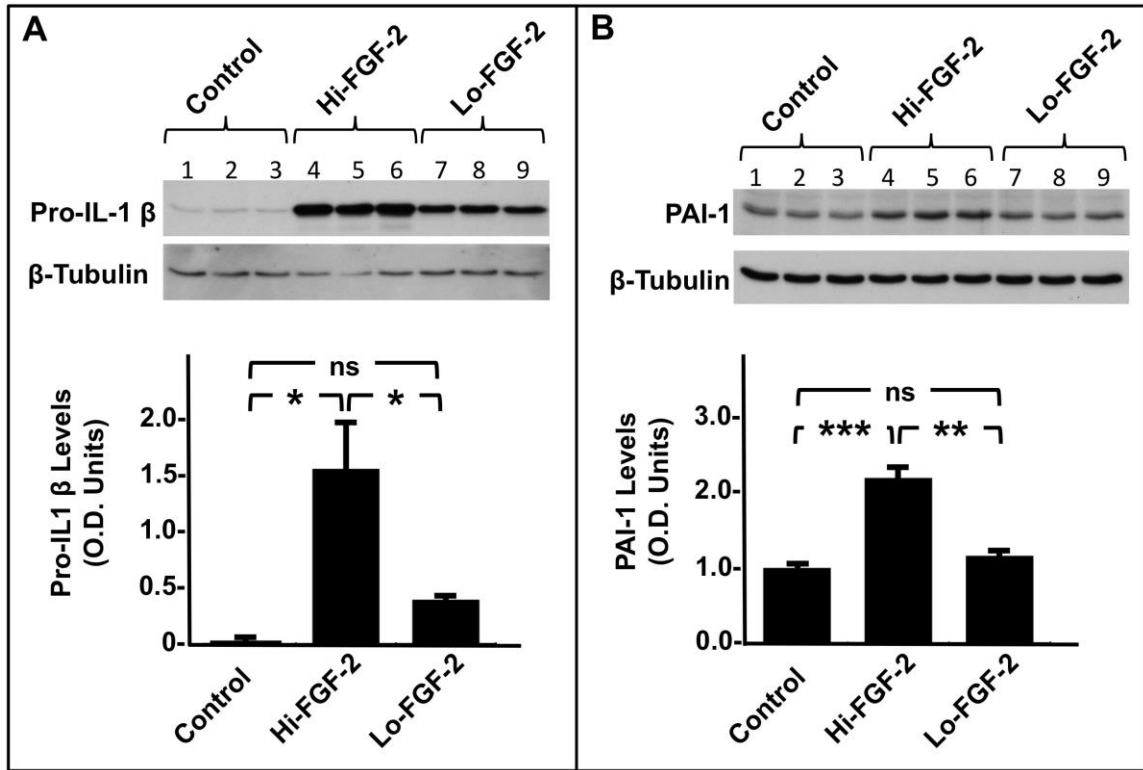


Figure 29/M2-Fig.8. Effect of extracellular-acting FGF-2 isoforms on the accumulation of pro-IL-1 β and PAI-1 by hMFs. **Panel A**, Western blot and corresponding cumulative data showing relative pro-IL-1 β levels (optical density, O.D. units) in hMF cell lysates from unstimulated cells (lanes 1,2,3) and cells stimulated with 10 ng/ml of a recombinant Hi-FGF-2 preparation (Hi, lanes 4,5,6) or 10 ng/ml of recombinant Lo-FGF-2 (Lo, lanes 7,8,9), as indicated. Both Hi- and Lo-FGF-2 upregulated pro-IL-1 β , although the effect of Hi-FGF-2 was significantly more potent. **Panel B**, Western blot and corresponding quantitative data showing relative PAI-1 levels (optical density, O.D. units) in hMF cell lysates from unstimulated cells (lanes 1,2,3) and cells stimulated with Hi-FGF-2 (Hi, lanes 4,5,6) or Lo-FGF-2 (Lo, lanes 7,8,9), as indicated. Hi- but not Lo-FGF-2 upregulated PAI-1 levels. Brackets mark comparisons between groups where *, **, ***, and ns denotes $P < 0.05$, $P < 0.01$, $P < 0.001$, and $P > 0.05$ respectively.

Figure 30/M2-Fig.9

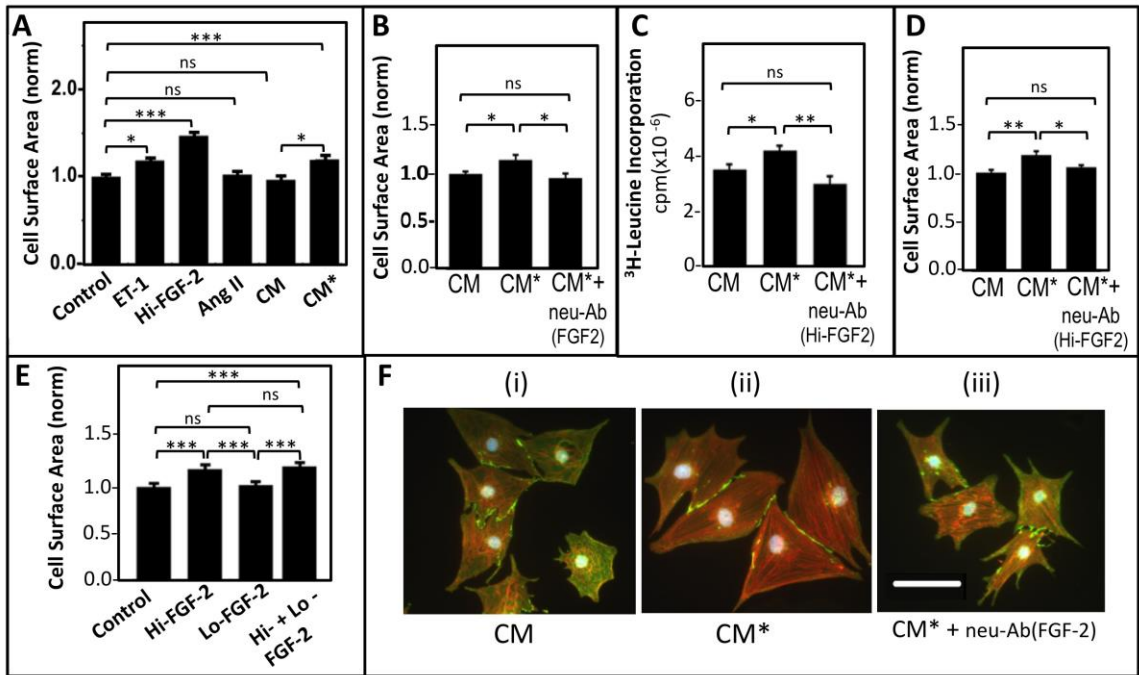


Figure 30/M2-Fig.9. Human Hi-FGF-2 exerts pro-hypertrophic effect.

Panel A. Neonatal rat cardiomyocyte cell surface area (normalized, assigning a value of 1 in control, untreated samples) is shown in response to stimulation with Endothelin 1 (ET-1), serving as a positive control, and a recombinant human Hi-FGF-2 preparation (10 ng protein/ml), $n=320$ myocytes/group. CM denotes conditioned medium obtained from unstimulated hMFs while CM* denotes conditioned medium from Ang II-stimulated hMFs. ET-1, recombinant human Hi-FGF-2, as well as CM* (but not CM, or Ang II added at 100 nM) increased myocyte cell surface area significantly. **Panel B.** Cardiomyocyte cell surface area (normalized) is shown as a function of incubation with CM, CM* or CM* supplemented with neutralizing antibodies to total FGF-2 (neu-Ab^{FGF-2}), as indicated; $n=480$ cells/group. Neutralization of total FGF-2 eliminated the ability of CM* to increase myocytes cell surface area compared to CM. **Panel C.** Protein synthesis (³H-Leucine incorporation) of cardiomyocytes incubated with CM, CM*, and CM* supplemented with 20 μ g/ml neutralizing anti-Hi-FGF-2 antibodies (CM* + neu-Ab^{Hi-FGF-2}). Neutralization of Hi-FGF-2 eliminated the ability of CM* to increase protein synthesis of cardiomyocytes compared to CM; $n=5$ plates/group. **D.** Cardiomyocyte cell surface area (normalized) is shown as a function of incubation with CM, CM*, and CM* + neu-Ab^{Hi-FGF-2}. Neutralization of Hi-FGF-2 eliminated the ability of CM* to increase surface area of cardiomyocytes compared to CM; $n=480$ /group. Please note that for the experiments shown in B,C,D panels the conditioned media in the first two groups (CM, CM*) were supplemented with non-specific rabbit IgG, at 20 μ g/ml. **E.**

Representative images of cardiomyocytes stained for anti-N-cadherin (green), alpha-actinin (red) and nuclei (blue), and incubated with CM, CM*, and CM* +neu-Ab (FGF-2). Sizing bar in (iii) corresponds to 100 μ M. In all graphs, brackets show comparison between groups, where *, **, ***, ns correspond to $P < 0.05$, < 0.01 , < 0.001 , or $P > 0.05$.

4.1 Rodent Hi-FGF-2

Part of the discussion in this section was obtained from Manuscript 1 (M1).

4.1.1 The mechanism of rat Hi-FGF-2 export requires caspase-1 activity

Fibroblasts/myofibroblasts are as a known source of FGF-2 (of unknown isoform composition) in the heart (Pellieux *et al.*, 2001). Our data demonstrated that the bulk of fibroblast-produced FGF-2 is composed of the Hi-FGF-2 isoforms (Santiago *et al.*, 2011). Compared with fibroblasts, cardiomyocytes appeared to produce less Hi-FGF-2 on a per mass unit basis. Our *in vitro* studies were concordant with our *in vivo* findings since, in adult cardiac sections, the anti-FGF-2 staining was more pronounced mainly in the non-myocyte cell populations.

For endogenous rat myofibroblast-expressed Hi-FGF-2 to be a candidate for auto- or paracrine functions, it needs to be exported to the extracellular environment. We have found this to be the case, *in vitro*, as Hi-FGF-2 was detected in both extracellular pools traditionally assigned to Lo-FGF-2. These pools included FGF-2 tightly bound to the cell surface/matrix due to its affinity for heparan sulfate proteoglycans, and FGF-2 present in cell conditioned media (Santiago *et al.*, 2011).

In the rat cell model, Hi-FGF-2 became detectable in the conditioned medium only after Ang II treatment, suggesting that Ang II may have actively promoted Hi-FGF-2 export and/or Hi-FGF-2 'liberation' from the matrix. It is possible that the strong overall Hi-FGF-2 up-regulation by Ang II could allow

proportionally more Hi-FGF-2 to be exported and to 'escape' to the soluble phase, possibly by saturating FGF-2-binding sites at the extracellular space. Alternatively or concurrently, Ang II may have actively promoted 'liberation' of cell- or matrix-bound FGF-2 to the medium by promoting matrix degradation. In support of the latter, Ang II/AT1 signaling increases matrix metalloproteinase (MMP) activity which in turn is responsible for shedding another matrix-bound factor, heparin-bound epidermal growth factor, to the medium (Jaffre *et al.*, 2009). Thus, MMP action may also contribute to the release of cell-bound Hi-FGF-2, as has been demonstrated for 'FGF-2' in the retina (Tholozan *et al.*, 2007).

Because neither Ang II nor the high salt wash stimulated the release of a cytosolic enzyme, LDH, an indicator of cellular injury (Santiago *et al.*, 2011), the increase in extracellular Hi-FGF2 was not a consequence of injury (Clarke *et al.*, 1995). Rather, we postulate that the mechanism(s) mediating Hi-FGF-2 export by myofibroblasts follows the non-conventional pathways of secretion operating for several proteins lacking a signal peptide for secretion. One of these pathways requires caspase-1 activity (Keller *et al.*, 2008). Because caspase-1 inhibition, by YVAD, diminished the Ang II-induced increases in extracellular Hi-FGF-2 (both cell/matrix-bound and in the soluble phase), but not the Ang II increase in intracellular Hi-FGF-2, we conclude that caspase-1 targets (directly or indirectly) the Hi-FGF-2 export mechanism and does not affect protein accumulation *per se*.

Caspase-1 is a protease activated by inflammasome(s), innate immune response protein complex(es) forming in response to stress signals (Keller *et al.*,

2008). Activated caspase-1 cleaves and activates immunological cytokines such as interleukin 1 β , stimulating their secretion; and it is also required for the cellular export of several other unconventionally secreted cytokines (Dinarello, 2002). Hi-FGF-2 export by rat myofibroblasts is thus linked to a generalized cellular response to stress stimuli mediated by caspase-1. It remains to be determined whether caspase-1 acts as a cargo protein, transporting Hi-FGF-2 to the cell exterior, or whether it affects another process linked to Hi-FGF-2 export. Regardless, it is of interest that failing human and murine hearts have elevated caspase-1 activities, and caspase-1 deletion is protective from myocardial infarction-induced heart failure (Merkle *et al.*, 2007). Caspase-1 deletion/inhibition would decrease externalized Hi-FGF-2 and thus reduce paracrine Hi-FGF-2 effects *in vivo* including hypertrophy, inflammation, and fibrosis.

4.1.2 Biological effects of extracellular-acting rat Hi-FGF-2

We provided the following evidence that Hi-FGF-2, secreted by Ang II-stimulated myofibroblasts, is capable of inducing cardiomyocyte hypertrophy in a paracrine manner because: (i) conditioned medium from stimulated myofibroblasts, containing Hi-FGF-2 but undetectable levels of Lo-FGF-2, increased myocyte size, in a manner similar to that of recombinant rat Hi-FGF-2 and (ii) this effect was reversed by antibodies capable of neutralizing the activity of both Hi- and Lo-FGF-2. Thus, using the conditioned media from Ang II-stimulated cells, our data suggest that endogenous, paracrine-acting rat Hi-FGF-

2 would be capable of contributing to the Ang II-induced hypertrophy *in vivo*. There is correlative evidence that endogenous mouse Hi-FGF-2 plays a hypertrophic role *in vivo*: a strong Hi-FGF-2 upregulation was observed in the hearts of transgenic mice displaying exaggerated cardiac hypertrophy and fibrosis (Ahmadie *et al.*, 2010).

In addition to cardiomyocytes, extracellular-acting Hi-FGF-2 was shown to affect cardiac myofibroblasts specifically matricellular protein production. Using LC MS/MS analysis of myofibroblast secretome, validated by Western blot data with specific antibodies, we have shown that stimulation with Hi-FGF-2 is more potent than Lo-FGF-2 in stimulating secretion of several matricellular proteins by cardiac myofibroblasts. These include periostin, follistatin-like protein 1, plasminogen activator inhibitor-1, and tenascin C; these four proteins were selected for validation because they displayed pronounced upregulation by Hi-FGF-2.

Matricellular proteins are non-structural secreted glycoproteins that help cells communicate with their surrounding ECM (Frangogiannis, 2012). Unlike structural matrix proteins, they do not seem to be primary determinants of overall tissue architecture, however these proteins are induced following injury and modulate cell-cell and cell-matrix interactions and tissue remodeling (Frangogiannis, 2012). The role of FGF-2 isoform in matricellular protein accumulation and secretion has not been studied previously.

Stimulation with rat Hi-FGF-2 was observed to induce a more robust upregulation of periostin secretion in myofibroblasts, compared to Lo-FGF-2. Hi-

FGF-2 also promoted a significant increase in cell associated periostin; the effect of Lo-FGF-2 showed a trend towards increasing cell-associated periostin. In agreement with our findings from extracellular-acting FGF-2 isoforms, endogenous expression of only Hi-FGF-2, or Lo-FGF-2 in mouse embryonic fibroblasts was also associated with significant upregulation of cell-associated periostin. This effect was more pronounced in the presence of Hi-FGF-2 expression. It is of interest that complete lack of FGF-2 expression diminished periostin accumulation in MEFs. Thus FGF-2 expression and/or stimulation by extracellular-acting FGF-2 isoforms is required for periostin protein accumulation by myofibroblasts. Pilot studies (unpublished observations) suggested that Hi- or Lo-FGF-2 had no significant effect on the periostin mRNA levels, assessed by q-PCR, suggesting that the mechanism of periostin upregulation by FGF-2 is post-transcriptional. Lack of an observed effect at the mRNA level is in agreement with a previous study (Lindner *et al.*, 2005) reporting that Lo-FGF-2 stimulation had no effect on periostin mRNA levels in cells with relatively high levels of endogenous FGF-2 expression such as rat aortic smooth muscle cells. The ability of Hi-FGF-2, and to some extent Lo-FGF-2, to upregulate periostin is important in view of the critical role of periostin in tissue remodeling. Periostin is upregulated after injury, and while considered important for correct early tissue repair, it becomes deleterious/profibrotic if it remains chronically upregulated after the conclusion of the healing response (Conway *et al.*, 2014). In the heart, periostin is exclusively upregulated in the interstitium/non-myocytes during surgically induced pressure overload hypertrophy, contributes to pro-hypertrophic

signaling (Oka *et al.*, 2007). Loss of periostin at the late stages of healing from myocardial infarction was considered beneficial, reducing fibrosis and scar expansion (Oka *et al.*, 2007).

Plasminogen activator inhibitor 1 (PAI-1) was also preferentially upregulated by extracellular acting Hi-FGF-2 in rat myofibroblasts. PAI-1 is a secreted serine protease inhibitor, resulting, ultimately, in the prevention of plasmin production and MMP activation (Ghosh *et al.*, 2012). Levels of PAI-1 are elevated in fibrotic tissues, and it is believed that PAI-1 contributes to fibrogenesis by preventing degradation of matrix components (Ghosh *et al.*, 2012). Hi-FGF-2 may therefore contribute to a fibrotic response by upregulating PAI-1. It should be noted that cell-associated PAI-1 levels were found to be unaffected by endogenous expression of only Hi- or Lo-FGF-2 in MEFs. It is possible that signaling pathways leading to upregulation of PAI-1 are selectively activated by extracellular-acting Hi-FGF-2.

Tenascin C is another matricellular protein which is upregulated by Hi-FGF-2 stimulation in cardiac myofibroblasts and which is also known to be upregulated during tissue remodeling and inflammation *in vivo* (Imanaka-Yoshida, 2012). Tenascin C is not expressed in normal hearts but becomes upregulated in several pathologies, including after myocardial infarction (Nishioka *et al.*, 2010). Myocardial infarction patients with high serum levels of tenascin C are more likely to present with maladaptive cardiac remodeling and have poor prognosis (Sato *et al.*, 2006). There is evidence that tenascin C plays an adverse role in the remodeling process after myocardial infarction, as studies employing

targeted deletion of this protein reduced myocardial fibrosis and stiffness (Nishioka *et al.*, 2010). Tenascin C upregulation by extracellular-acting Hi-FGF-2 would therefore be expected to contribute to pathological changes in the heart. Tenascin C levels however were not affected by endogenous Hi-FGF-2 compared to Lo-FGF-2 expression in MEFs. It is possible that mouse MEFs respond differently than rat cardiac myofibroblasts in regards to tenascin C. Another possibility is that extracellular-acting added Hi-FGF-2 provided a stronger stimulus than does endogenously expressed Hi-FGF-2.

Follistatin-like protein 1 (FSTL1) secretion by rat myofibroblasts was also upregulated preferentially by Hi-FGF-2. FSTL1 is described as a cardiac tissue-secreted glycoprotein (“cardiokine”), and reported to exert beneficial, cardioprotective effects, suppressing cell death, and inflammation, during ischemia-reperfusion (Ogura *et al.*, 2012). FSTL1 has also been reported to prevent cardiomyocyte hypertrophy (Shimano *et al.*, 2011). Other studies show however that elevated serum FSTL1 levels in human heart failure patients were positively correlated with left ventricular hypertrophy (El-Armouche *et al.*, 2011). It is possible that FSTL1 upregulation represents a compensatory response during cardiac stress. Overall our data suggest that extracellular-acting Hi-FGF-2 is likely to play an important role in tissue remodeling, given its ability to upregulate secretion of proteins involved in modulating fibrosis and hypertrophy.

MEFs from FGF-2 transgenic mice were used to address the role of endogenous Hi- or Lo-FGF-2 on the expression/accumulation of selected extracellular matrix proteins. With the exception of periostin, where results from

exogenous addition were similar to those of endogenous expression of FGF-2 isoforms, expression/accumulation of PAI-1, tenascin C or FSTL1 did not change as a function of FGF-2 isoform expression. We examined the possibility that differential FGF-2 isoform expression in MEFs might have altered their degree of differentiation into myofibroblasts, which could result in differential regulation of extracellular matrix protein production. Endogenous expression of only Hi-FGF-2 (in K02 MEFs) was associated with elevated levels of pro-collagen I as well as EDA-Fibronectin, suggesting that endogenous expression of Hi-FGF-2 can promote some aspects of myofibroblast differentiation. On the other hand, endogenous expression of Hi- versus Lo-FGF-2 did not alter the expression of α -SMA, which is considered to be an important marker of myofibroblasts (Hinz *et al.*, 2007). Furthermore, complete lack of FGF-2 expression (in K01 MEFs) was associated with increased SMemb, which is also considered as a marker of myofibroblast differentiation. These pilot studies with MEFs from FGF-2 transgenic mice have not provided a clear answer as to their degree of differentiation into myofibroblasts. Endogenous expression of Hi- versus Lo-FGF-2 isoforms exerts complex regulation of proteins associated with myofibroblast differentiation. The role of endogenous Hi-FGF-2 versus Lo-FGF-2 expression in the process of fibroblast differentiation into myofibroblasts needs further investigation.

4.2 Human Hi-FGF-2

The high molecular weight isoforms of FGF-2 have been largely ignored in studies of human cardiac physiology and pathology. This is likely due to the

presumption that Hi-FGF-2 (unlike Lo-FGF-2) is not amongst the cytokines/growth factors that are secreted to the extracellular space and mediate tissue remodeling by an autocrine and/or paracrine mechanism. The present study challenges this perception by drawing attention to the expression and potential pathological role of Hi-FGF-2 in the human heart. We have shown, for the first time, that human Hi-FGF-2 (i) represents a substantial fraction of total FGF-2 in atrial tissue and in pericardial fluid, (ii) is exported to the extracellular space by human myofibroblasts, hMFs, (iii) is upregulated by Ang II via both AT-1R and AT-2R receptor-activated pathways, and (iv) can exert autocrine (pro-fibrotic, pro-inflammatory) and paracrine (pro-hypertrophic) biological activities. Human Hi-FGF-2 emerges therefore as a likely contributor to maladaptive cardiac remodeling *in vivo*.

4.2.1 Hi-FGF-2 in the human atria

The presence of Hi-FGF-2 in human atrial tissue extracts was documented by Western blotting-based detection of 22-22.5 and 24 kDa immunoreactive bands, in addition to the 18 kDa Lo-FGF-2, using well-characterized antibodies capable of detecting all FGF-2 isoforms. The sizes of immunoreactive bands were identical to those previously described in the literature (Arnaud *et al.*, 1999; Valtink *et al.*, 2012). All patient tissue extracts examined (n=60) contained both Hi- and Lo-FGF-2 isoforms, although the relative contribution, as well as absolute amount, of each type of isoform varied considerably between individuals. At this stage, and taking into account the

relatively small number of samples analyzed, no attempt was made to investigate whether a potential relationship exists between isoform distribution/concentration and patient age, gender, history, pathology or medications; a larger scale, targeted study will be required to address these issues.

Immunolocalization using anti-human Hi-FGF-2-specific antibodies corroborated the Western blotting data, and in addition showed that this protein was present in atrial cardiomyocytes, interstitial, fibroblastic cells, endothelial cells, and vimentin-positive cells at or near the epicardium. All of these cells are expected to contribute to the Hi-FGF-2 content of tissue lysates. Detection of Hi-FGF-2 in the cytosol of cardiomyocytes *in vivo*, and as discussed later, in the cytosol of cardiac myofibroblasts *in vitro*, goes against the commonly held notion that Hi-FGF-2 is an exclusively nuclear protein (Bugler *et al.*, 1991; Chlebova *et al.*, 2009), but is consistent with a potential for it to be exported by the expressing cells. Cardiac muscle cells are known to release FGF-2 to the extracellular space on a beat-to-beat basis, through transient disruptions of their plasma membrane (Clarke *et al.*, 1995). Detection of Hi-FGF-2 in the cytoplasm of atrial cardiomyocytes suggests that these cells might be a source of exported Hi-FGF-2 *in vivo*.

The presence of Hi-FGF-2, in addition to Lo-FGF-2, in human atria raised the question of functional roles of the different isoforms. Lo-FGF-2 is well documented to exert mitotic, cytoprotective, as well as angiogenic effects in animal models as well as humans (Kardami *et al.*, 2007). To begin addressing the function, as well as regulation, of human Hi-FGF-2, a series of *in vitro*

experiments were conducted investigating the expression and secretion of Hi-FGF-2 (compared to Lo-FGF-2) by cells such as hMFs that play a central role in tissue remodeling. Potential biological activities of extracellular-acting Hi-FGF-2 relating to tissue remodeling were also investigated.

4.2.2 Expression of human Hi-FGF-2 in hMFs

Fibroblasts are responsible for the production and homeostasis of the extracellular matrix in normal tissue. Various stress stimuli, such as chronic adrenergic or neurohumoral stimulation, as well as ischemia and reperfusion damage, promote the transformation of fibroblasts to the hypersynthetic, hypersecretory and hypercontractile myofibroblast phenotype. While myofibroblasts are important in cardiac repair and scar formation, persistent presence of these cells plays a central role in maladaptive remodeling and eventual failure (Porter *et al.*, 2009; Weber *et al.*, 2013). The primary hMF cultures used in the present study model the 'activated fibroblast', myofibroblast, phenotype (Santiago *et al.*, 2010).

Human myofibroblasts were found to express predominantly Hi-FGF-2, at over 80% of total FGF-2. All human Hi-FGF-2 isoforms, namely the 22, 22.5, 24 and 34 kDa proteins were produced by hMFs. The 34 kDa FGF-2 is a uniquely human isoform, which has not been detected previously in primary, non-transformed cells (Arnaud *et al.*, 1999; Valtink *et al.*, 2012). It is possible that expression of 34 kDa FGF-2 occurs preferentially in human myofibroblasts, as it was not detected in primary human endothelial cells. The functional role of 34

kDa FGF-2 is currently unknown, although overexpression studies have suggested that it enhances cell survival (Arnaud *et al.*, 1999; Valtink *et al.*, 2012).

4.2.3 The role of Ang II signaling in human Hi-FGF-2 accumulation by hMFs

Ang II upregulated human Hi-FGF-2 accumulation in hMFs, suggesting that Hi-FGF-2 may contribute to the diverse cardiac pathologies associated with Ang II elevation *in vivo*. Chronic activation of the renin angiotensin system causes maladaptive cardiac remodeling including fibrosis and hypertrophy in ventricles as well as atria (Boldt *et al.*, 2006), and is managed by angiotensin converting enzyme (ACE) inhibitors and/or Ang II receptor AT-1 antagonists (Bommer, 2008). The beneficial effects of ACE inhibitors and AT-1R receptor antagonists on patients could be attributed, to some extent, to a reduction in Hi-FGF-2 levels, as losartan attenuated the Ang II-induced human Hi-FGF-2 upregulation. Nevertheless, as shown here, AT-2R was also implicated in the Ang II-induced Hi-FGF-2 upregulation, and would be expected to sustain elevated Hi-FGF-2 expression even when AT-1R is blocked. The role of AT-2R in cardiac pathology is poorly understood. It is generally believed that, unlike AT-1R, AT-2R has beneficial effects counteracting several of the effects triggered by AT-1R (Aranguiz-Urroz *et al.*, 2009; Porrello *et al.*, 2009). On the other hand, there is some evidence that AT-2R may exert similar effects as AT-1R, by mediating left ventricular hypertrophy and fibrosis in Ang II-induced hypertensive disease (Ichihara *et al.*, 2001). It is of interest that unlike AT-1R, AT-2R levels are elevated in fibrillating and fibrotic atria and also in the failing heart (Tsutsumi *et*

al., 1998; Goette *et al.*, 2000), a situation that might perpetuate a pathology-inducing stimulus by upregulating Hi-FGF-2.

The signal transduction pathway(s) leading to increased human Hi-FGF-2 accumulation downstream of Ang II /AT-1R or Ang II/AT-2R remain to be determined. While both AT-1R and AT-2R belong to the G protein-coupled receptor superfamily, they are known to activate different downstream pathways. AT-1R is linked to growth factor signaling pathways, requiring tyrosine kinase receptors, and kinase-driven phosphorylations, while AT-2R is linked to activation of several types of phosphatases that are believed to counteract the phosphorylation events induced by AT-1R; for a detailed description of Ang II receptor signaling pathways the readers are referred to (Lemarie *et al.*, 2010). The present study shows that the Ang II-induced Hi-FGF-2 upregulation requires the ERK activating pathway, in agreement with previous work regarding expression of FGF-2 of unknown isoform composition by cardiac fibroblasts (Tholozan *et al.*, 2007; Thum *et al.*, 2008). In addition, both AT-1R and AT-2R were found to mediate the Ang II-induced ERK activation. While AT-1R has been linked to the Ang II-induced activation of ERK (Hunyady *et al.*, 2006), AT-2R is reported to inhibit the AT-1R-induced ERK activation (Cui *et al.*, 2001). In other cell models, AT-2R is reported to activate the ERK pathway (Stroth *et al.*, 2000), in agreement with our present findings. Endogenous FGF-2 expression would also be expected to contribute to overall levels of activated ERK in hMFs via both intracrine and autocrine routes, as we have documented in previous studies (Ma *et al.*, 2007). In agreement, inhibition of extracellular-acting FGF-2 in our system

decreased the magnitude of Ang-II-associated ERK activity, which decreased further, and significantly, with concurrent inhibition of AT-1R and/or AT-2R. We suggest that the ability of Ang II to upregulate FGF-2/Hi-FGF-2 requires ERK activation which occurs downstream of AT-1R and/or AT-2R as well as downstream from extracellular-acting FGF-2.

Inhibition of MMP activity was found to prevent the Ang II-induced Hi-FGF-2 upregulation in hMFs, but the timing and immediate targets of MMP action are not known. MMP activity is reported to mediate the Ang II-induced secretion of several cytokines (IL-6, IL-1 β , tumor necrosis factor α , transforming growth factor β) by cardiac fibroblasts (Jaffre *et al.*, 2009); and FGF-2 release from the extracellular matrix of the lens (Tholozan *et al.*, 2007). It remains to be determined whether MMP inhibition prevents the release of cytokines and growth factors, including FGF-2, by hMFs, and therefore blocked an autocrine and/or auto-stimulatory component in the Ang II-induced FGF-2, and Hi-FGF-2 upregulation. In addition, extracellular-acting FGF-2 had no effect on MMP-2 activity as shown in Figure 23/M2-FigS7. Other MMPs, such as MMP-9, can also mediate the effects of Ang II. Thus, future studies are required to investigate if other MMPs (MMP-9 and/or MT-MMP) are affected by extracellular-acting FGF-2. In addition, there have been concerns that zymography does not measure activity of MMP-2 directly but rather only measures the levels, thus future studies should include ELISA-based approaches.

4.2.4 Secretion/release of human Hi-FGF-2

We have shown for the first time that human Hi-FGF-2 is released to the extracellular environment by cardiac cells, hMFs, *in vitro*, and that Ang II elicited a significant increase in exported Hi-FGF-2, which paralleled the increase in total cell-associated Hi-FGF-2. In addition, it would appear that, as in rat myofibroblasts, caspase-1 activity is required for the export of human Hi-FGF-2, linking human Hi-FGF-2 production to the innate inflammation response.

Detection of Hi-FGF-2 in patient pericardial fluid (Figure 24C) demonstrated that, in addition to Lo-FGF-2, Hi-FGF-2 can also be released or secreted by cells *in vivo*. This is in apparent contrast to a previous report that only the 18 kDa Lo-FGF-2 is secreted into the pericardial fluid (Corda *et al.*, 1997). A likely explanation for the discrepancy may be the inadequate prevention of proteolysis, which can occur even when FGF-2 is bound to heparin-Sepharose. This proteolysis converts Hi-FGF-2 to a Lo-FGF-2-like protein, by truncating the N-terminal extension (Doble *et al.*, 1990). The ELISA-based approaches widely used for measuring FGF-2 in biological fluids do not distinguish between isoforms.

The exact cellular source of Hi- and Lo-FGF-2 in pericardial fluid is not currently known. The pericardial fluid in addition to being a passive ultrafiltrate of plasma, can also reflect the composition of cardiac interstitium, and the local production of bioactive molecules (growth factors, brain natriuretic peptides) in health and disease (Corda *et al.*, 1997; Fujita *et al.*, 1998; Tanaka *et al.*, 1998). In humans, the FGF-2 concentration in pericardial fluid was 20-fold higher than in serum, correlating with high FGF-2 content in atrial biopsies, suggestive of local,

myocardial production (Corda *et al.*, 1997). Based on available information, we suggest that all cardiac cells are capable of releasing Hi-FGF-2 to the interstitial space, either through injury or via a regulated export process, would be expected to contribute to the FGF-2 content and isoform composition in the myocardium as well as the pericardial fluid. One can extrapolate that during the development of hypertrophic and fibrotic heart disease hypersecretory myofibroblastic cells would be likely to increase interstitial and pericardial Hi-FGF-2 content.

The function of Hi-FGF-2 in the pericardial fluid, which bathes the heart and thus allows for, potentially, a broader range of action compared to matrix-retained proteins, remains to be investigated. Based on our *in vitro* studies discussed in the following section, it is reasonable to expect that Hi-FGF-2 in pericardial fluid may contribute to cardiomyocyte hypertrophy even in the presence of Lo-FGF-2.

4.2.5 Biological activity of human Hi-FGF-2

We have shown, for the first time, that human Hi-FGF-2 displays pro-fibrotic as well as pro-inflammatory potential. In primary hMF cultures it was found that endogenous, extracellular-acting human Hi-FGF-2 promotes or maintains the activated fibroblast phenotype, as well as upregulating periostin accumulation and therefore can be considered as pro-fibrotic. Treatment of hMFs with neu-Ab^{Hi-FGF-2}, expected to blunt the autocrine action of Hi-FGF-2, but not Lo-FGF-2, elicited significant decreases in α -SMA, EDA-Fibronectin, SMemb, procollagen, and periostin, without affecting housekeeping proteins. Alpha-SMA

represents a widely used marker for the myofibroblast contractile phenotype (Dobaczewski *et al.*, 2010), while EDA-Fibronectin is considered pro-fibrotic and pro-inflammatory (Muro *et al.*, 2008). Decreased levels of α -SMA when the extracellular action of Hi-FGF-2 is neutralized suggests that endogenous Hi-FGF-2 stimulates α -SMA accumulation in an autocrine fashion. This finding is in contrast with the effect of extracellular-acting Lo-FGF-2, reported to decrease α -SMA expression in interstitial cells (Maltseva *et al.*, 2001; Cushing *et al.*, 2008) and represents a novel, distinct activity for Hi- compared to Lo-FGF-2.

Another novel finding is the ability of extracellular-acting recombinant human Hi-FGF-2 to robustly upregulate proteins linked with the innate inflammatory signaling pathway such as pro-IL-1 β and PAI-1. IL-1 β is an early mediator and prominent marker of inflammation (Turner *et al.*, 2013). IL-1 β is expressed as inactive precursor, pro-IL-1 β , which is then converted to the mature, active form by the inflammasome-activated cysteine protease caspase-1 (Dinarello, 2002). Kawaguchi and colleagues have demonstrated that inflammasome activation, and hence IL-1 β production, occurs in cardiac fibroblasts, not in cardiomyocytes, and represents a crucial step in the initial inflammatory response after myocardial injury (Kawaguchi *et al.*, 2011). Lo-FGF-2 was also found to upregulate pro-IL-1 β in hMFs, however the effect was much less pronounced compared to Hi-FGF-2. In addition, unlike Hi-FGF-2, Lo-FGF-2 had no discernible effect on the accumulation of PAI-1 by hMFs. PAI-1 is a member of the serine protease inhibitor gene family and the major physiological inhibitor of the serine proteases, urokinase-type plasminogen activator, and

tissue-type plasminogen activator. Increased levels of PAI-1 are implicated in a number of pathophysiological complications including fibrosis and inflammation (Ghosh *et al.*, 2012). It is of interest that Ang II has also been reported to upregulate PAI-1 expression (Kawano *et al.*, 2000), as well as IL-1 β (Xu *et al.*, 2011). These effects of Ang II may be mediated or reinforced by the Ang II-induced Hi-FGF-2 increases shown here.

The mechanism by which extracellular-acting Hi- and Lo-FGF-2 exert differential effects on cardiac hMFs and myocytes need to be identified. Previous studies have indicated that Hi- and Lo-FGF-2 isoforms are similarly potent in activating the tyrosine kinase FGF-2 cell surface receptors (FGFR) and pathways downstream of FGFR (Piotrowicz *et al.*, 1999). This would suggest that differential effects are not mediated by differences in receptor binding or activation. It should, however, be noted, that the FGFR family has many members, not only products of different genes, but also products of differential splicing, and subjected to variable degrees of post-translational modifications (Eswarakumar *et al.*, 2005). There is as yet no information as to which FGFR isoform(s) are expressed by activated human cardiac myofibroblasts, or whether they may display isoform-specific preferences. It should also be noted that extracellular FGF-2-triggered signal transduction includes not only plasma membrane FGFR-mediated signals (which may be common between Hi- and Lo-FGF-2) but also direct nuclear signals exerted by internalized FGF-2, which may be isoform-specific. It is of relevance that Hi- and Lo-FGF-2 localize to distinct

nuclear locations, and have been proposed to exert distinct effects on nuclear function (Claus *et al.*, 2003).

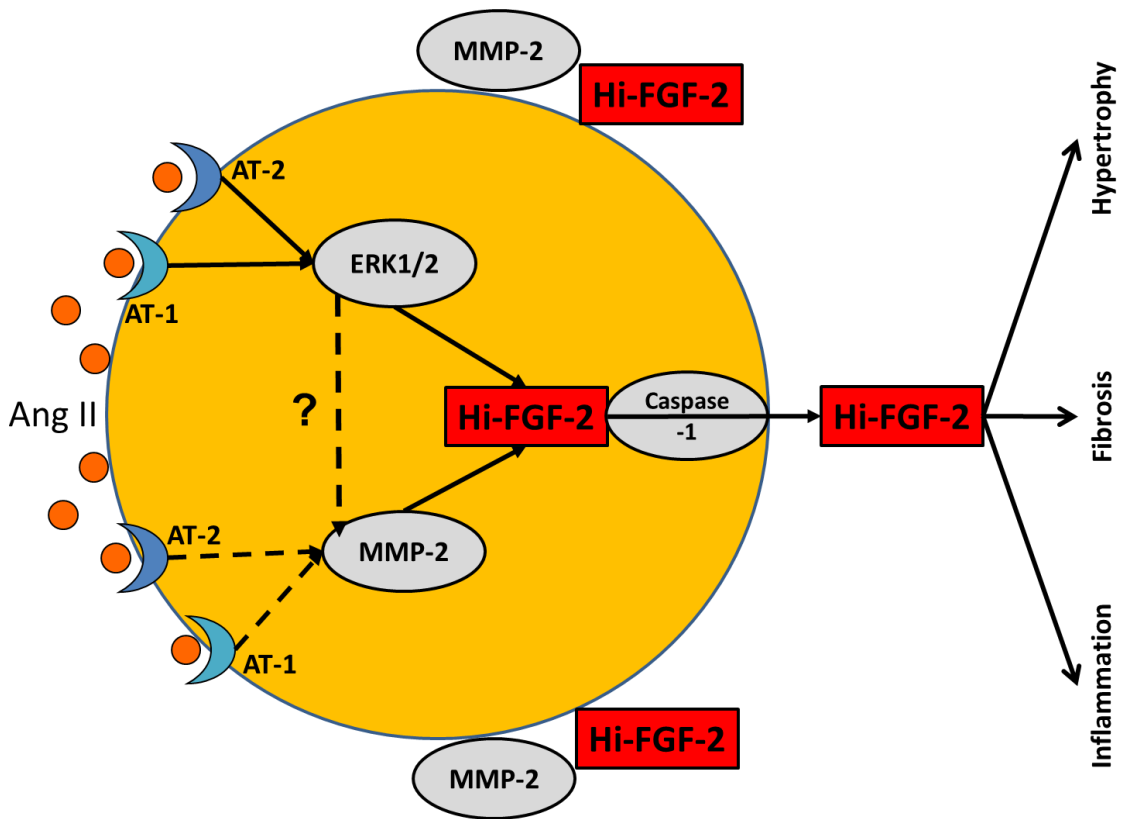
Extracellular-acting human Hi-FGF-2, either recombinant or endogenously produced, was found to be pro-hypertrophic *in vitro*, similar to rat Hi-FGF-2 (Jiang *et al.*, 2007). It is therefore reasonable to expect that just like rat Hi-FGF-2, human Hi-FGF-2, but not Lo-FGF-2, is likely to play a pro-hypertrophic role in the human heart *in vivo*. The relative total and Hi-FGF-2 levels in human heart-derived hMFs were found to be 4-fold higher than those of their rat counterparts, suggesting a potential for a more prominent role for Hi-FGF-2 in humans as compared to rodent models. We propose that selective neutralization of secreted Hi-FGF-2 in humans would be expected to prevent or attenuate fibrosis and hypertrophy without affecting beneficial (cytoprotective and angiogenic) effects of co-expressed Lo-FGF-2.

Chapter 5: Conclusions: Clinical Relevance and Future Directions

We have conducted a series of studies addressing aspects of the biology of FGF-2 isoforms in rodent (mainly rat) and human hearts. Major findings were similar between myofibroblasts from rat and human species. We have demonstrated that cardiac myofibroblasts, major cell populations in the chronically stressed heart, predominantly express and export the Hi-FGF-2 isoform, via a caspase-1-mediated export pathway. Extracellular-acting Hi-FGF-2 has pro-hypertrophic, pro-fibrotic, and pro-inflammatory activities: in both rat and human myofibroblasts, extracellular-acting Hi-FGF-2 upregulated periostin, and PAI-1. Periostin is linked to the induction of cardiac hypertrophy and fibrosis, while PAI-1 is linked to fibrosis and inflammation. Pilot MS/MS data indicated that extracellular-acting rat Hi-FGF-2 is more potent than Lo-FGF-2 in upregulating extracellular levels of fibrillar collagens; a positive link between collagen I and Hi-FGF-2 stimulation was also observed in human cells. Further studies with the secretome analysis is highly warranted in regards to the other proteins indicated by the thermal map, for example proteins that were downregulated, which may also shed insights to the isoform specific effects of FGF-2. In addition, total and Hi-FGF-2 accumulation and export were shown to be upregulated by the Ang II/AT-1R receptor axis. Current treatments for heart disease that target AT-1R activity would be predicted to also reduce endogenous Hi-FGF-2 levels and associated detrimental effects.

In contrast to our findings with rat ventricular myofibroblasts, human Hi-FGF-2 upregulation by Ang II was also mediated by the AT-2R. This may

represent a species-specific difference or may reflect tissue of origin such as ventricle (rat) versus atria (human). Thus, it will be important to determine the role of AT-2R in Hi-FGF-2 production in rat atrial myofibroblasts and human ventricular myofibroblasts to resolve this issue. Nonetheless, the schematic diagram below depicts the major findings of the thesis with respect to Hi-FGF-2:



Summary of signaling pathways leading to the upregulation and secretion of human Hi-FGF-2. The Ang II-induced accumulation of Hi-FGF-2 is dependent on AT-1 and AT-2 receptors as well as ERK1/2 and MMP-2 activities. The secretion of Hi-FGF-2 is dependent on Caspase-1 activity. Extracellular-acting Hi-FGF-2 is pro-hypertrophic, pro-fibrotic, and pro-inflammatory. Whether the activity of MMP-2 is dependent on activation of ERK1/2 is still unknown in human cardiac myofibroblasts.

The work done in this thesis is mostly based on *in vitro* work using rat and human cardiac myofibroblasts. Findings presented from *in vitro* studies will thus need to be validated in *in vivo* models. Another limitation of our studies is the fact that the isolated cells were cultured on non-compliant plates. Appropriate 3-D gel culture system can offer a more compliant extracellular matrix that is closer to the *in vivo* environment than culture dish and may reveal novel isoform specific effects of FGF-2 not seen in our work. Furthermore, atrial tissues were collected from patients undergoing coronary bypass surgery indicated that existing medical conditions are present. Analysis of the patient demographics may correlate the expression of Hi- versus Lo-FGF-2 to specific diseases.

Our studies have described all Hi-FGF-2 isoforms under the generic term “Hi-FGF-2”. Future studies should address potentially the distinct functions of the 21-23 kDa Hi-FGF-2 isoforms in the rat or the 22-34 kDa in human. The role of the uniquely human 34 kDa Hi-FGF-2 isoform, which was present in all human primary myofibroblast cultures, remains completely unknown and merits further investigation. Better understanding of the translational and post-translational regulation of FGF-2 isoforms is needed to be able to selectively regulate their accumulation and function. Interacting factors associated exclusively with Hi-FGF-2 may provide clues regarding the elusive translational regulation of FGF-2. Worked done in supervisor’s laboratory has shown that eukaryotic initiation factor-3 (eIF3) and heterogeneous nuclear ribonucleoprotein A1 (hnRNP A1) are associated with specifically to Hi-FGF-2. In addition, hnRNP A1, involved in pre-mRNA processing, has been shown to bind to hairpin-loop structures within the

FGF-2 mRNA and control the initiation of translation of FGF-2 (Bonnal *et al.*, 2005). Future studies on the translational regulation of FGF-2 are highly warranted. Furthermore, elucidation of the mechanism by which Hi- and Lo-FGF-2 exert their distinct biological effects would provide a means to selectively modulate their activities.

In conclusion, we have confirmed our hypotheses, and have clearly documented that endogenous Hi-FGF-2, considered by many to exert exclusively nuclear intracrine activities can also be released into the extracellular environment in both physiological and pathological conditions indicating a paracrine and autocrine mode of action. Furthermore, we have validated our findings using human tissues, pericardial fluid, and human atrial-derived myofibroblasts, rendering this clinically relevant with translational potential, particularly in patients with atrial fibrillation. Thus, the regulation of Hi-FGF-2 expression and release by cardiac non-myocyte myofibroblasts provides a possible therapeutic target to combat heart disease.

Chapter 6 References

- Abraham JA, Mergia A, Whang JL, Tumolo A, Friedman J, Hjerrild KA, et al.** Nucleotide sequence of a bovine clone encoding the angiogenic protein, basic fibroblast growth factor. *Science* 1986; 233:545-548.
- Ahmadie R, Santiago JJ, Walker J, Fang T, Le K, Zhao Z, et al.** A High-Lipid Diet Potentiates Left Ventricular Dysfunction in Nitric Oxide Synthase 3-Deficient Mice after Chronic Pressure Overload. *J Nutr* 2010; 140:1438-1444.
- Amerlin HA.** Pituitary extracts and steroid hormones in the control of 3T3 cell growth. *Proc Natl Acad Sci USA* 1973; 70:2702-2706.
- Anderson JE, Liu L, Kardami E.** Distinctive patterns of basic fibroblast growth factor (bFGF) distribution in degenerating and regenerating areas of dystrophic (mdx) striated muscles. *Dev Biol* 1991; 147:96-109.
- Anderson KR, Sutton MG, Lie JT.** Histopathological types of cardiac fibrosis in myocardial disease. *J Pathol* 1979; 128:79-85.
- Aranguiz-Urroz P, Soto D, Contreras A, Troncoso R, Chiong M, et al.** Differential participation of angiotensin II type 1 and 2 receptors in the regulation of cardiac cell death triggered by angiotensin II. *Am J Hypertens* 2009; 22:569-576.
- Arese M, Chen Y, Florkiewicz RZ, Gualandris A, Shen B and Rifkin DB.** Nuclear activities of basic fibroblast growth factor: potentiation of low-serum growth mediated by natural or chimeric nuclear localization signals. *Mol Biol Cell* 1999; 10:1429-1444.
- Arnaud E, Touriol C, Boutonnet C, Gensac MC, Vagner S, Prats H, et al.** A new 34-kilodalton isoform of human fibroblast growth factor 2 is cap dependently synthesized by using a non-AUG start codon and behaves as a survival factor. *Mol Cell Biol* 1999; 19:505-514.
- Azhar M, Yin M, Zhou M, Li H, Mustafa M, Nusayr E, et al.** Gene targeted ablation of high molecular weight fibroblast growth factor-2. *Dev Dyn* 2009; 238(2):351-357.
- Baird A, Walicke PA.** Fibroblast growth factors. *Br Med Bull* 1989; 45:438-452.
- Berry C, Touyz R, Dominiczak AF, Webb RC, Johns DG.** Angiotensin receptors: signaling, vascular pathophysiology, and interactions with ceramide. *Am J Physiol Heart Circ Physiol* 2001; 281:H2337-2365.

Bertrand S, Somorjai I, Garcia-Fernandez J, Lamonerie T, Escriva H. *BMC Evol Biol* 2009; 9:226.

Biernacka A, Dobaczewski M, Frangogiannis NG. TGF- β signaling in fibrosis. *Growth Factors* 2011; 29:196-202.

Biernacka A, Frangogiannis NG. Aging and cardiac fibrosis. *Aging Dis* 2011; 2:158-173.

Bikfalvi A, Klein S, Pintucci G and Rifkin DB. Biological roles of fibroblast growth factor-2. *Endocr Rev* 1997; 18:26-45.

Boldt A, Scholl A, Garbade J, Resetar ME, Mohr FW, Gummert JF, et al. ACE-inhibitor treatment attenuates atrial structural remodeling in patients with lone chronic atrial fibrillation. *Basic Res Cardiol* 2006; 101:261-267.

Bommer WJ. Use of angiotensin-converting enzyme inhibitor/angiotensin receptor blocker therapy to reduce cardiovascular events in high-risk patients: part 2. *Prev Cardiol* 2008; 11:215-222.

Bonnal S, Schaeffer C, Creancier L, Clamens S, Moine H, Prats AC, et al. A single internal ribosome entry site containing a G quartet RNA structure drives fibroblast growth factor 2 gene expression at four alternative translation initiation codons. *J Biol Chem* 2003; 278:39330-39336.

Bonnal S, Pileur F, Orsini C, Parker F, Pujol F, Prats AC, et al. Heterogenous nuclear ribonucleoprotein A1 is a novel internal ribosome entry site trans-acting factor that modulates alternative initiation of translation of the fibroblast growth-2 mRNA. *J Biol Chem* 2005; 280:4144-4153.

Bornstein P, Sage EH. Matricellular proteins: extracellular modulators of cell function. *Curr Opin Cell Biol* 2002; 14:608-616.

Bossard C, Laurell H, Van den Berghe L, Meunier S, Zanibellato C, Prats H. Translokin is an intracellular mediator of FGF-2 trafficking. *Nat Cell Biol* 2003; 5:433-439.

Bouche G, Gas N, Prats H, Baldin V, Tauber JP, Teissie J, et al. Basic fibroblast growth factor enters the nucleolus and stimulates the transcription of ribosomal genes in ABAE cells undergoing G0---G1 transition. *Proc Natl Acad Sci USA* 1987; 84:6770-6774.

Brilla CG, Zhou G, Matsubara L, Weber KT. Collagen metabolism in cultured adult rat cardiac fibroblasts: response to angiotensin II and aldosterone. *J Mol Cell Cardiol* 1994; 26:809-820.

Bruns AF, Grothe C, Claus P. Fibroblast growth factor-2 (FGF-2) is a novel substrate for arginine methylation by PRMT5. *Biol Chem* 2009; 390:59-65.

Bugler B, Amalric F, Prats H. Alternative initiation of translation determines cytoplasmic or nuclear localization of basic fibroblast growth factor. *Mol Cell Biol* 1991; 11:573-577.

Burstein B, Libby E, Calderone A, Nattel S. Differential behaviors of atrial versus ventricular fibroblasts: a potential role for platelet-derived growth factor in atrial-ventricular remodeling differences. *Circulation* 2008; 117:1630-1641.

Camelliti P, Devlin GP, Matthews KG, Kohl P, Green CR. Spatially and temporally distinct expression of fibroblast connexins after sheep ventricular infarction. *Cardiovasc Res* 2204; 62:415-425.

Campbell SE, Katwa LC. Angiotensin II stimulated expression of transforming growth factor-beta 1 in cardiac fibroblasts and myofibroblasts. *J Mol Cell Cardiol* 1997; 29:1947-1958.

Chen VC, Kristensen AR, Foster LJ, Naus CC. Association of connexin43 with E3 ubiquitin ligase TRIM21 reveals a mechanism for gap junction phosphodegron control. *J Proteome Res* 2012; 11:6134-6146.

Chlebova K, Bryja V, Dvorak P, Kozubik A, Wilcox WR, Krejci P. High molecular weight FGF2: the biology of a nuclear growth factor. *Cell Mol Life Sci* 2009; 66:225-235.

Chua CC, Rahimi N, Forsten-Williams K, Nugent MA. Heparan sulfate proteoglycans function as receptors for fibroblast growth factor-2 activation of extracellular signal-regulated kinases 1 and 2. *Circ Res* 2004; 94: 316-323.

Cilvik SN, Wang JI, Lavine KJ, Uchida K, Castro A, Gierasch CM, et al. Fibroblast growth factor receptor 1 signaling in adult cardiomyocytes increases contractility and results in a hypertrophic cardiomyopathy. *PLoS One* 2013; 8:e82979.

Clarke MS, Caldwell RW, Chiao H, Miyake K, McNeil PL. Contraction-induced cell wounding and release of fibroblast growth factor in heart. *Circ Res* 1995; 76:927-934.

Claus P, Doring F, Gringel S, Muller-Ostermeyer F, Fuhrlrott J, et al. Differential intranuclear localization of fibroblast growth factor-2 isoforms and specific interaction with the survival of motoneuron protein. *J Biol Chem* 2003; 278:479-485.

- Conway SJ, Molkentin D.** Periostin as a heterofunctional regulator of cardiac development and disease. *Curr Genomics* 2008; 9:548-555.
- Conway SJ, Izuhara K, Kudo Y, Litvin J, Markwals R, Ouyang G, et al.** The role of periostin in tissue remodeling across health and disease. *Cell Mol Life Sci* 2014; 71:1279-1288.
- Conda S, Mebazaa A, Gandolfini MP, Fitting C, Marotte F, et al.** Trophic effect of human pericardial fluid on adult cardiac myocytes. Differential role of fibroblast growth factor-2 and factors related to ventricular hypertrophy. *Circ Res* 1997; 81:679-687.
- Cui T, Nakagami H, Iwai M, Takeda Y, Shiuchi T, et al.** Pivotal role of tyrosine phosphatase SHP-1 in AT2 receptor-mediated apoptosis in rat fetal vascular smooth muscle cell. *Cardiovasc Res* 2001; 49:863-871.
- Cushing MC, Mariner PD, Liao JT, Sims EA, Anseth KS.** Fibroblast growth factor represses Smad-mediated myofibroblast activation in aortic valvular interstitial cells. *FASEB J* 2008; 22:1769-1777.
- Davis J, Molkentin JD.** Myofibroblasts: Trust your heart and let fate decide. *J Mol Cell Cardiol* 2014; 70:9-18.
- Delrieu I.** The high molecular weight isoforms of basic fibroblast growth factor (FGF-2): an insight into an intracrine mechanism. *FEBS Lett* 2000; 468:6-10.
- Dinarello CA.** The IL-1 family and inflammatory diseases. *Clin Exp Rheumatol* 2002; 20:S113.
- Ding L, Donate F, Parry GC, Guan X, Maher P, Levin EG.** Inhibition of cell migration and angiogenesis by the amino-terminal fragment of 24kD basic fibroblast growth factor. *J Biol Chem* 2002; 277:31056-31061.
- Dobaczewski M, Gonzalez-Quesada C, Frangogiannis NG.** The extracellular matrix as a modulator of the inflammatory and reparative response following myocardial infarction. *J Mol Cell Cardiol* 2010; 48:504-511.
- Doble BW, Fandrich RR, Liu L, Padua RR, Kardami E.** Calcium protects pituitary basic fibroblast growth factors from limited proteolysis by co-purifying proteases. *Biochem Biophys Res Commun* 1990; 173:1116-1122.
- Doble BW, Kardami E.** Basic fibroblast growth factor stimulates connexin-43 expression and intercellular communication of cardiac fibroblasts. *Mol Cell Biochem* 1995; 143:81-87.

Doble BW, Chen Y, Bosc DG, Litchfield DW, Kardami E. Fibroblast growth factor-2 decreases metabolic coupling and stimulates phosphorylation as well as masking of connexin43 epitopes in cardiac myocytes. *Circ Res* 1996; 79:647-658.

Doble BW, Dang X, Ping P, Fandrich RR, Nickel BE, et al. Phosphorylation of serine 262 in the gap junction protein connexin-43 regulates DNA synthesis in cell-cell contact forming cardiomyocytes. *J Cell Sci* 2004; 117:507-514.

Dono R, Texido G, Dussel R, Ehmke H and Zeller R. Impaired cerebral cortex development and blood pressure regulation in FGF-2-deficient mice. *Embo J* 1998; 17:4213-4225.

Dorn GW, 2nd. The fuzzy logic of physiological cardiac hypertrophy. *Hypertension* 2007; 49: 962-970.

Dunham-Ems SM, Lee YW, Stachowiak EK, Pudavar H, Claus P, Prasad PN, et al. Fibroblast growth factor receptor-1 (FGFR1) nuclear dynamics reveal a novel mechanism in transcription control. *Mol Biol Cell* 2009; 20:2401-2412.

Ebert AD, Laussmann M, Wegehingel S, Kaderali L, Erfle H, Reichert J, et al. Tec-kinase-mediated phosphorylation of fibroblast growth factor 2 is essential for unconventional secretion. *Traffic* 2010; 11:813-826.

El-Armouche A, Ouchi N, Tanaka K, Doros G, Wittkopper K, Schulze T, et al. Follistatin-like 1 in chronic systolic heart failure: a marker of left ventricular remodeling. *Circ Heart Fail* 2011; 4:621-627.

Eswarakumar VP, Lax I, Schlessinger J. Cellular signaling by fibroblast growth factor receptors. *Cytokine Growth Factor Rev* 2005; 16:139-149.

Fedak PW, Bai L, Turnbull J, Ngu J, Narine K, Duff HJ. Cell therapy limits myofibroblast differentiation and structural cardiac remodeling: basic fibroblast growth factor-mediated paracrine mechanism. *Circ Heart Fail* 2012; 5:349-356.

Ferrario CM. Role of angiotensin II in cardiovascular disease therapeutic implications of more than a century of research. *Journal of Renin-Angiotensin-Aldosterone System* 2006; 7:3-14.

Foletti A, Vuadens F and Beermann F. Nuclear localization of mouse fibroblast growth factor 2 requires N-terminal and C-terminal sequences. *Cell Mol Life Sci* 2003; 60:2254-2265.

Frangogiannis NG. Matricellular proteins in cardiac adaptation and disease. *Physiol Rev* 2012; 92:635-688.

Frey N , Olson EN. Cardiac hypertrophy: the good, the bad, and the ugly. *Annu Rev Physiol* 2003; 65:45-79.

Fujita M, Ikemoto M, Tanaka T, Tamaki S, Yamazato A, et al. Marked elevation of vascular endothelial growth factor and basic fibroblast growth factor in pericardial fluid of patients with angina pectoris. *Angiogenesis* 1998; 2:05-108.

Galvez-Contreras AY, Gonzalez-Casteneda RE, Luquin S, Guzman-Muniz J, Quinones-Hinojosa A, Moy-Lopez NA, et al. Diphenylhydantoin promotes proliferation in the subventricular zone and dentate gyrus. *Am J Neurosci* 2012; 3:1-9.

Galy B, Creancier L, Prado-Lourenco L, Prats AC, Prats H. p53 directs conformational change and translation initiation blockade of human fibroblast growth factor 2 mRNA. *Oncogene* 2001; 20:4613-4620.

Galzie Z, Kinsella AR, Smith JA. Fibroblast growth factors and their receptors. *Biochem Cell Biol* 1997; 75: 69-685.

Ghosh AK, Vaughan DE. PAI-1 in tissue fibrosis. *J Cell Physiol* 2012; 227:493-507.

Goette A, Arndt M, Rådcken C, Spiess A, Staack T, et al. Regulation of Angiotensin II Receptor Subtypes During Atrial Fibrillation in Humans. *Circulation* 2000; 101:2678-2681.

Gospodarowicz D, Jones KL, Sato G. Purification of a growth factor for ovarian cells from bovine pituitary glands. *Proc Natl Acad Sci USA* 1974; 71:2295-2296.

Gray MO, Long CS, Kalinyak JE, Li HT, Karliner JS. Angiotensin II stimulates cardiac hypertrophy via paracrine release of TGF β 1 and endothelin-1 from fibroblasts. *Cardiovasc Res* 1998; 40:352-363.

Hasenfuss G. Animal models of human cardiovascular disease, heart failure and hypertrophy. *Cardiovasc Res* 1998; 39:60-76.

Heim A, Zeuke S, Weiss S, Ruschewski W, Grumbach IM. Transient induction of cytokine production in human myocardial fibroblasts by coxsackievirus B3. *Circ Res* 2000; 86:753-759.

Hinescu ME, Gherghiceanu M, Mandache E, Ciontea SM, Popescu LM. Interstitial Cajal-like cells (ICLC) in atrial myocardium: ultrastructural and immunohistochemical characterization. *J Cell Mol Med* 2006; 10:243-257.

Hinz B, Phan SH, Thannickal VJ, Galli A, Bochaton-Piallat ML, Gabbiani G. The myofibroblasts: one function, multiple origins. *Am J Pathol* 2007; 170:18007-18016.

Hinz B, Gabbiani G. Fibrosis: recent advances in myofibroblasts biology and new therapeutic perspectives. *Biol Rep* 2010; 2:78.

Hirst CJ, Herlyn M, Cattini PA, Kardami E. High levels of CUG-initiated FGF-2 expression cause chromatin compaction, decreased cardiomyocyte mitosis, and cell death. *Mol Cell Biochem* 2003; 246: 111-116.

Hoerstrup SP, Zund G, Schnell AM, Kolb SA, Visjager JF, Schoeberlein A, et al. Optimized growth conditions for tissue engineering of human cardiovascular structures. *Int J Artif Organs* 2000; 23:817-823.

Hunter JJ, Chien KR. Signaling pathways for cardiac hypertrophy and failure. *N Engl J Med* 1999; 341:1276-1286.

Hunyady L, Catt KJ. Pleiotropic AT1 receptor signaling pathways mediating physiological and pathogenic actions of angiotensin II. *Mol Endocrinol* 2006; 20:953-970.

Ichihara S, Senbonmatsu T, Price E, Jr., Ichiki T, Gaffney FA, et al. Angiotensin II type 2 receptor is essential for left ventricular hypertrophy and cardiac fibrosis in chronic angiotensin II-induced hypertension. *Circulation* 2001; 104:346-351.

Imanaka-Yoshida K. Tenascin-C in cardiovascular tissue remodeling: from development to inflammation and repair. *Circ J* 2012; 76:25132520.

Isoyama S, Nitta-Komatsubara Y. Acute and chronic adaptation to hemodynamic overload and ischemia in the aged heart. *Heart Fail Rev* 2002; 7:63-69.

Itoh N, Ornitz D. Fibroblast growth factors: from molecular evolution to roles in development, metabolism and diseases. *J Biochem* 2011; 149:121-130.

Iwakura A, Fujita M, Ikemoto M, Hasegawa K, Nohara R, et al. Myocardial ischemia enhances the expression of acidic fibroblast growth factor in human pericardial fluid. *Heart Vessels* 2000;15:112-116.

Jaffre F, Bonnin P, Callebert J, Debbabi H, Setola V, Doly S, et al. Serotonin and angiotensin receptors in cardiac fibroblasts coregulate adrenergic-dependent cardiac hypertrophy. *Circ Res* 2009; 104:113-123

Jiang ZS, Srisakuldee W, Soulet F, Bouche G, Kardami E. Non-angiogenic FGF-2 protects the ischemic heart from injury, in the presence or absence of reperfusion. *Cardiovasc Res* 2004; 62:154-166.

Jiang ZS, Jeyaraman M, Wen GB, Fandrich RR, Dixon IM, Cattini PA, et al. High- but not low-molecular weight FGF-2 causes cardiac hypertrophy *in vivo*; possible involvement of cardiotrophin-1. *J Mol Cell Cardiol* 2007; 42:222-233.

Jimenez SK, Sheikh F, Jin Y, Detillieux KA, Dhaliwal J, Kardami E, et al. Transcriptional regulation of FGF-2 gene expression in cardiac myocytes. *Cardiovasc Res* 2004; 62:548-557.

Kardami E, Fandrich RR. Basic fibroblast growth factor in atria and ventricles of the vertebrate heart. *J Cell Biol* 1989; 109:1865-1875.

Kardami E, Murphy LJ, Liu L, Padua RR, Fandrich RR. Characterization of two preparations of antibodies to basic fibroblast growth factor which exhibit distinct patterns of immunolocalization. *Growth Factors* 1990; 4:69-80.

Kardami E, Jiang ZS, Jimenez SK, Hirst CJ, Sheikh F, Zahradka P, Cattini PA. Fibroblast growth factor 2 isoforms and cardiac hypertrophy. *Cardiovasc Res* 2004; 63:458-466.

Kardami E, Detillieux K, Ma X, Jiang Z, Santiago JJ, Jimenez SK, et al. Fibroblast growth factor-2 and cardioprotection. *Heart Fail Rev* 2007; 12:267-277.

Kaschina E, Unger T. Angiotensin AT1/AT2 receptors: regulation, signaling and function. *Blood Press* 2003; 12:70-88.

Kawaguchi M, Takahashi M, Hata T, Kashima Y, Usui F, et al. Inflammasome activation of cardiac fibroblasts is essential for myocardial ischemia/reperfusion injury. *Circulation* 2011; 123:594-604.

Kawano H, Do YS, Kawano Y, Starnes V, Barr M, et al. Angiotensin II has multiple profibrotic effects in human cardiac fibroblasts. *Circulation* 2000; 101: 1130-1137.

Keller M, Ruegg A, Werner S, Beer HD. Active caspase-1 is a regulator of unconventional protein secretion. *Cell* 2008; 132:818-831.

Khalil N, Xu YD, O'Connor R, Duronio V. Proliferation of pulmonary interstitial fibroblasts is mediated by transforming growth factor-beta1-induced release of extracellular fibroblast growth factor-2 and phosphorylation of p38 MAPK and JNK. *J Biol Chem* 2005; 280:4300- 43009.

Kim HD. Expression of intermediate filament desmin and vimentin in the human fetal heart. *Anat Rec* 1996; 246:271-278.

Kim I, Moon S, Yu K, Kim U, Koh GY. A novel fibroblast growth factor receptor-5 preferentially expressed in the pancreas(1). *Biochim Biophys Acta* 2001; 1518:152-156.

Klint P and Claesson-Welsh L. Signal transduction by fibroblast growth factor receptors. *Front Biosci* 1999; 4:D165-177.

Kohli S, Ahuja Suchit, Rani V. Transcription factors in heart: promising therapeutic targets in cardiac hypertrophy. *Curr Cardiol Rev* 2011; 7:262-271.

Krenz M, Robbins J. Impact of beta-myosin heavy chain expression on cardiac function during stress. *J Am Coll Cardiol* 2004; 44:2390-2397.

Kuhn H, Weser L, Gessner C, Hammerschmidt S, Wirtz H. Release of bFGF following apoptosis and necrosis in NSCLC cells: effects on chemosensitivity to cisplatin. *Oncol Rep* 2005; 14:759-762.

Lafontant PJ,, Burns AR, Donnachie E, Haudek SB, Smith CW, Entman ML. Oncostatin M differentially regulates CXC chemokines in mouse cardiac fibroblasts. *Am J Physiol Cell Physiol* 2006; 291:C18-26.

Lemarie CA, Schiffrin EL. The angiotensin II type 2 receptor in cardiovascular disease. *J Renin Angiotensin Aldosterone Syst* 2010; 11:19-31.

Li H, Zhang J, Jia W. Fibroblast growth factor 21: a novel metabolic regulator from pharmacology to physiology. *Front Med* 2013; 7:25-30.

Liao S, Bodmer J, Pietras D, Azhar M, Doetschman T, Schultz Jel J. Biological functions of the low and high molecular weight protein isoforms of fibroblast growth factor-2 in cardiovascular development and disease. *Dev Dyn* 2009; 238:249-264.

Liao S, Bodmer JR, Azhar M, Newman G, Coffin JD, Doetschman T, et al. The influence of FGF2 high molecular weight (HMW) isoforms in the development of cardiac ischemia-reperfusion injury. *J Mol Cell Cardiol* 2010; 48:1245-1254.

Lindner V, Wang Q, Conley BA, Friesel RE, Vary CP. Vascular injury induces expression of periostin: implications for vascular cell differentiation and migration. *Arterioscler Thromb Vasc Biol* 2005; 25:77-83.

Liu L, Doble BW, Kardami E. Perinatal phenotype and hypothyroidism are associated with elevated levels of 21.5- to 22-kDa basic fibroblast growth factor in cardiac ventricles. *Dev Biol* 1993; 157:507-516.

Liu AY, Zheng H, Ouyang G. Periostin, a multifunctional matricellular protein in inflammatory and tumor microenvironments. *Matrix Biol* 2014; S0945-053x(14)00066-3.

Ma X, Dang X, Claus P, Hirst C, Fandrich RR, et al. Chromatin compaction and cell death by high molecular weight FGF-2 depend on its nuclear localization, intracrine ERK activation, and engagement of mitochondria. *J Cell Physiol* 2007; 213:690-698.

Mahadavan G, Nguyen TH, Horowitz JD. Brain natriuretic peptide: a biomarker for all cardiac disease. *Curr Opin Cardiol* 2014; 29:160-166.

Maher PA. Nuclear Translocation of fibroblast growth factor (FGF) receptors in response to FGF-2. *J Cell Biol* 1996; 134:529-536.

Malecki J, Wesche J, Skjerpen CS, Wiedlocha A and Olsnes S. Translocation of FGF-1 and FGF-2 across vesicular membranes occurs during G1-phase by a common mechanism. *Mol Biol Cell* 2004; 15:801-814.

Maltseva O, Folger P, Zekaria D, Petridou S, Masur SK. Fibroblast growth factor reversal of the corneal myofibroblast phenotype. *Invest Ophthalmol Vis Sci* 2001; 42:2490-2495.

Meij JT, Sheikh F, Jimenez SK, Nickerson PW, Kardami E, Cattini PA. Exacerbation of myocardial injury in transgenic mice overexpressing FGF-2 is T cell dependent. *Am J Physiol Heart Circ Physiol* 2002; 282:H547-555.

Merkle S, Frantz S, Schon MP, Bauersachs J, Buitrago M, Frost RJ, et al. A role for caspase-1 in heart failure. *Circ Res* 2007; 100:645-653.

Mehta PK, Griendling KK. Angiotensin II cell signaling: physiological and pathological effects in the cardiovascular system. *Am J Physiol Cell Physiol* 2007; 292:C82-C97.

Mihl C, Dassen WR, Kuipers H. Cardiac remodeling: concentric versus eccentric hypertrophy in strength and endurance athletes. *Neth Heart J* 2008; 16:129-133.

Molkentin JD. Calcineurin-NFAT signaling regulates the cardiac hypertrophic response in coordination with MAPKs. *Card Res* 2004; 63:467-475.

Moscatelli D. High and low affinity binding sites for basic fibroblast growth factor on cultured cells: absence of a role for low affinity binding in the stimulation of plasminogen activator production by bovine capillary endothelial cells. *J Cell Physiol* 1987; 131: 123-130.

Muro AF, Moretti FA, Moore BB, Yan M, Atrasz RG, Wilke CA, et al. An essential role for fibronectin extra type III domain A in pulmonary fibrosis. *Am J Respir Crit Care Med* 2008; 177:638-645.

Narine K, Ke Wever O, Van Valckenborgh D, Francois K, Bracke M, DeSmet S, et al. Growth factor modulation of fibroblast proliferation, differentiation, and invasion; implications for tissue valve engineering. *Tissue Eng* 2006; 12:2707-2716.

Netticadan T, Yu L, Dhalla NS, Panagia V. Palmitoyl carnitine increases intracellular calcium in adult rat cardiomyocytes. *J Mol Cell Cardiol* 1999; 31:1357-1367.

Nickel W, Rabouille C. Mechanisms of regulated unconventional protein secretion. *Nat Rev Moll Cell Biol* 2009; 10:148-155.

Nishioka T, Onishi K, Shimojo N, Nagano Y, Matsusaka H, Ikeuchi M, et al. Tenascin-C may aggravate left ventricular remodeling and function after myocardial infarction in mice. *Am J Physiol Heart Circ Physiol* 2010; 298: H1072-H1078.

Nusayr E, Sadideen DT, Doetschman T. FGF-2 modulates cardiac remodeling in an isoform- and sex-specific manner. *Physio Rep* 2013; 1:1-14.

Nusayr E, Doetschman T. Cardiac development and physiology are modulated by FGF-2 in an isoform- and sex-specific manner. *Physiol Rep* 2013; 1:e00087.

Ogura Y, Ouchi N, Ohashi K, Shibata R, Kataoka Y, Kambara T, et al. Therapeutic impact of follistatin-like 1 on myocardial ischemic injury in preclinical models. *Circulation* 2012; 126:1728-1738.

Oka T, Xu J, Kaiser RA, Melendez J, Hambleton M, Sargent MA, et al. Genetic manipulation of periostin expression reveals a role in cardiac hypertrophy and ventricular remodeling. *Circ Res* 2007; 101:313-321.

Opie LH, Commerford PJ, Gersh BJ, Pfeffer MA. Controversies in ventricular remodeling. *Lancet* 2006; 367:356-367.

Ornitz DM, Itoh N. Fibroblast growth factors. *Genome Biol* 2001; 2:REVIEWS3005.

Ortega S, Ittmann M, Tsang SH, Ehrlich M and Basilico C. Neuronal defects and delayed wound healing in mice lacking fibroblast growth factor 2. *Proc Natl Acad Sci USA* 1998; 95:5672-5677.

Padua RR, Kardami E. Increased basic fibroblast growth factor (bFGF) accumulation and distinct patterns of localization in isoproterenol-induced cardiomyocyte injury. *Growth Factors* 1993; 8:291-306.

Pasumarthi KB, Doble BW, Kardami E, Cattini PA. Over-expression of CUG- or AUG-initiated forms of basic fibroblast growth factor in cardiac myocytes results in similar effects on mitosis and protein synthesis but distinct nuclear morphologies. *J Mol Cell Cardiol* 1994; 26:1045-1060.

Pasumarthi KB, Kardami E, Cattini PA. High and low molecular weight fibroblast growth factor-2 increase proliferation of neonatal rat cardiac myocytes but have differential effects on binucleation and nuclear morphology. Evidence for both paracrine and intracrine actions of fibroblast growth factor-2. *Circ Res* 1996; 78:126-136.

Pellieux C, Foletti A, Peduto G, Aubert JF, Nussberger J, Beermann F, et al. Dilated cardiomyopathy and impaired cardiac hypertrophic response to angiotensin II in mice lacking FGF-2. *J Clin Invest* 2001; 108:1843-1851.

Piotrowicz RS, Martin JL, Dillman WH, Levin EG. The 27-kDa heat shock protein facilitates basic fibroblast growth factor release from endothelial cells. *J Biol Chem* 1997; 272:7042-7047.

Piotrowicz RS, Maher PA, Levin EG. Dual activities of 22-24 kDa basic fibroblast growth factor: inhibition of migration and stimulation of proliferation. *J Cell Physiol* 1999; 178:144-153.

Piotrowicz RS, Ding L, Maher P, Levin EG. Inhibition of cell migration by 24-kDa fibroblast growth factor-2 is dependent upon the estrogen receptor. *J Biol Chem* 2001; 276:3963-3970.

Porrello ER, Delbridge LM, Thomas WG. The angiotensin II type 2 (AT2) receptor: an enigmatic seven transmembrane receptor. *Front Biosci* 2009; 14:958-972.

Porter KE, Turner NA. Cardiac fibroblasts: at the heart of myocardial remodeling. *Pharmacol Ther* 2009; 123:255-278.

Prats AC, Prats H. Translational control of gene expression: role of IRESs and consequences for cell transformation and angiogenesis. *Prog Nucleic Acid Res Mol Biol* 2002; 72:367-413.

Quarto N, Fong KD, Longaker MT. Gene profiling of cells expressing different FGF-2 forms. *Gene* 2005; 356:49-68.

Riese J, Zeller R and Dono R. Nucleo-cytoplasmic translocation and secretion of fibroblast growth factor-2 during avian gastrulation. *Mech Dev* 1995; 49:13-22.

Sabbah HN, Sharov VG, Lesch M, Goldstein S. Progression of heart failure: a role for interstitial fibrosis. *Mol Cell Biochem* 1995; 147:29-34.

Sadoshima J, Izumo S. Molecular characterization of angiotensin-induced hypertrophy of cardiac myocytes and hyperplasia of cardiac fibroblasts. Critical role of the AT-1 receptor subtype. *Circ Res* 1993; 73:413-423.

Santiago JJ, Dangerfield AL, Rattan SG, Bathe KL, Cunnington RH, et al. Cardiac fibroblast to myofibroblast differentiation *in vivo* and *in vitro*: expression of focal adhesion components in neonatal and adult rat ventricular myofibroblasts. *Dev Dyn* 2010; 239:1573-1584.

Santiago JJ, Ma X, McNaughton LJ, Nickel BE, Bestvater BP, et al. Preferential accumulation and export of high molecular weight FGF-2 by rat cardiac non-myocytes. *Cardiovasc Res* 2011; 89:139-147.

Santiago JJ, McNaughton LJ, Koleini N, Ma X, Bestvater B, Nickel B, et al. High molecular weight fibroblast growth factor-2 in the human heart is a potential target for prevention of cardiac remodeling. *PLoS One* 2014; 9:e97281.

Sato A, Aonuma K, Imanaka-Yoshida K, Yoshida T, Isobe M, Kawase D, et al. Serum tenascin-C might be a novel predictor of left ventricular remodeling and prognosis after acute myocardial infarction. *J Am Coll Cardiol* 2006; 47: 2319-2325.

Schultz JE, Witt SA, Nieman ML, Reiser PJ, Engle SJ, Zhou M, et al. Fibroblast growth factor-2 mediates pressure-induced hypertrophic response. *J Clin Invest* 1999; 104:709-719.

Sheng Z, Lewis JA, Chirico WJ. Nuclear and nucleolar localization of 18-kDa fibroblast growth factor-2 is controlled by C-terminal signals. *J Biol Chem* 2004; 279:40153-40160.

Shibata F, Baird A, Florkiewicz RZ. Functional characterization of the human basic fibroblast growth factor gene promoter. *Growth Factors* 1991; 4:277-287.

Shimano M, Ouchi N, Nakamura K, van Wijk B, Ohashi K, Asaumi Y, et al. Cardiac myocytes follistatin-like 1 functions to attenuate hypertrophy following pressure overload. *Proc Natl Acad Sci USA* 2011; 108:E899-906.

Shimasaki S, Emoto N, Koba A, Mercado M, Shibata F, et al. Complementary DNA cloning and sequencing of rat ovarian basic fibroblast growth factor and tissue distribution study of its mRNA. *Biochem Biophys Res Commun* 1998; 157: 256-263.

Shinde AV, Frangogiannis NG. Fibroblasts in myocardial infarction: a role in inflammation and repair. *J Moll Cell Cardiol* 2014; 70C:74-82.

Shi-Wen X, Chen Y, Denton CP, Eastwood M, Renzoni EA, Bou-Gharios G, et al. Endothelin-1 promotes myofibroblasts induction through the ETA receptor via a *rac*/phosphoinositide 3-kinase/Akt-dependent pathway and is essential for the enhanced contractile phenotype of fibrotic fibroblasts. *Mol Biol Cell* 2004; 15:2707-2719.

Silva PN, Altamentova SM, Kilkenny DM, Rocheleau JV. Fibroblast growth factor receptor like-1 (FGFRL1) interacts with SHP-1 phosphatase at insulin secretory granules and induces beta-cell ERK1/2 protein activation. *J Biol Chem* 2013; 288:17859-17870.

Simons M, Ware JA. Therapeutic angiogenesis in cardiovascular disease. *Nat Rev Drug Discov* 2003; 2:863-871.

Sleeman M, Fraser J, McDonald M, Yuan S, White D, Grandison P, et al. Identification of a new fibroblast growth factor receptor, FGFR5. *Gene* 2001; 271:171-182.

Srisakuldee W, Jeyaraman MM, Nickel BE, Tanguy S, Jiang ZS, Kardami E. Phosphorylation of connexin-43 at serine 262 promotes a cardiac injury-resistant state. *Cardiovasc Res* 2009; 83:672-681.

Sorensen V, Nilsen T, Wiedlocha A. Functional diversity of FGF-2 isoforms by intracellular sorting. *Bioessays* 2006 ;28:504-514.

Stachowiak MK, Fang X, Myers JM, Dunham SM, Berezney R, Maher PA, Stachowiak EK. Integrative nuclear FGFR1 signaling (INFS) as a part of a universal "feed-forward-and-gate" signaling module that controls cell growth and differentiation. *J Cell Biochem* 2003; 90:662-691.

Stroth U, Blume A, Mielke K, Unger T. Angiotensin AT(2) receptor stimulates ERK1 and ERK2 in quiescent but inhibits ERK in NGF-stimulated PC12W cells. *Brain Res Mol Brain Res* 2000; 78:175-180.

Sun G, Doble BW, Sun JM, Fandrich RR, Florkiewicz R, Kirshenbaum L, et al. CUG-initiated FGF-2 induces chromatin compaction in cultured cardiac myocytes and *in vitro*. *J Cell Physiol* 2001; 186:457-467.

Swynghedauw B. Molecular mechanisms of myocardial remodeling. *Physiol Rev* 1999; 79:215-262.

Szebenyi G, Fallon JF. Fibroblast growth factors as multifunctional signaling factors. *Int Rev Cytol* 1999; 185-45-106.

Tanaka T, Hasegawa K, Fujita M, Tamaki SI, Yamazato A, et al. Marked elevation of brain natriuretic peptide levels in pericardial fluid is closely associated with left ventricular dysfunction. *J Am Coll Cardiol* 1998; 31:399-403.

Taverna S, Gherzi G, Ginestra A, Rigogliuso S, Pecorella S, Alaimo G, et al. Shedding of membrane vesicles mediates fibroblast growth factor-2 release from cells. *J Biol Chem* 2003; 278:51911-51919.

Temmerman K, Ebert AD, Muller HM, Sinning I, Tews I, Nickel W. A direct role for phosphatidylinositol-4,5-bisphosphate in unconventional secretion of fibroblast growth factor 2. *Traffic* 2008; 9:1204-1217.

Teshima-Kondo S, Kondo K, Prado-Lourenco L, Gonzalez-Herrera IG, Rokutan K, Bayard F, et al. Hyperglycemia upregulates translation of the fibroblast growth factor 2 mRNA in mouse aorta via internal ribosome entry site. *Faseb J* 2004; 18:1583-1585.

Tessler S, Neufeld G. Basic fibroblast growth factor accumulates in the nuclei of various bFGF-producing cell types. *J Cell Physiol* 1990; 145:310-317.

Tholozan FM, Gribbon C, Li Z, Goldberg MW, Prescott AR, McKie N, et al. FGF-2 release from the lens capsule by MMP-2 maintains lens epithelial cell viability. *Mol Biol Cell* 2007; 18:4222-4231.

Thum T, Gross C, Fiedler J, Fischer T, Kissler S, Bussen M, et al. MicroRNA-21 contributes to myocardial disease by stimulating MAP kinase signaling in fibroblasts. *Nature* 2008; 456:980-984.

Tomasek JJ, Gabbiani G, Hinz B, Chaponnier C, Brown RA. Myofibroblasts and mechano-regulation of connective tissue remodeling. *Nat Rev Mol Cell Biol* 2002; 3:349-363.

Touriol C, Roussigne M, Gensac MC, Prats H and Prats AC. Alternative translation initiation of human fibroblast growth factor 2 mRNA controlled by its 3'-untranslated region involves a Poly(A) switch and a translational enhancer. *J Biol Chem* 2000; 275:19361-19367.

Tsutsumi Y, Matsubara H, Ohkubo N, Mori Y, Nozawa Y, et al. Angiotensin II type 2 receptor is upregulated in human heart with interstitial fibrosis, and cardiac fibroblasts are the major cell type for its expression. *Circ Res* 1998; 83:1035-1046.

Turner NA. Effects of interleukin-1 on cardiac fibroblast function: Relevance to post-myocardial infarction remodeling. *Vascul Pharmacol* 2013.

Vagner S, Touriol C, Galy B, Audigier S, Gensac MC, Amalric F, et al. Translation of CUG- but not AUG-initiated forms of human fibroblast growth factor 2 is activated in transformed and stressed cells. *J Cell Biol* 1996; 135:1391-1402.

Valtink M, Knels L, Stanke N, Engelmann K, Funk RH, Lindemann D. Overexpression of human HMW FGF-2 but not LMW FGF-2 reduces the cytotoxic effect of lentiviral gene transfer in human corneal endothelial cells. *Invest Ophthalmol Vis Sci* 2012; 53:3207-3214.

Vlodavsky I, Bashkin P, Ishai-Michaeli R, Chajek-Shaul T, Bar-Shavit R, Haimovitz-Friedman A, et al. Sequestration and release of basic fibroblast growth factor. *Ann N Y Acad Sci* 1991; 638:207-220.

Weber KT, Sun Y, Bhattacharya SK, Ahokas RA, Gerling IC. Myofibroblast-mediated mechanisms of pathological remodeling of the heart. *Nat Rev Cardiol* 2013; 10:15-26.

Weber KT. Cardiac interstitium in health and disease: the fibrillar collagen network. *J Am Coll Cardiol* 1989; 13:1637-1652

Wu M, Massaelli H, Durston M, Mesaelli N. Differential expression and activity of matrix metalloproteinase-2 and -9 in the calreticulin deficient cells. *Matrix Biol* 2007; 26:463-472.

Wuechner C, Nordqvist AC, Winterpacht A, Zabel B, Schalling M. Developmental expression of splicing variants of fibroblast growth factor receptor 3 (FGFR3) in mouse. *Int J Dev Biol* 1996; 40:1185-1188.

Xu S, Zhi H, Hou X, Cohen RA, Jiang B. I κ B β attenuates Angiotensin II-induced cardiovascular inflammation and fibrosis in mice. *Hypertension* 2011; 58:310-316.

Yamashita T, Yoshioka M and Itoh N. Identification of a novel fibroblast growth factor, FGF-23, preferentially expressed in the ventrolateral thalamic nucleus of the brain. *Biochem Biophys Res Commun* 2000; 277:494-498.

Yeh J, Osathanondh R. Expression of messenger ribonucleic acids encoding for basic fibroblast growth factor (FGF) and alternatively spliced FGF receptor in human fetal ovary and uterus. *J Clin Endocrinol Metab* 1993; 77:1367-1371.

Yu PJ, Ferrari G, Galloway AC, Mignatti P and Pintucci G. Basic fibroblast growth factor (FGF-2): the high molecular weight forms come of age. *J Cell Biochem* 2007; 100:1100-1108.

Yu PJ, Ferrari G, Pirelli L, Galloway AC, Mignatti P, Pintucci G. Thrombin cleaves the high molecular weight forms of basic fibroblast growth factor (FGF-2): a novel mechanism for the control of FGF-2 and thrombin activity. *Oncogene* 2008; 27:2594-2601.

Zehe C, Engling A, Wegehingel S, Schafer T and Nickel W. Cell-surface heparan sulfate proteoglycans are essential components of the unconventional export machinery of FGF-2. *Proc Natl Acad Sci USA* 2006; 103:15479-15484.

Zhang S, Smartt H, Holgate ST, Roche WR. Growth factors secreted by bronchial epithelial cells control myofibroblast proliferation: an *in vitro* co-culture model of airway remodeling in asthma. *Lab Invest* 1999; 79:395-405.

Zhang L, Parry GC, Levin EG. Inhibition of tumor cell migration by LD22-4, an N-terminal fragment of 24 kDa FGF-2, is mediated by Neuropilin 1. *Cancer Res* 2013; 73:3316-3325.

Zhao S, Wu H, Xia W, Chen X, Zhu S, Zhang S, et al. Periostin expression is upregulated and associated with myocardial fibrosis in human failing hearts. *J Cardiol* 2014; 63:373-378.

Zhou M, Sutliff RL, Pau RJI, Lorenz JN, Hoying JB, Haudenschild CC, et al. Fibroblast growth factor 2 control of vascular tone. *Nat Med* 1998; 4:201-207.

Appendix A

Figure 13 was completed by Dr. Barb E Nickel, **Figures 15 and 16** were completed by Dr. Xin Ma (as part of his PhD thesis), and **Figures 22 and 23** were completed by Dr. Navid Koleini. Permission was granted to use the following in the thesis:

Manuscript 1 (M1). By Santiago *et al.*, “Preferential accumulation and export of high molecular weight of FGF-2 by rat cardiac non-myocytes”. *Cardiovasc Res* 2011;89:139-147 (please note email below):

Dear Jon-Jon Rodrin Santiago,

Re: Jon-Jon Santiago, Xin Ma, Leslie J. McNaughton *et al.*, Preferential accumulation and export of high molecular weight FGF-2 by rat cardiac non-myocytes *Cardiovasc Res* (2011) 89 (1): 139-147

Thank you for your request. As part of your copyright agreement with Oxford University Press you have retained the right, after publication, to include the article in full or in part in a thesis or dissertation, provided that this is not published commercially. Please be advised that in terms of electronic versions of your thesis, you are permitted to include ‘a post print’ of your article (accepted manuscript PDF) and public availability outside your study institution should be delayed until 12 months after first online publication in the journal. Please include the following credit line:

This is a pre-copy-editing, author-produced PDF of an article accepted for publication in [insert journal title] following peer review. The definitive publisher-authenticated version [insert complete citation information here] is available online at: xxxxxxx [insert URL that the author will receive upon publication here].

For full details of the self-archiving policy for this journal please follow this link:

http://www.oxfordjournals.org/access_purchase/self-archiving_policyb.html

Kind regards,

Guffi Chohdri (Ms)
Rights Assistant

Academic Rights & Journals

Tel: +44 (0)1865 354454

Email: guffi.chohdri@oup.com

Manuscript 2 (M2). By Santiago *et al.*, “High molecular fibroblast growth factor-2 in the human heart is a potential target for prevention of cardiac remodeling”. PLoS One, in press, 2014 (please note email below):

Dear Mr. Santiago,

Thank you for contacting PLOS ONE.

All content of articles published in PLOS journals is open access. You can read about our open access license here: <http://www.plos.org/about/open-access/>. To summarize, this license allows you to download, reuse, reprint, modify, distribute, and/or copy articles or images in PLOS journals, so long as the original creators are credited (e.g., including the article’s citation and/or the image credit).

There are many ways to access our content, including HTML, XML, and PDF versions of each article. Higher resolution versions of figures can be downloaded directly from the article. Additionally, our articles are archived at PubMed Central (<http://www.pubmedcentral.gov/>), which offers a public FTP service from which you can download a complete site of files for each of our articles. See <http://www.pubmedcentral.gov/about/openftlist.html> for links to the FTP site, file list, and organizational directory.

Kind Regards,

**Anna Collier
PLOS ONE
Staff EO**

**Case Number: 03401332
ref:_00DU0Ifis._500U0C7HLk:ref**